Epigenetic regulation of thyroid development

Inauguraldissertation

zur
Erlangung der Würde eines Doktors der Philosophie
vorgelegt der
Philosophisch-Naturwissenschaftlichen Fakultät
der Universität Basel

von

Sanjay Gawade

aus Pune, Indien

Basel, 2016

Genehmigt von der Philosophisch-Naturwissenschaftlichen Fakultät auf Antrag von

Prof. Dr. Antonius Rolink
Prof. Dr. Georg A. Holländer
PD Dr. Gabor Szinnai

Basel, den 8. December 2015

Prof. Dr. Jörg Schibler

Dekan der Philosophisch-
Naturwissenschaftlichen
Fakultät

ABSTRACT

Focusing on the molecular mechanisms of normal and abnormal thyroid development, this work had two main aims:

1) To establish a flow cytometry protocol for the developing and adult murine thyroid.

2) To analyze whether epigenetic mechanisms are regulating thyroid development.

Project 1: A new tool for thyroid research: Flow cytometry of the thyroid gland

The thyroid is composed of endocrine epithelial cells, blood vessels and mesenchyme. However, no data exist so far on absolute cell numbers, relative distribution, and proliferation of the different cell populations of the thyroid. First, we established a gating strategy for flow cytometry that is able to identify seven distinct cell populations in the embryonic and adult thyroid. Second, a detailed analysis of cell populations *in vivo* revealed unexpected frequencies and cell growth dynamics of the different cell populations at distinct embryonic stages and in adult tissues, extending our current knowledge on normal thyroid development. Finally, a yet unknown and uncharacterized cell population present in embryonic and adult thyroids at a frequency between 5-20% has been identified, that needs further detailed characterization. In summary, our approach provides a useful new tool for cell function analyses in murine thyroid disease models.

Project 2: A new concept: Epigenetic regulation of thyroid development

Abnormal thyroid development results in thyroid dysgenesis (TD). TD causes congenital hypothyroidism in neonates. Monozygotic twin are discordant for TD, suggesting epigenetic mechanisms. This epigenetic concept is further supported by disrupted histone acetylation in thyroid cancer and pathologic development of organs after inhibition of histone deacetylases (HDAC). To investigate the role of HDACs for normal and abnormal thyroid development, we first documented physiological dynamic changes of HDAC activity, HDAC expression and histone acetylation in the thyroid between E13.5-E17.5 *in vivo*. Second, we investigated the effect of HDAC inhibition on thyroid development in an *ex vivo* embryonic thyroid culture model. HDAC inhibition induced decreased HDAC activity and increased histone acetylation. HDAC inhibition resulted in profoundly disordered thyroid development compatible with all aspects of TD: reduced follicle formation, decreased endocrine cell mass,

and disturbed angiogenesis. Hence, our data supports the concept of epigenetic regulation of thyroid development, and suggests a new molecular mechanism of TD.

TABLE OF CONTENTS

LIST OF ABBREVIATIONS

7AAD	7 amino actinomycin D
BrdU	Bromodeoxyuridine (5-bromo-2'-deoxyuridine)
C-cells	Calcitonin-producing cells
CH	Congenital hypothyroidism
CNV	Copy number variations
cAMP	Cyclic adenosine monophosphate
d	day(s)
DNA	Deoxyribonucleic acid
DAPI	4',6-diamidino-2-phenylindole
E	Embryonic days
EpCam	Epithelial cell adhesion molecule
FOXE1	Forkhead Box E1
GW	Gestational weeks
H3	Histone H3
H4	Histone H4
H3K9ac	Acetyl histone H3 lysine 9
H3K9me3	Tri-methyl histone H3 lysine 9
HAT	Histone acetyl transferase
HDAC	Histone deacetylase
HDACi	Histone deacetylase inhibitor
HMTase	Histone methyltransferase
HDMs	Histone demethylases
MFI	Mean florescence intensity
NIS	Sodium iodide symporter
NKX2-1	NK2 Homeobox 1
NuRD	Nucleosome remodeling and deacetylase complex
PAX8	Paired box gene 8
PBS	Phosphate-buffered saline
PDGFRa	Platelet-derived growth factor receptor, alpha
Pecam	Platelet endothelial cell adhesion molecule

PI	Propidium iodide
RFU	Reference Fluorescence Units
Rpd3	Reduced potassium dependency
RT	Room temperature
SD	Standard deviation
SIRT	Sirtuins
T3	Triiodothyronine
T4	Thyroxine
TD	Thyroid dysgenesis
TDHG	Thyroid dyshormonogenesis
TG	Thyroglobulin
TPO	Thyroperoxidase
TSA	Trichostatin A
TSH	Thyroid stimulating hormone
TSHR	Thyroid stimulating hormone receptor
TUNEL	Terminal deoxynucleotidyl transferase (TdT) dUTP Nick-End Labeling
VPA	Valproic acid

1. INTRODUCTION

The thyroid gland is the first endocrine gland to develop in the embryo and is responsible for the synthesis and secretion of thyroid hormones. Thyroid hormones act on virtually every cell in the body to affect body growth, metabolic rate and development, and under or over production of these hormones have potent effects. Since thyroid hormones are essential for physical and mental development, hypothyroidism in utero and postnatally might cause mental impairment and reduced physical growth (Braverman and Cooper, 2012).

The anatomy and physiology of thyroid gland is very well studied. However, the relative distribution of all the major cell types in embryonic and adult thyroid as well as the growth dynamics during embryonic development is not well characterized. One previous study in the adult dog thyroid had quantified the different cell populations by transmission electron microscopy. They showed 70% of thyroid cells were epithelial cells, 6% endothelial cells, and 24% fibroblasts. However, these results were never confirmed in other species (Dow et al., 1986). Another study in adult rat thyroids had quantified TFCs *in vivo* by flow cytometry observed 40% TG-positive TFCs, and 2-4% calcitonin-positive C-cells (Moerch et al., 2007). However, the remaining cell types were not characterized and quantified.

CH is the most frequent endocrine disease in infants, with an incidence of about 1:3000 to 1:4000 newborns (Rastogi and La Franchi, 2010). The most common cause of CH in the developed world is defects in the various important steps of thyroid development that result in thyroid dysgenesis (TD). TD is characterized by a spectrum of developmental defects of the thyroid ranging from complete absence of thyroid gland (athyreosis), abnormally located thyroid gland (ectopic), a normally located but smaller in size thyroid (hypoplastic) or orthotopic thyroid of normal size without function.

TD is believed to be a sporadic disease (98% of cases are non-familial). Also, human genetic studies suggest that TD has a discordance rate of 92% in monozygotic twins (Perry et al., 2002). Mutations in transcription factors that are expressed in developing and in functioning adult thyroid gland have been implicated as a cause of TD, however these are found in only 2% of the cases. An exact cause in the remaining of the cases still remains unknown. Recent findings suggest that genetics of TD mostly do not follow Mendelian patterns and alternative

mechanisms such as multigenic defects and epigenetic processes need to be considered (Vassart and Dumont, 2005; Szinnai, 2014a). In thyroid cancer cells, changes in gene expression due to epigenetic mechanisms involving aberrant modifications by histone acetylation or methylation have been shown (Kondo et al., 2008; Russo et al., 2011). There is increasing evidence of epigenetic mechanisms, especially histone modifications being critical during murine embryonic development of pancreas (Haumaitre et al., 2008), intestine (Tou et al., 2004) and kidney (Chen et al., 2011).

Two main important questions are addressed in this thesis:

1. Development of a new tool for thyroid research by using flow cytometry for characterization and growth dynamics of mouse thyroid gland during embryonic development and in adult stage.
2. Analyze the role of HDACs and histone acetylation for the regulation of thyroid development.

1.1 Thyroid gland

1.1.1 Anatomy and histology

Thyroid gland is a butterfly-shaped endocrine organ located in the anterior neck, on the trachea and inferior to the larynx. Two lateral thyroid lobes are connected by median isthmus. The main function of the thyroid gland is to store iodide and make it available for the synthesis of thyroid hormones. Each lobe is composed of two distinct endocrine cell types - the Thyroid follicular cells (TFCs) and the Parafollicular cells or C-cells.

TFCs are organized into thyroid follicles, the structural and functional unit of the gland (Figure 1). Thyroid follicles are made up of monolayer of TFCs enclosing the follicular lumen, which is filled with colloid. Colloid contains iodothyroglobulin, a precursor of thyroid hormones (Tortora and Derrickson, 2008; Polak and Szinnai, 2013). Thyroid hormones are synthesized and stored in the follicles. Follicles vary in size, depending upon the degree of distention, and are surrounded by dense network of capillaries, lymphatic vessels, sympathetic nerves and angiofollicular unit. The TFCs produce thyroid hormones Tetraiodothyronine or "T4" and Triiodothyronine or "T3" (Tortora and Derrickson, 2008; Polak and Szinnai, 2013).

C-cells or parafollicular cells constitute 2-4% of all cells in an adult thyroid and are located adjacent to the follicles and produce the hormone calcitonin that helps in maintaining calcium homeostasis. The four parathyroid glands are an independent endocrine organ located near the posterior aspect of the thyroid gland. These glands produce parathyroid hormone (PTH), which has effects antagonistic to those of calcitonin and helps in maintaining calcium and phosphate homeostasis (Tortora and Derrickson, 2008).

The anatomy and physiology of thyroid gland is very well studied. However, the relative distribution of all the major cell types in embryonic and adult thyroid as well as the growth dynamics during embryonic development is not well characterized. One of the oldest studies in the adult dog thyroid had quantified the different cell populations by transmission electron microscopy. They showed that 70% of the thyroid cells were epithelial cells, 6% endothelial cells, and 24% were fibroblasts. However, these results were never confirmed in other species (Dow et al., 1986). Another study in adult rat thyroids had quantified TFCs *in vivo* by flow cytometry observed 40% TG-positive TFCs, and 2-4% calcitonin-positive C-cells (Moerch et al., 2007). However, the remaining cell types were not characterized and quantified.

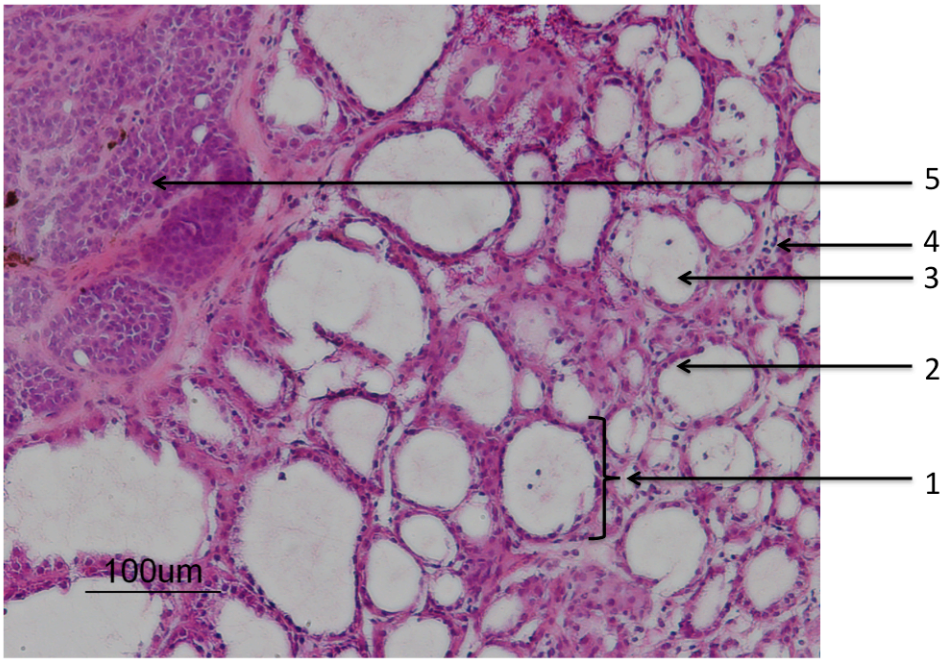

Figure 1. Adult thyroid gland of the mouse. Hematoxylin and Eosin staining of an adult mouse thyroid gland. 1) thyroid follicle, 2) monolayer TFC epithelium, 3) follicular lumen filled with colloid, 4) C-cells, 5) parathyroid gland.

Sanjay Gawade, Unpublished data.

1.1.2 Thyroid hormone synthesis

The synthesis of thyroid hormones takes place in the thyroid follicles and requires a normally developed thyroid gland, an adequate nutritional intake of iodide, and a series of sequential biochemical steps. The TFCs synthesize and secrete hormones T3 and T4 as follows:

Iodide trapping

Active transport of iodide into the thyroid gland is a crucial and rate-limiting step in the biosynthesis of thyroid hormones (Dai et al., 1996; Szinnai et al., 2007; Spitzweg and Morris, 2010; Portulano et al., 2014). TFCs trap iodide ions (I^-) by actively transporting them from the blood into the cytosol. As a result, the thyroid gland normally contains most of the iodide in the body. Sodium iodide symporter (NIS) is the protein responsible for iodide uptake at the basolateral membrane and is encoded by the *SLC5A5* gene. NIS co-transports two sodium ions along with one iodide ion, with the transmembrane sodium gradient serving as the driving force for iodide uptake. This sodium gradient that provides the energy for this transfer is generated by Na+/K+-ATPase. Following the active transport, iodide is translocated across the apical membrane by passive or facilitated transport into the follicular lumen by

chloride/iodide transporter pendrin (*SLC26A4/ PDS*) (Royaux et al., 2000; Bizhanova and Kopp, 2009; Pesce et al., 2011; Darrouzet et al., 2014).

Synthesis of thyroglobulin

TFCs synthesize thyroglobulin (TG), a large glycoprotein that is produced in the rough endoplasmic reticulum, modified in the Golgi complex, and packaged into secretory vesicles. The vesicles then undergo exocytosis, which releases TG into the lumen of the follicle. TG serves as matrix for TH synthesis and storage (Lee et al., 2009; Tortora and Derrickson, 2008; Polak and Szinnai, 2013).

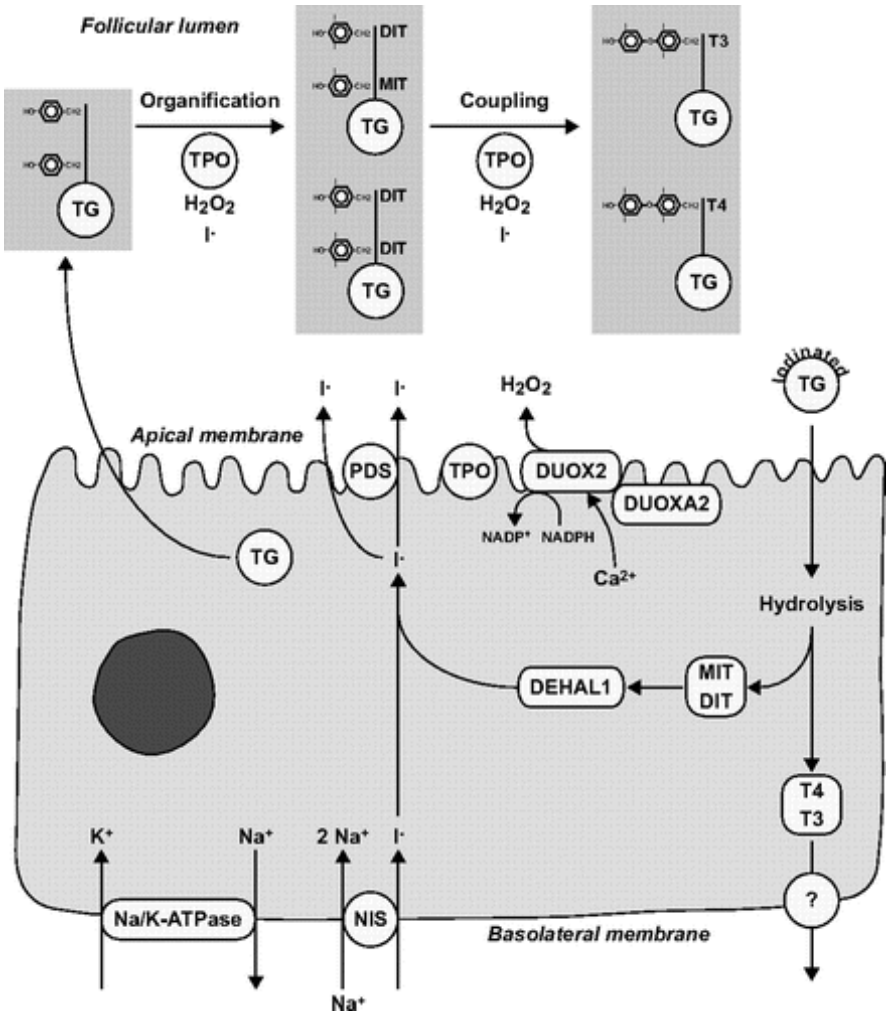

Figure 2: Main steps involved in the thyroid hormone synthesis. At the basolateral membrane, iodide is transported into thyrocytes by the sodium iodide symporter (NIS). At the apical membrane, iodide efflux is mediated by pendrin (PDS). Iodide is oxidized by TPO in the presence of H_2O_2. Thyroglobulin (TG) secreted into the follicular lumen serves as matrix for synthesis of T_3 and T_4. First, TPO catalyzes iodination of selected tyrosyl residues (organification) to form monoiodotyrosine (MIT) and diiodotyrosine (DIT). Subsequently, TPO catalyzes the coupling of two iodotyrosines to form either T_4 or T_3. Iodinated TG is stored as colloid in the follicular lumen until needed. For the release of thyroid hormones, TG is internalized into the follicular cell by pinocytosis and digested in lysosomes. These processes generate T_4 and T_3 that are released into the bloodstream through unknown mechanisms. The unused MIT and DIT are retained in the cell and deiodinated by the dehalogenase 1 (DEHAL1). The released iodide is recycled for thyroid hormone synthesis.

Taken from Bizhanova and Kopp, 2009.

Oxidation of iodide and iodination of tyrosine

Iodide ions undergo oxidation to form iodine that binds to tyrosine in TG. Thyroid (TPO) catalyzes two key steps of thyroid hormone synthesis, namely organification and coupling (Figure 2). Organification of iodide to bind iodine to tyrosyl residues in TG needs the presence of hydrogen peroxide (H_2O_2), resulting in the production of monoiodotyrosine (MIT) and diiodotyrosine (DIT). Then, coupling of one MIT and one DIT or two DIT residues takes place, resulting in iodinated TG molecules forming T3 or T4 respectively. H_2O_2 is generated by two nicotinamide adenine dinucleotide phosphate (NADPH) oxidases called dual oxidases 1 and 2 (DUOX1 and DUOX2). Generation of H_2O_2 as well as binding of oxidized iodide to tyrosine residues of TG and formation of THs are activated by the TSH-dependent phospholipase C-Ca^{2+} pathway and inhibited by cyclic adenosine monophosphate (cAMP) signaling cascades (Stathatos, 2006; Song et al., 2007; Grasberger, 2010).

Thyroglobulin pinocytosis and secretion of thyroid hormones

For the release of thyroid hormones, iodinated TG molecules are reabsorbed into the follicular cells by pinocytosis. These molecules undergo lysosomal digestion that release T4 and T3 into the bloodstream via the basolateral membrane through an unknown mechanism. The unused MIT and DIT undergoes deiodination that is mediated by iodotyrosine dehalogenase 1 (DEHAL1), representing an important mechanism of iodine recycling within the TFCs for future TH synthesis (Figure 2) (Bizhanova and Kopp, 2009; Kleinau et al., 2013; Iglesias et al., 2014).

Control of thyroid hormone synthesis

Iodine availability and thyroid-stimulating hormone (TSH) are the two most important factors controlling thyroid hormone synthesis. Deficient amounts of iodine leads to decreased thyroid hormone production, increased secretion of TSH, and in an attempt to compensate may also cause goiter. In contrast, higher concentration of iodide acutely inhibits thyroid hormone synthesis by inhibiting the generation of H_2O_2 (the Wolff-Chaikoff effect) (Wolff and Chaikoff, 1948) and thus blocking TG iodination (Dunn and Dunn, 2001).

The plasma levels of THs are under the regulation of the hypothalamic-pituitary-thyroid (HPT) axis. When the serum levels of T4 and T3 are low, TSH is released from the anterior pituitary gland. TSH is considered to be the key regulatory factor controlling the synthesis

and secretion of THs. Thyrotropin-releasing hormone (TRH) secreted from the hypothalamus controls the release of TSH. (Costa-e-Sousa and Hollenberg, 2012). TSH binding to TSHR leads to the activation of the enzyme adenylate cyclase (AC). The consequent increase in cAMP intracellular levels together with the activation of cAMP-dependent protein kinase A (PKA) mediate the TSH-dependent synthesis of THs (Yen, 2001; Rivas and Santisteban, 2003; Kleinau et al., 2013). TSH stimulates nearly every step along the process of THs synthesis and secretion. TSH stimulates the synthesis of NIS, TPO, TG, generation of H_2O_2, internalization of TG by TFCs, its degradation and the subsequent release of THs into the blood circulation (Stathatos, 2006).

The thyroid specific expression of the proteins involved in thyroid hormone synthesis, TG, TPO, NIS and PDS requires transcription factors such as NKX2-1 (NK2 Homeobox 1/ also known as thyroid transcription factor 1 (TTF-1), FOXE1 (Forkhead Box E1/ also known as thyroid transcription factor 2 (TTF-2) and PAX8 (Paired Box 8) (Kambe and Seo, 1997; De Felice and Di Lauro, 2004; Fernandez et al., 2015). Binding sites of NKX2-1, FOXE1 and PAX8 are present in the promoters of TG and TPO, NKX2-1 and PAX8 in the NIS upstream enhancer and NKX2-1 in the promoter of PDS (Damante and Di Lauro, 1994; Di Palma et al., 2003; Christophe, 2004; Dentice et al., 2005; Portulano et al., 2014).

1.2. Normal thyroid development

1.2.1 Key steps of thyroid development

The thyroid gland originates from a median anlage and two lateral anlages (ultimobranchial bodies), which fuses during development (De Felice and Di Lauro, 2004; Szinnai, 2014a). The median anlage originates from the foregut endoderm, while the lateral anlages are of neuroectodermal origin and derived from the 4th pharyngeal pouches (Szinnai, 2014a). As mentioned earlier, the thyroid gland has two distinct cell types: 1) The TFC precursor cells that are derived from the foregut endoderm, and 2) C-cells that are derived from the lateral anlages. After migrating from their respective sites of origin, cells from both the thyroid anlage and the lateral anlages ultimately merge in the definitive thyroid gland. After merging, TFCs originating from the thyroid anlage organize into thyroid follicles, whereas the C-cells scatter in the interfollicular space (De Felice and Di Lauro, 2004; Nilsson and Fagman, 2013; Szinnai, 2014a).

All major morphogenetic steps of the thyroid are conserved in humans and mice:

A) Specification and budding of the thyroid primordium from the foregut endoderm.
B) Migration of the median anlage to its final pretracheal position.
C) Fusion of median anlage with the ultimobranchial bodies (lateral anlages).
D) Terminal differentiation with the onset of thyroid hormone synthesis (De Felice and Di Lauro, 2004; Trueba et al., 2005; Fagman et al., 2006; Szinnai, 2007).

The sequence of these key steps of thyroid development is identical in humans and mice and can be correlated (Table 1).

Table 1: Correlation of the timing of relevant events during thyroid development in humans and mice. (E- Embryonic day; GW- Gestational week).

EVENTS	**HUMAN** (Embryonic day and gestational week)	**MOUSE** (Embryonic day)
Specification of the median anlage	E22	E8.5
Budding of the median anlage	E26	E9.5
Migration of median and lateral anlages	E28-48	E10.5-13.5
Fusion of median and lateral anlages	E44	E13
Terminal differentiation	E48-80; GW 7-11	E14.5- 16.5
Follicle formation	E73-80; GW 10-11	E15.5
Onset of thyroid hormone synthesis	E80; GW 11	E16.5

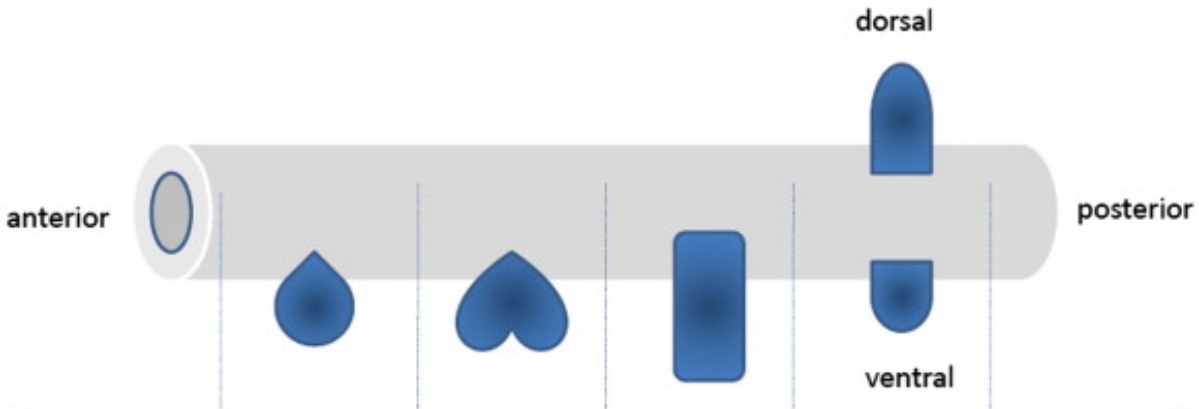

Transcription factors	Thyroid progenitors	Lung progenitors	Hepato-blasts	Pancreatic progenitors	Expression outside of foregut
Pax8	⟷				kidney
Foxe1	⟷				thymus
Nkx2-1	⟷	⟷			brain
Hhex	⟷		⟷		brain
Hes1	⟷			⟷	brain

Figure 3. Transcription factors in the endoderm. The schematic representation of the mouse E8.5–E9.5 gut tube shows the expression of the transcription factors Pax8, Foxe1, Nkx2-1, Hhex, and Hes1 along its anterior–posterior axis and in regions that contribute to other endodermal organs.

Taken from Szinnai, 2014.

1.2.2 Endodermal origin of the thyroid gland

Following gastrulation of vertebrate embryos (embryonic day E7.5 in mice), the definitive endoderm undergoes complex morphogenetic changes that form primitive gut tube. Invagination of the endoderm at the anterior end (the foregut) contributes to the formation of thyroid, thymus, parathyroid, pancreas and the liver. The cells of these organs that undergo specification and development are controlled by transcriptional regulators and by signals from the surrounding tissues such as heart and notochord (Zorn and Wells, 2009; Kraus and Grapin-Botton, 2012). Transcription factors that are expressed early in the endoderm, such as Foxa1 (Forkhead Box A1), Foxa2 (Forkhead Box A2), Gata4 (GATA binding protein) and Gata6 are necessary for the differentiation, survival and morphogenesis of the foregut (Ang and Rosant, 1994; Kuo et al., 1997; Morrisey et al., 1998).

At E8-9.5, the expression of transcription factors such as Foxa1, Foxa2, Hhex (hematopoietically expressed homeobox), Pdx1 (pancreatic and duodenal homeobox 1) and

Nkx2-1 along the anterior-posterior axis of the ventral foregut marks organ specific domains. Foxa1 and Foxa2 are expressed in the ventral foregut in the liver, lung and pancreas field (Kaestner et al., 1993; Wan et al., 2005; Lee et al., 2005; Zaret, 2008). Hhex is expressed in the forebrain, thyroid and liver (Thomas et al., 1998; Martinez-Barbera et al., 2000). Nkx2-1 is expressed in the thyroid and lung (Lazzaro et al., 1991; Kimura et al., 1996; Cardoso and Lü, 2006). Hes1 (hairy/enhancer of split 1) is expressed in TFC progenitors and pancreatic progenitors, while Pax8 and Foxe1 endodermic expression occurs exclusively in the thyroid. The endodermal cells of the thyroid domain acquire a specific molecular signature by E8.5 in the mouse with co-expression of the transcription factors Pax8, Foxe1, Nkx2-1, Hhex, and Hes1 in the mouse (Plachov et al., 1990; Lazzaro et al., 1991; Zanini et al., 1997; Thomas et al., 1998; Parlato et al., 2004; Carre et al., 2011; Fernández et al., 2015) (Figure 3).

1.2.3 Budding and migration of the median thyroid anlage

By E9.0 in mouse and E22 in human embryo, the median anlage is visible as a thickening of the endodermal epithelium in the foregut, which is referred to as thyroid anlage. Thickening in a restricted region of a cell layer is an essential event in the generation of signals required for the continuation of organogenesis (Kenyon et al., 2003). The thyroid anlage evaginates from the floor of the pharynx by E9.5 and E26 respectively. The bud forms a diverticulum that starts to migrate caudally into the mesenchyme by E10.5 and E32 respectively. The molecular mechanism of thyroid migration remains largely unknown. Epithelial to mesenchymal transition, a conserved mechanism of active cell migration in development and cancer does not play a role as shown by Fagman et al (Fagman et al, 2003). Until now, only Foxe1 has been shown to play a specific role in this process, as 50% of Foxe1-/- embryos developed thyroid ectopy (De Felice et al., 1998; Trueba et al., 2005; Nilsson and Fagman, 2013; Fernández et al., 2015).

1.2.4 Fusion of the median thyroid anlage with the ultimobranchial bodies

By E12.5 in mouse and E48 in human, the median anlage reaches its definitive pre-tracheal position and just before reaching the definitive pretracheal position, the thyroid anlage fuses with the ultimobranchial bodies. Between E13.0-13.5 in mouse, the thyroid anlage develops into two lobes and a narrow isthmus that connects these two lateral lobes (Trueba et al., 2005; Fagman et al., 2006; Kusakabe et al., 2006b). Studies on transgenic mice show that Nkx2-1,

Pax8 and Shh (Sonic hedgehog) play an important role for correct symmetrical lobulation of the median anlage (Fagman et al., 2004; Amendola et al., 2005).

1.2.5 Terminal differentiation of the thyroid gland

Terminal differentiation or functional differentiation is the final step of thyroid development and results in the onset of thyroid function. It starts by E14.5 in mouse and 7 gestational weeks (GW) in the human, and is completed by E16.5 and 11 GW respectively. Terminal differentiation comprises structural and functional changes. Structural changes include polarization and adhesion of each TFCs to form thyroid follicles, the functional unit of thyroid gland. This is followed by angiogenesis forming a dense three-dimensional capillary network around each follicle and functional transition from non-functional TFC precursors to mature TFC capable of TH synthesis. Active uptake of iodide, Tg synthesis and H_2O_2 generation are the most essential mechanisms for thyroid hormone synthesis (De Felice and Di Lauro, 2004; Szinnai, 2014a,b).

In mouse, thyroid specific genes that are typical of the developmental stage appear according to a given temporal pattern: By E14.5 Tg, Tpo, and Tshr genes are expressed; by E16 Nis is detected. T4 synthesis starts at E16.5. For thyroid hormone biosynthesis, the precise timing of the expression of each of these genes is necessary, indicating that a genetic mechanism must be necessary for such a control. However, the key players of such a mechanism are unknown (Lazzaro et al., 1991; Zannini et al., 1997; Postiglione et al., 2002; Nilsson and Fagman, 2013; Szinnai, 2014a).

In humans, terminal differentiation of the thyroid is completed at 11 GW and is characterized by the onset of follicle formation and thyroid hormone synthesis. The three growth stages representing the structural differentiation of the human thyroid gland histologically are precolloid, a beginning colloid and a follicular growth stage has been described in a historical landmark paper by Shepard et al. (Shepard et al., 1964). From 7 to 9 GW in embryos, the precolloid stage is found characterized by compact unpolarized TFC precursors. From 10 to 11 GW, the beginning colloid stage is characterized by the appearance of small follicles formed by polarizing TFCs. From 12 GW on, progressive follicular growth occurs (Shepard et al., 1964). From the autoradiographic studies, iodide accumulation and thyroid hormone synthesis occurs during the beginning colloid stage in fetal thyroid (Shepard, 1967; Olin et al., 1970). T4 in the fetal thyroid gland is present from GW 11 (Szinnai et al., 2007) and in fetal

blood from GW 12 on (Thorpe-Beeston et al., 1991). The onset of iodide uptake in fetal thyroid occurs at GW 11 as observed by accidental radioablation of the fetal thyroid in pregnant women exposed to radioactive iodide during the first trimester. The molecular mechanisms underlying the onset of human thyroid function remained largely unknown (Szinnai et al., 2007).

The human and mouse data suggest that the structural and functional differentiation are interdependently linked. The expression patterns of the transcription factors PAX8, NKX2-1 and FOXE1 in the human embryo are described by Trueba et al. (Trueba et al., 2005), the sequence of expression of functional proteins involved in thyroid hormone synthesis in the human thyroid during differentiation are then shown by Szinnai et al. (Szinnai et al., 2007). Mouse data indicating the precise timing of expression of thyroid specific gene necessary for thyroid hormone synthesis suggests a genetic mechanism may be responsible for such a control (De Felice and Di Lauro, 2004).

1.3. Thyroid dysgenesis- abnormal thyroid development

1.3.1 Thyroid dysgenesis causes congenital hypothyroidism

Congenital hypothyroidism (CH) is defined as the deficiency of thyroid hormones at birth or postnatally. Thyroid hormone deficiency at birth is mostly caused either by disorder in thyroid gland development (dysgenesis; 80-85% of all cases) or a defect in thyroid hormone biosynthesis (dyshormonogenesis; 10-15% of all cases) (Park and Chatterjee, 2005; Rastogi and La Franchi, 2010; Szinnai, 2014a).

The most common signs of CH are umbilical hernia, macroglossia, mottled skin, persistent jaundice, wide posterior fontanel and poor feeding (Figure 4). A few infants with CH may have a palpable goiter due to TDHG (Grant et al., 1992). Symptoms of CH in the newborns include quiet newborns, may sleep longer than normal, hoarse cry, constipation and hyperbilirubinemia for more than 3 weeks (Rastogi and La Franchi, 2010).

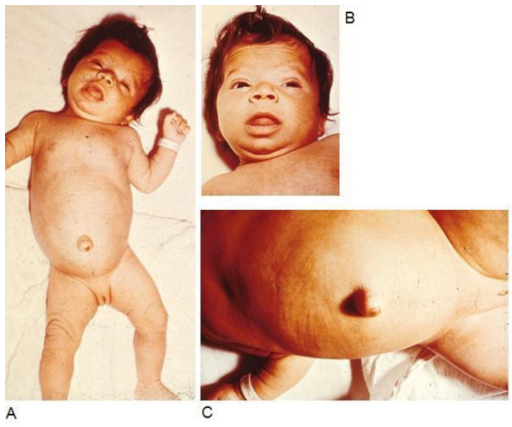

Figure 4: Signs of congenital hypothyroidism. A - 3 months old hypothyroid infant with untreated CH shows hypotonic posture, wide posterior fontanelle, myxedematous facies, macroglossia, and umbilical hernia. B – Magnified image of the same patient with myxedematous facies, macroglossia, and mottled skin. C - Same patient with abdominal distension and umbilical hernia.

Taken from Rastogi, 2010.

TD includes a spectrum of defects in development of the thyroid gland: thyroid agenesis, ectopy or athyreosis, thyroid hypoplasia and pretracheal thyroid without function (Figure 5). Agenesis occurs in 20-30% of TD cases, due to defect in survival of TFC precursors. Thyroid ectopy involves sublingually located thyroid and occurs in 50-60% of TD cases, due to defect in migration of thyroid anlage. Thyroid hypoplasia occurs in 5% of TD cases. Further, normally located thyroid without function are the mildest form of TD (10%) (Devos et al., 1999; Brown and Demmer, 2002; Rastogi and La Franchi, 2010; Szinnai, 2014a). The specific form of TD is dependent at what stage of thyroid development the physiological process is disrupted (Figure 5).

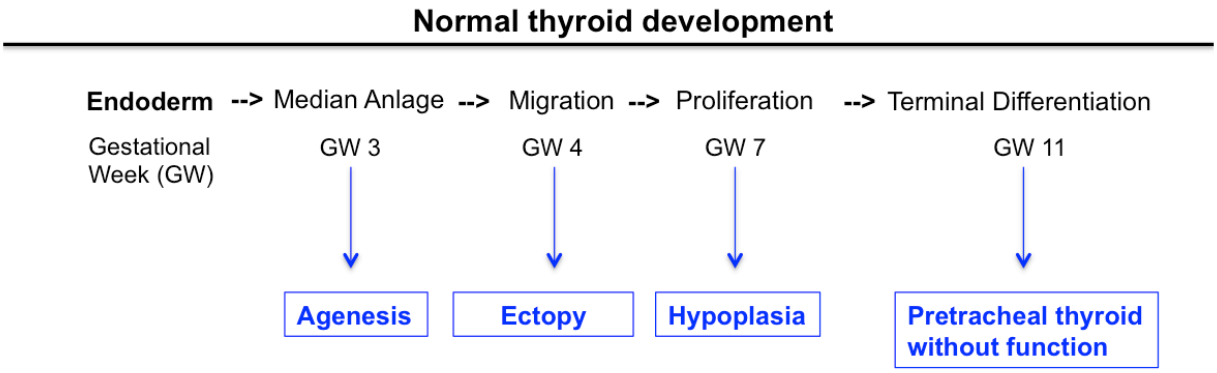

Figure 5: Sequence of processes during normal thyroid development and specific forms of thyroid dysgenesis resulting from disrupted development at defined time points.

TD is typically a sporadic disorder, however recent evidence suggests the involvement of genetic component. Of all the cases of TD, one study found that 2% were familial in occurrence (Castanet et al., 2000). Thus, the underlying cause in most of the cases still remains unknown. Mutational screening of cohort of TD patients and phenotypes from

transgenic mouse models has identified mutations in genes that are involved during thyroid development. These include *TSHR*, *PAX8*, *FOXE1 NKX2-1*, and *TBX21* (Figure 6). These genes encode for transcription factors that are expressed during thyroid development and in the normal functioning of adult thyroid. Mutations in these genes are found only in a small percentage of TD patients (Sunthornthepvarakul et al., 1995; Abramowicz et al., 1997; Clifton-Bligh et al., 1998; Macchia et al., 1998; Vilain et al., 2001; Krude et al., 2002; Pohlenz et al., 2002; De Felice and Di Lauro, 2004; Dentice et al., 2006; Moya et al., 2006; Al Taji et al., 2007; Ferrara et al., 2008).

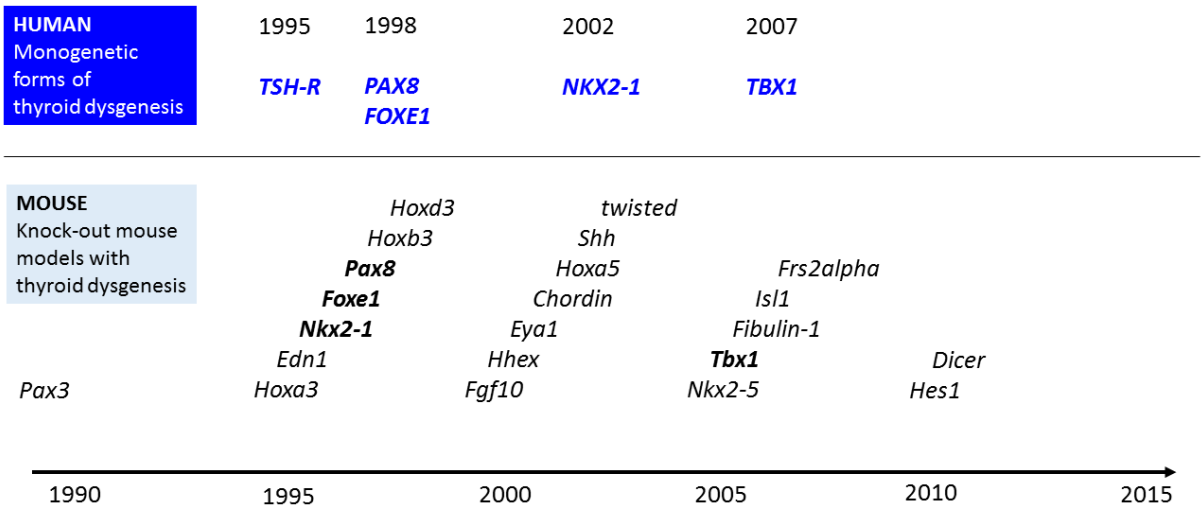

Figure 6: Sequence of genes identified in normal thyroid development in human and mouse and their specific time points of identification.

1.3.2 Thyroid dyshormonogenesis

Genetic defects in each of the various steps involved in the biosynthesis of THs are the cause of CH due to thyroid dyshormonogenesis (TDHG). These include defects in iodide transport due to mutations in sodium iodide symporter gene (*NIS* or *SLC5A5*) (Stanbury and Chapman, 1960; Fujiwara et al., 1997), partial defects in the organification of iodide (PIOD) leading to Pendred syndrome (PDS) (Morgans and Trotter, 1958; Everett et al., 1997; Kopp and Bizhanova, 2011), defects in iodination and coupling of tyrosyl moieties due to mutations in thyroid peroxidase (*TPO*) gene (Avbelj et al., 2007), mutations in the gene encoding *DUOX2* (Knobel and Medeiros-Neto, 2003; Grasberger, 2010; Fugazzola et al., 2013) and in the gene encoding for the dual oxidase maturation factor 2 (*DUOXA2*) (Zamproni et al., 2008) leads to dyshormonogenesis due to H_2O_2 deficiency, inactivating mutations of the *TG* gene causes defects in thyroglobulin synthesis (Rivolta et al., 2005; Targovnik et al., 2010), and mutations

in iodotyrosine deiodinase (*DEHAL1*, *IYD*) leads to iodotyrosine deiodinase deficiency associated with defective intrathyroidal iodide recycling and excessive blood and urinary secretion of MIT and DIT (Moreno et al., 2008).

1.3.3 Insights from transgenic mouse models

Pax8

Gene encoding Pax8 (mouse *Pax8* and human *PAX8*) is located on chromosome 2 (Plachov et al., 1990; Stapleton et al., 1993). It is expressed in the thyroid, kidney and in the myelencephalon (Plachov et al., 1990). It binds to the specific DNA sequences in the promoter region of Tg, Tpo and Nis and is detected at E8.5 in the developing murine thyroid. Its expression is maintained in TFCs during all the stages of thyroid development and in adult thyroid (De Felice and Di Lauro, 2004).

Heterozygous $Pax8^{+/-}$ mice show no phenotype, whereas homozygous $Pax8^{-/-}$ mice show growth retardation and die within 2–3 weeks. In $Pax8^{-/-}$ mice, the thyroid gland shows neither follicle formation nor TFCs and is composed only of C-cells. These mice die due to hypothyroidism and administration of T4 helps them to survive. At E12.5 in *Pax8* null embryos, the TFCs are absent after normal budding and migration process. Thus, Pax8 is necessary for thyroid precursor cell survival and for thyroid development and functional differentiation (Plachov et al., 1990; Mansouri et al., 1998; Magliano et al., 2000; Fernández et al., 2015).

Heterozygous mutations in *PAX8* cause athyreosis or thyroid hypoplasia. Since *PAX8* is also expressed in the mesonephros and ureteric buds, there are cases of genitourinary malformations in patients with CH (Kumar et al., 2009).

Foxe1

Gene encoding Foxe1 is located on chromosome 4 in mouse (Zannini et al., 1997) and on chromosome 9 in humans (Chadwick et al., 1997). It recognizes a DNA sequence present on both Tg and Tpo promoters under hormone stimulation (Civitareale et al., 1989) and is expressed in the developing thyroid, tongue, epiglottis, esophagus and palate (Dathan et al., 2002).

$Foxe1^{-/-}$ mice show either athyreosis or an ectopic thyroid, elevated TSH levels and die within

first 2 days of birth. In these mice, thyroid budding occurs normally, however thyroid migration is not initiated. These non-migrating cells differentiate and synthesize Tg. Thus, Foxe1 is essential for migration and survival of TFC precursors (Zannini et al., 1997; De Felice et al., 1998; Fernández et al., 2015).

Patients born with a homozygous missense mutation in *FOXE1* causes a Bamforth-Lazarus Syndrome of CH characterized by thyroid dysgenesis (mostly athyreosis), bifid epiglottis, choanal atresia, cleft palate, spiky hair and with or without facial dysmorphism and porencephaly (Clifton-Bligh et al., 1998; Castanet et al., 2002; Vieira et al., 2005).

Nkx2-1

Nkx2-1 belongs to the Nkx2 family of transcription factors (Price et al., 1992) and was identified as nuclear protein able to bind the specific DNA sequences in the promoter region of *Tg* (Guazzi et al., 1990) and enhancer region of *TPO* (Mizuno et al., 1991). Mouse *Nkx2-1* is located on chromosome 12, whereas the human NKX2-1 is on 14q13 (Civitareale et al., 1989; Guazzi et al., 1990; De Felice and Di Lauro, 2004). *Nkx2-1* is expressed in the precursors and differentiated TFCs and C-cells (Suzuki, 1998), adult thyroid, lung epithelium, posterior pituitary and in the forebrain.

Nkx2-1$^{-/-}$ mice show athyreosis with absence of TFCs and C-cells, impaired lung morphogenesis, lack of pituitary, alteration in the forebrain and death at birth (Kimura et al., 1996). At E11 in *Nkx2-1*$^{-/-}$ embryos, no thyroid cells are detectable. This data and the presence of apoptotic cells suggest that *Nkx2-1* is necessary to prevent the initiation of apoptosis (Kimura et al., 1999). *Nkx2-1*$^{+/-}$ mice have normal thyroid size, but showed decreased coordination and mild hyperthyrotropinemia. Disturbed follicular architecture and function is seen in adult thyroid of the conditional knockout mice (Kusakabe et al., 2006a; Fernández et al., 2015).

Mutations in *NKX2-1* causes brain-lung-thyroid syndrome characterized by congenital hypothyroidism, infant respiratory distress syndrome (IRDS), ataxia and benign chorea (Krude et al., 2002; Willemsen et al., 2005; Moya et al., 2006).

Hhex

Gene encoding Hhex (Hematopoietically expressed homeobox) is located on chromosome 19 in mouse (Ghosh et al., 1999) and on chromosome 10 in humans (Hromas et al., 1993). Hhex

is expressed in the primitive endoderm and from E8.5 onwards in the primordium of thyroid, thymus, pancreas, liver, foregut and lungs. Hhex is highly expressed in developing and adult thyroid (Thomas et al., 1998; Bogue et al., 2000).

Hhex$^{-/-}$ mice show severe defects during the development of the liver, the thyroid, the forebrain and the heart. In thyroid, Hhex is an early marker of thyroid cells and is essential for thyroid morphogenesis as observed in *Hhex*$^{-/-}$ embryos where the development of the thyroid is arrested at the thyroid bud stage at E9.5 (Barbera et al., 2000).

Hes1

Hes1 encodes for a basic Helix-Loop-Helix (bHLH) transcriptional repressor regulated by the Notch pathway (Kageyama et al., 2007). It regulates the morphogenesis of various tissues by maintaining the undifferentiated progenitor state by negatively regulating bHLH transcription factors such as Mash1 in the nervous system and Ngn3 in the pancreas. Hes1 was detected from E9.5 onwards in the median anlage, and at E11.5 in the ultimobranchial bodies during normal mouse thyroid development (Carré et al., 2011).

Hes1$^{-/-}$ mice embryos showed severe neuronal developmental defects and pancreatic hypoplasia (Ishibashi et al., 1995; Murata et al., 2005). Furthermore, thyroid hypoplasia and abnormal fusion of the thyroid anlagen is observed in *Hes1*$^{-/-}$ mutants (Carré *et al.*, 2011). It is shown that *Hes1* regulates the number of progenitors of thyrocytes and C-cells present in both thyroid anlagen and is involved in determining the normal size of the thyroid gland. Reduced endocrine thyroid function in both, the thyrocytes and the C-cells was observed, as demonstrated by a profound decrease in both T4 and calcitonin positive surface areas. Thus, they have shown that *Hes1* is crucial for normal mouse thyroid organogenesis as it assures the proper fusion of the thyroid anlagen.

Tshr

Gene encoding Tshr is located on chromosome 12 in mouse (Taylor et al., 1996) and on chromosome 14 in humans (Libert et al., 1990) and encodes for a G protein coupled receptors (Parmentier et al., 1989). Expression of Tshr is seen in TFCs from E15.5 in mouse and is profoundly upregulated by E17-E18. The expression pattern of Tshr mRNA is coincident with the completion of migration process, up-regulation of thyroid specific genes, beginning of

colloid formation and folliculogenesis (Vassart and Dumont, 1992; Postiglione et al., 2002). Thyroid hypoplasia with severe hypothyroidism in adult thyroid is seen in *Tshr*$^{hyt/hyt}$ mice, which is characterized by a spontaneous loss-of-function mutation in Tshr gene, and in *Tshr*$^{-/-}$ mice. Expression of Tpo and Nis is down regulated, but Tg expression is slightly decreased in these mice (Stein et al., 1994; Marians et al., 2002).

Mutations in the *TSHR* result in resistance to TSH, which causes a reduction in thyroid hormone production, athyreosis or thyroid hypoplasia and normal thyroid with severe hypothyroidism (Sunthornthepvarakul et al., 1995; Refetoff, 2003). Loss-of-function mutations in the *TSHR* gene are inherited in an autosomal dominant way and lead to euthyroid hyperthyrotropinemia and severe CH (Refetoff, 2003; Beck-Peccoz et al., 2006).

1.3.4 Alternative mechanisms for TD

TD cases due to mutations in *NKX2.1*, *PAX8*, *TSHR*, *FOXE1* and *NKX2-5* are very few. Genetic linkage analysis of these genes showed no significant LOD (logarithm (base 10) of odds) scores in a large cohort of multiplex families. Therefore, other mechanisms are suggested for the vast majority of TD cases (Clifton-Bligh et al., 1998; Macchia et al., 1998; Castanet et al., 2002; Castanet et al., 2005; Al Taji et al., 2007; Narumi et al., 2010).

Multigenic origin of TD

The evidence for the multigenic origin of TD in mice has been provided by Amendola et. al (Amendola, 2005). Pax8 and Nkx2-1 double heterozygous mice (Pax8$^{+/-}$Nkx2-1$^{+/-}$) exhibited severe TD with thyroid hypoplasia and hemiagenesis, while both single heterozygous mice had no TD phenotype (Amendola et al., 2005).

In humans, multiple loci responsible for the pathogenesis of TD have been suggested. Few patients with digenic origin of TD are reported. Mutations in *TSHR* in combination with mutations in *DUOX2* (Narumi et al., 2011a), *TPO* (Sriphrapradang et al., 2011) and *GNAS* (Lado-Abeal et al., 2011) have been shown. One case with mutation in *PAX8* and *NKX2.5* has been shown (Hermanns et al., 2011). However, no TD cases with digenic defects were identified in either a cohort of 170 Czech patients with TD (Al Taji et al., 2007) screened for all known genetic aberrations in genes encoding for PAX8, NKX2.1, FOXE1, NKX2.5, HHEX and TSHR. Only one patient has exhibited digenic cause of TD from the cohort of 102 Japanese patients with CH (Narumi et al., 2010). This suggests that genes that are not

associated with TD might be responsible for the pathogenesis of TD.

Early somatic mutations

Somatic mutations are recently shown to cause congenital neurological disease (Poduri et al., 2013). Somatic loss-of-function mutation has to occur very early during the developmental process in the common ancestral cell of all the cells committed to the thyroid fate to lead to a phenotype (Deladoëy et al., 2007). Until now, a somatic heterozygous mutation in *PAX8* has been reported in a female patient and her two siblings having TD due to a germ line mutation in *PAX8* (Narumi et al., 2011b). The patient had normal thyroid function but underwent hemithyroidectomy due to a thyroid adenoma. Histological analysis of the patient's thyroid revealed adenoma tissue, embryonic thyroid tissue in the follicular growth stage and normal thyroid tissue. Since somatic mutation was only observed in tissue with embryonic features and not in normal or adenoma tissue, it indicates the existence of early somatic mutations. Apart from thyroid, *PAX8* mutation was also observed in lymphocytes and nails that are derived from mesoderm and ectoderm respectively, suggesting its early occurrence during embryogenesis (Narumi et al., 2011b).

Copy number variations

Recently, an increasing number of copy number variations (CNVs) associated with congenital human diseases have been reported (Erdogan et al., 2008; Hitz et al., 2012; Southard et al., 2012). To determine the role of CNVs in the etiology of TD, Thorwarth et al. have screened 80 TD patients and two pairs of discordant monozygotic twins (Thorwarth et al., 2010). Of all patients screened, 8.75% of the patients with athyreosis and hypoplasia had shown potential nonrecurrent CNVs, six duplications and four deletions. However, no CNV encompassed genes known to be involved in thyroid morphogenesis. No differences in CNVs between the affected and the healthy twins were found in the two pairs of monozygotic twins discordant for TD. In another study by Abu-Khudir (Abu-Khudir et al., 2010), CNVs were assessed in three human ectopic thyroid tissues in combination with gene expression analysis. Though the gene expression studies showed differences in normal and ectopic thyroids, these differences were independent of the identified thyroid specific CNVs. Thus, high frequencies of CNVs in screened TD patients suggest the involvement of CNVs in the pathogenesis of TD. However, lack of recurrence, absence of differences in CNVs in monozygotic discordant twins and lack of gene expression dependence on CNVs in ectopic thyroid tissues suggests that CNVs do not play a major role in the pathogenesis of TD (Abu-Khudir et al., 2010).

Epigenetic mechanisms

Apart from monogenic, multigenic, somatic mutations and CNVs, epigenetic mechanisms such as DNA methylation and histone modifications might play a role in the pathogenesis of TD. High discordance rate (92%) between the monozygotic twins and the non-Mendelian mechanisms that are consistent with the sporadic occurrence of TD in majority of the cases (98%) strongly suggests that epigenetic mechanisms need to be investigated to confirm their involvement in TD (Perry et al., 2002; Vassart and Dumont, 2005; Deladoëy et al., 2007). Epigenetic mechanisms involving aberrant modifications by histone acetylation or methylation have been shown to change gene expression in thyroid cancer cells (Kondo et al., 2008; Russo et al., 2011). Their role in TD remains unknown.

1.4. Epigenetic regulation during embryonic development

1.4.1 Definition of epigenetics

Conrad Waddington coined the term "Epigenetics" in 1940 and defined it as the study of causal interactions between genes and their products that bring the phenotype into being. The definition of epigenetics has changed over the years and currently is defined as the study of mitotically and/or meiotically heritable changes in gene function that do not undergo a change in DNA sequence (Dupont et al., 2009). The basic building block of chromatin is the nucleosome. 146-147 base pairs of DNA wraps around a histone octamer that is composed of one (H3–H4) tetramer capped by two H2A–H2B dimers and each octamer is linked to other by the linker histone H1. This forms the nucleosome (Luger, 1997). Modifications of DNA and histones alter the accessibility of DNA to transcription machinery and therefore influence gene activity and expression (Jaenisch and Bird, 2003; Grewal and Moazed, 2003; Reik, 2007).

1.4.2 Different forms of epigenetic regulation

DNA methylation

DNA methylation involves covalent addition of a methyl group to cytosine bases and occurs mainly on CpG islands. DNA methylation is initiated (de novo methylation) and maintained by the enzymatic activity of the DNA methyltransferases (DNMTs) (Goll and Bestor, 2005).

DNMT enzymes DNMT3A and DNMT3B set up a new methylation pattern on the unmodified DNA molecules during development and hence are called as de novo DNMTs (Okano, 1999). The promoter regions of silenced genes possess significantly more methylated cytosines as compared with actively transcribed genes. Thus, the canonical function of DNA methylation is to mediate transcriptional repression at promoter elements (Reddington et al., 2013).

MicroRNAs

Recently, MicroRNAs (miRNAs) have been established as important mediators of gene regulation. Endogenous miRNAs have been shown to play an important role in developmental processes, including differentiation, proliferation, and apoptosis (Ambros, 2004) and regulate expression at posttranscriptional level. Further, it has been shown that during embryonic development, miRNA expression is tissue specific, which implicates that they are important to establish and maintain cell type and tissue identity (Giraldez et al., 2005; Wienholds et al., 2005; Zhang et al., 2015).

Histone modifications and histone code

The flexible N-terminal tail of histones undergoes several post-translational modifications, such as acetylation, methylation, phosphorylation, ubiquitylation, sumoylation, ADP ribosylation, glycosylation and carbonylation (Bernstein et al., 2007; Kouzarides, 2007; Kurdistani, 2007). Histone acetylases (HATs), histone deacetylases (HDACs), histone methyltransferases (HMTs) and histone demethylases are few examples of enzymes responsible for histone modifications. The highly dynamic changes in the chromatin structure takes place during many fundamental cellular processes, like gene transcription, DNA replication or DNA damage. The type and position of modification over histone residue determines the chromatin state as euchromatic or heterochromatic. The ‘histone code’ hypothesis states that a combination of various modifications over histone residues allows the gene expression status to interchangeably switch between on and off and regulate chromatin structure (Strahl and Allis, 2000; Jenuwein and Allis, 2001; Margueron et al., 2005).

1.4.3 Histone acetylation

Histone proteins have N- and/or C-terminal tails that extend out from the core surface and undergo various post-translational modifications, such as acetylation, methylation,

phosphorylation, ubiquitination, and sumoylation. These post-translational modifications of the residues on the histone tails make them an important switch points for chromatin condensation or decondensation, thus altering their interactions with DNA and nuclear proteins. Out of all the histone H2A, H2B, H3 and H4 tails, the histone H3 N-terminal tail is the most extensively studied and modifications on residues K4, K9, and K27 have the most significant effect on transcriptional regulation (Figure 7). K4, K9 and K27 can be methylated and acetylated (Strahl and Allis, 2000).

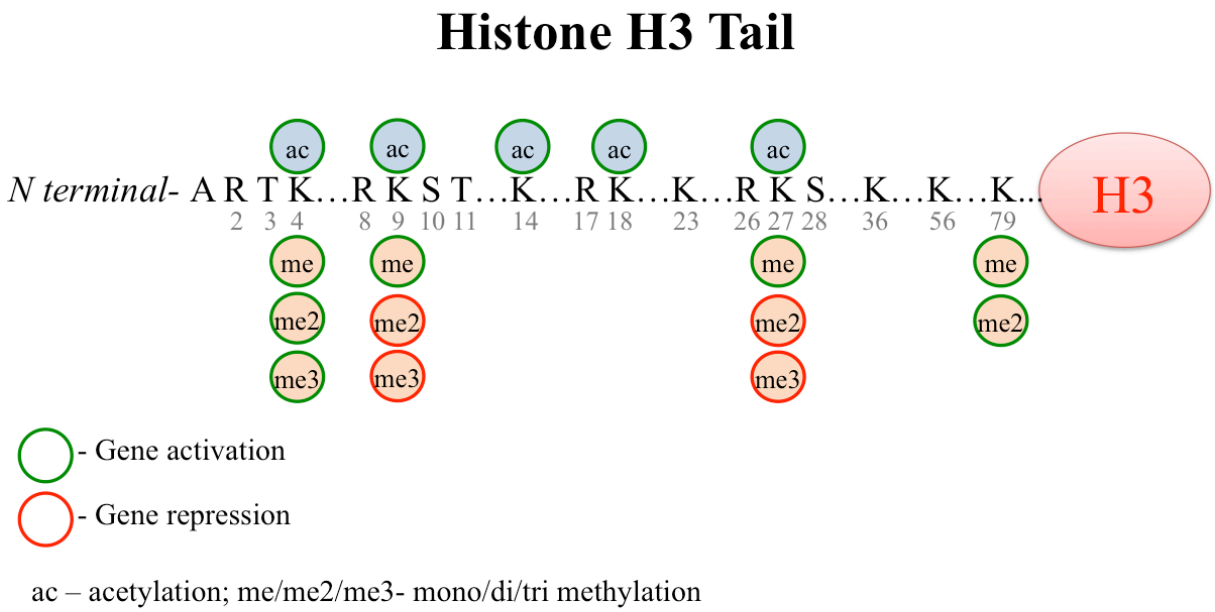

Figure 7. Schematic diagram of the covalent post-translational modifications of histone H3 N-terminal tail. The different modifications are indicated (ac, acetylation; me/me/me3 as mono/di/tri-methylation, with green and red indicating marks that are associated with activation and repression, respectively.

Sanjay Gawade, Unpublished data.

Acetylation of histones on lysine residues is a dynamic reversible process controlled by histone deacetylases (HDACs) and histone acetyltransferases (HATs) (Figure 8). The balance between these two processes together with other proteins and DNA modifications such as DNA methylation regulates chromatin accessibility and gene expression. HATs regulate gene activation by adding acetyl groups to the histones that leads to a change in the net positive charge of histone tails causing chromatin relaxation (Chen et al., 2001; Roth et al., 2001; Xu et al., 2007). HDACs regulate gene silencing by removing acetyl groups from histones and thus interact more closely with the DNA causing chromatin condensation (Roth and Allis, 1996; Svaren and Hörz, 1993). HDACs also deacetylate non-histone proteins, such as

transcription factors like E2F1 (Martinez-Balbas et al., 2000), p53 (Luo et al., 2000) and the cytoskeletal protein tubulin (Hubbert et al., 2002; Glozak et al., 2005).

In humans, 18 HDACs have been identified and are divided into four classes based on their homology to yeast HDACs, their subcellular localization and their enzymatic activities (Thiagalingam et al., 2003):

A) The class I HDACs (HDAC1, HDAC2, HDAC3 and HDAC8) has homology to the yeast RPD3 protein and can generally be detected in the nucleus.
B) Class II HDACs (HDAC4, HDAC5, HDAC6, HDAC7, HDAC9 and HDAC10) have homology to the yeast Hda proteins and can be detected in nucleus and the cytoplasm.
C) The class III HDACs, also called as Sirtuins (SIRTl, 2, 3, 4, 5, 6 and 7) are homologues of the yeast protein Sir2 and require NAD+ for their activity.
D) HDAC11 is the sole member of class IV HDACs.

HDACs contain zinc in their catalytic site and are inhibited by drugs such as trichostatin A (TSA) and vorinostat [suberoylanilide hydroxamic acid (SAHA)] except sirtuins, which do not contain zinc in their catalytic site and are not inhibited by either TSA or vorinostat (Grozinger and Schreiber, 2002; Dokmanovic et al., 2007; Marks and Xu, 2009). Drugs like TSA and SAHA are part of histone deacetylase inhibitors (HDACi) as they inhibit the action of HDACs. HDAC knockout mice studies have provided highly specific information about the functions of individual HDACs in development and disease (Table 2).

HATs and HDACs play a very vital role in developmental processes and normal physiology, and their deregulation is linked to disease states. Deletion of each member of the class I HDAC family leads to lethality, indicating a unique role of each HDAC in development (Haberland et al., 2009a). Typically HDACs are present within multi-subunit protein complexes together with other components that determine HDAC target gene specificity due to the interactions with sequence-specific DNA-binding proteins (Cunliffe 2008; Yang and Seto, 2008). These complexes may be made up of one or more HDACs. Without binding to DNA directly, HDACs are part of multi protein complexes that include co-repressors and coactivators, which interact with DNA (Xu et al, 2007). Class I HDACs are found in repressive complexes known as the Sin3, NuRD, CoREST and NCoR/SMRT complexes (Yang and Seto, 2008).

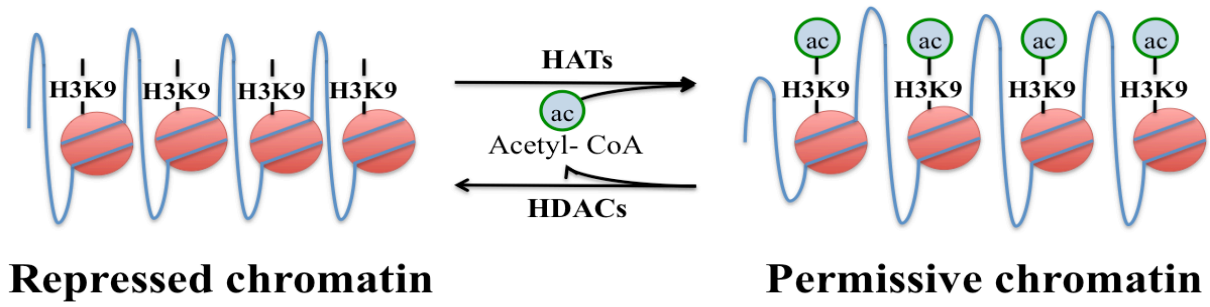

Figure 8. Schematic of the reversible histone acetylation changes in chromatin organization. HATs- Histone acetyl transferases, HDACs- Histone deacetylases. Acetyl residues from acetyl-CoA are added by HATs on lysine residues of the histone tails that results in active chromatin, whereas removal of acetyl residues by HDACs results in repressed chromatin.

Sanjay Gawade, Unpublished data.

Table 2: Classification of histone deacetylase (HDAC) superfamily, time point of lethality of the knockouts and loss-of-function phenotypes in mice.
(E- embryonic day; P- days postnatal)

Adapted from Haberland et al. (Haberland et al., 2008).

Class	HDACs	Time of lethality	Phenotype
Class I	HDAC1	E10.5	Proliferative defects (Lagger et al., 2002)
	HDAC2	P1	Cardiac malformations (Trivedi et al., 2007)
	HDAC3	E9.5	Gastrulation defects (Bhaskara et al., 2008)
	HDAC8	P1	Craniofacial defects (Haberland et al., 2009b)
Class IIa	HDAC4	P7-P14	Chondrocyte differentiation defect in growth plate (Vega et al., 2004)
	HDAC5	Viable	Exacerbate cardiac hypertrophy after stress (Chang et al., 2004)
	HDAC7	E11	Endothelial dysfunction (Chang et al., 2006)
	HDAC9	Viable	Exacerbate cardiac hypertrophy after stress (Zhang et al., 2002)

Class IIb	HDAC6	Viable	Increased tubulin acetylation (Zhang et al., 2009)
	HDAC10	Not determined	-
Class IV	HDAC11	Not determined	-

1.4.4 Epigenetic regulation by histone deacetylases during development and function

Class I members HDAC1 and HDAC2 are highly homologous (Tsai and Seto, 2002). Murine genes *Hdac1* and *Hdac2* are closely related and encode two enzymes with high sequence similarity (Khier et al., 1999). Global knockout of HDAC1 is lethal at E10.5 and embryos show growth retardation, disturbed head formation and proliferative defects (Lagger et al., 2002; Montgomery et al., 2007). Global knockout of HDAC2 is lethal at postnatal day 1 and shows cardiac malformations (Montgomery et al., 2007; Trivedi et al., 2007). Class I HDACs seem to play a primary role in cell survival and proliferation based on selective gene knockout studies, whereas class II HDACs have tissue specific roles (Lagger et al., 2002; Marks and Xu, 2009). HDAC1 and HDAC2 are involved in various developmental processes like neurogenesis, myogenesis, haematopoiesis and epithelial cell differentiation (Brunmeir et al., 2009). HDAC inhibitors (HDACi) are being used in various tissue culture models to investigate the role of HDACs for development and differentiation in various organs. *Ex vivo* studies on mouse intestine showed that class I HDACs are confined to the prospective epithelium. The levels of class I HDACs decline coincidently with the activation of differentiation genes. HDAC inhibitors activated the same genes prematurely and caused accelerated cytodifferentiation. Overexpression of HDAC1 and HDAC2 in these *ex vivo* cultures reversed expression of certain maturation markers (Tou et al., 2004). *Ex vivo* studies on rat pancreas showed modification in cell fate of pancreatic progenitor cells in endocrine and exocrine differentiation in the presence of HDACi (Haumaitre et al., 2008).

1.4.5 Role of epigenetic regulation for normal thyroid development and in thyroid dysgenesis

As stated before, the following arguments suggests a role of epigenetic regulation of thyroid development; a) Very low identified monogenetic forms of TD, b) Discordance of monozygotic twins for TD, c) Epigenetic changes during thyroid carcinogenesis. However, information on the role of epigenetic regulation for thyroid development by using knockout mice models has never been described.

Abu-Khudir et al assessed the role of altered DNA methylation profiles in the pathogenesis of TD by comparing ectopic thyroid tissue from TD patients with euthyroid tissues (Abu-Khudir et al., 2010). No difference in promoter and CpG island methylation profiles between the two tissues was observed. Also, correlation between the global DNA methylation profile and the differential expression in the tissues revealed no difference. However, clusters of genes that are repressed in ectopic tissues, involved genes incorporated in histone modifications. Therefore, role of differential histone modifications in the observed differential gene expression in ectopic thyroids cannot be excluded (Abu-Khudir et al., 2010).

2. AIM OF THE THESIS

The aim of this thesis work is to address the following unsolved questions in the context of molecular mechanisms of normal and abnormal thyroid development:

Aim of Project 1: A new tool for thyroid research: Flow cytometry of the thyroid gland

The thyroid is composed of endocrine epithelial cells, blood vessels and mesenchyme. Fluorescence-activated cell sorting (FACS) provides a tool for quantification of distinct cell populations. However, in the absence of an established tissue-specific protocol, no data exist on absolute cell numbers, relative distribution, and proliferation of the different cell populations in the developing and mature thyroid.

The aim of this project was to identify and quantify various cell populations in developing and adult mouse thyroids by establishing a new flow cytometry protocol.

Aim of Project 2: A new hypothesis: Epigenetic regulation of thyroid development

In the differentiating tissues, reversible histone acetylation represents a major epigenetic mechanism regulating gene expression. Acetylation of core histones is regulated by histone deacetylases and histone acetyltransferases in a reciprocal way.

Abnormal thyroid development results in TD. Several observations from clinics and biology suggest epigenetic regulation of thyroid development: 1) Discordance of monozygotic twins for TD, 2) disrupted histone acetylation in thyroid cancer being associated with loss of differentiation markers, and 3) pathologic development of organs after genetic deletion or pharmacological inhibition of histone deacetylases (HDAC).

The aim of this study was to analyze the role of HDACs and of histone acetylation for regulation of normal thyroid development.

3. MATERIALS AND METHODS

3.1 Mice

Wild type, outbred, male and female Swiss albino mice were obtained from Janvier Labs, Saint Berthevin Cedex, France and were used for all the experiments. All experiments were performed in accordance with the federal regulations.

3.2 Thyroid culture, HDACi / HATi treatments inhibition of angiogenesis

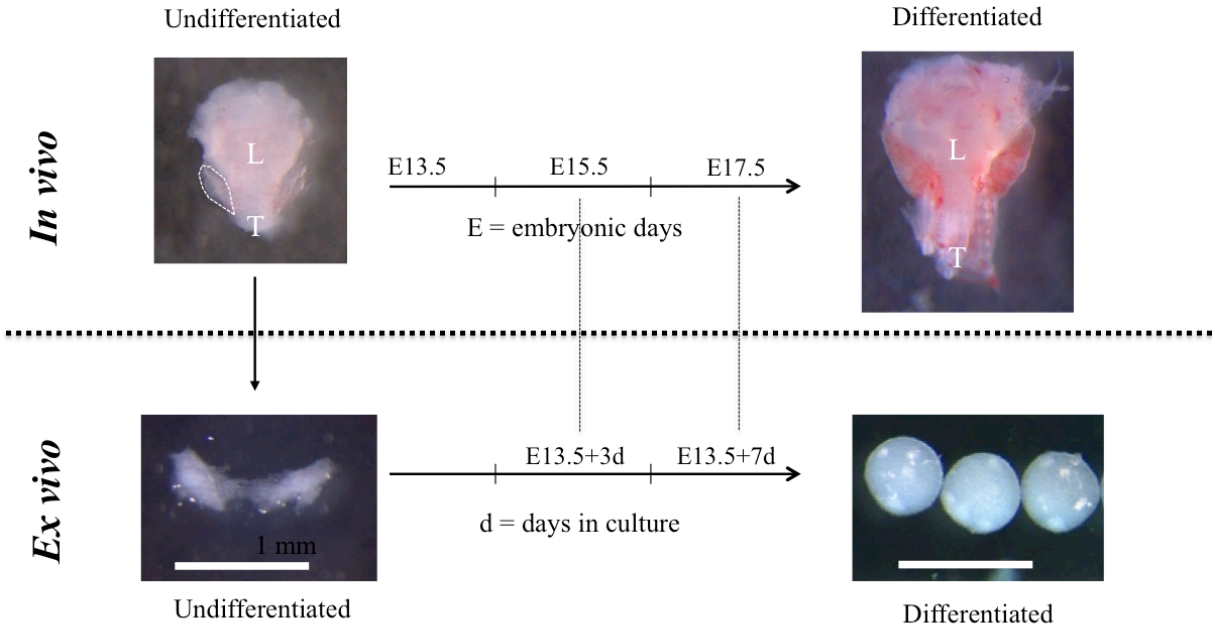

Figure 9. Murine thyroid culture model. *In vivo*, undifferentiated E13.5 mouse thyroid starts to undergo differentiation and angiogenesis. At E15.5, onset of thyroid follicle formation takes place and at E17.5 the thyroid is terminally differentiated. The *ex vivo* thyroid explant culture model recapitulates the developmental stages *in vivo*. E13.5 thyroids from mice are micro-dissected and cultured at air-surface medium for 3 days (E13.5+3d) that represents E15.5 *in vivo* and 7 days (E13.5+7d) that represents E17.5 *in vivo*.

After dissecting the E13.5 thyroids from the embryos, these were laid on 0.45 uM filters (Millipore) at the air-medium interface in petri dishes containing IMDM with 25 mM HEPES, 10% fetal calf serum, L-glutamine, Kanamycyin and 2 Mercaptoethanol 50 mM (Figure 9). Two thyroids were places together to form one thyroid explant. Thyroid stimulating hormone (TSH) was added to the culture medium to a final concentration of 100uU/ml. The explants were maintained at 37°C in humidified 95% air-10% CO_2 for 3 days (E13.5+3d) or 7 days (E13.5+7d). The medium and TSH were changed after every 48 h.

Explants were cultured in the presence of Histone deacetylase inhibitor (HDACi) Valproic acid (VPA- Sigma) or absence of VPA (Control). The optimal concentrations of VPA was decided by testing increasing doses of VPA (from 0.5 mM to 1.5 mM). VPA 1 mM was chosen for all the experiments as these concentrations led to phenotypic effects without any toxic effects. Untreated explants were used as control.

To check the effect of inhibition of angiogenesis during thyroid development, thyroid explants were treated with angiogenesis inhibitor Sunitinib 1uM (Selleckchem, USA) for 3 and 7 days.

3.3 Morphometric analysis

For the analysis of thyroid explant size and total number of thyroid follicles, cryosections of the explants were stained with Hematoxylin and Erythrosin B (HE). Thyroid explants were embedded in OCT (CellPath, Mid Wales, UK) using isopentane cooled in dry ice and stored at -80^{0}C at the end of 3 and 7 days. 10um thick cryosections were sliced in a Leica CM 3050 cryostat (Leica instruments GmbH, Nussloch, Germany), collected on SuperFrost-plus microscope slides and stored at -80^{0}C until use. For HE staining, slides were first air dried for 1 h at room temperature (RT). Tissue sections were fixed with 4% paraformaldehyde (PFA) at RT and washed with PBS. Sections were stained with Hematoxylin for 5 mins at RT and washed with lukewarm running tap water for 5 mins. Next, slides were counterstained with Erythrosin B for 5 mins at RT and washed in distilled water followed by serial washes with 70%, 95% and 100% ethanol. Slides were then mounted with entellan mounting medium (Merck KGaA, Darmstadt, Germany) and observed under Nikon Eclipse E600. At least 2 sections of each culture were photographed and further analyzed by ImageJ (version 1.45s, NIH, USA).

3.4 Immunohistochemistry

Immunohistochemistry was performed on frozen sections. Antibodies against NKX2-1 (clone 8G7G3/1, mouse monoclonal) was obtained from Dako, PECAM (390, rat monoclonal) from Biolegend, and Histone H3K9 acetyl, H3K9 tri methyl, HDAC1 from Abcam. Cryosections of thyroid explants were air dried for 30 mins before fixing with 4% PFA for 10 mins at RT. Slides were washed 3 times with PBS. Antigen retrieval was performed using 10mM sodium citrate (pH 6.0) with 0.05% Tween-20 in a pressure cooker for 5 mins at 120^{0}C. Once the

slides cooled down to room temperature, sections were washed with PBS with 0.1% Tween (PBST) followed by blocking, with blocking solution consisting of 10% goat serum in PBST for 1 h at RT. Sections were labeled overnight with primary antibody diluted in blocking solution, in a moist chamber in dark, and then the reaction was stopped by rinsing 3 times with PBST. The next step of the staining procedure was incubation with secondary antibody for 45 mins at RT and rinsing with PBST. Nuclei were stained with DAPI (Sigma, 1ug/ml). Slides were then mounted with hydromount mounting medium (National Diagnostics, USA) and observed under Zeiss 510 Meta Laser Scanning Microscope.

For the detection of BrdU labeled cells another protocol was followed. *Ex vivo* BrdU labeling of thyroid explants was done by adding BrdU (BD Pharmingen; final concentration of 10uM) for 2 h before snap freezing the tissues. Tissue sections were fixed with 4% PFA for 30 mins at 4^0C. Slides were washed with 0.1M Phosphate Buffered Saline (PBS) (pH 7.4) with 1% TritonX100 (PBST). Sections were incubated with HCl (1M) for 10 mins on ice to break open the DNA structure of the labeled cells followed by HCl (2 M) for 10 min at room temperature, then 20 min at 37°C. Sections were neutralized by incubating with 0.1 M borate buffer pH 8.5 for 10 mins at RT. Slides were washed with PBST and blocked with 5% goat serum in PBST containing 1M glycine for 1 h. Sections were then incubated overnight in a moist chamber at RT with anti BrdU FITC labeled antibody. After washing the slides with PBST, nuclei were stained with DAPI (Sigma, 1ug/ml) and slides were mounted with hydromount.

3.5 Cell suspension preparation and flow cytometry

Embryonic thyroids from E13.5, E15.5, E17.5 embryos and adult thyroids were micro-dissected, cleaned of fat and connective tissue and placed on ice cold PBS 2%FCS (Phosphate Buffer Saline containing 2% Fetal Calf Serum). All embryonic and adult thyroid tissues were micro-dissected on the same experimental day. Each experiment represents pooled tissues to get enough cells for analysis: E13.5 $n \geq 20$ pooled thyroids per sample, E15.5 $n \geq 13$ pooled thyroids per sample, E17.5 $n \geq 11$ pooled thyroids per sample and adult tissues $n \geq 1$ thyroid per sample. To reduce experimental variations as much as possible, for each analysis all 4 stages were analyzed within the same experiment on the same day.

Thyroids were enzymatically digested with 1 mg/ml collagenase/dispase and 2 ug/ml DNase I (Roche Diagnostics, Switzerland) at 37^0 C for 20 minutes until single cell suspension was

obtained. Adult thyroids were first cut into small pieces using sterile scissors before enzymatic digestion. After obtaining the single cell suspension, cells were spun down with PBS 2%FCS for 5 minutes at 1500 rpm. Cells were then stained with cell surface markers for 20 mins on ice.

Prior to intracellular staining, cells were fixed and permeabilised using the BD Cytofix/CytopermTM Fixation/Permeabilization solution kit (BD Bioscience) according to the manufacturer's guidelines. Cells were then treated with 10% goat serum for 45 mins at room temperature. Intracellular staining with anti- NKX2-1 antibody was done for 45 mins at room temperature followed by secondary antibody for 30 mins at room temperature. Non-nucleated cells were excluded by staining with DAPI; (4',6-Diamidine-2'-phenylindole dihydrochloride; Roche Diagnostics, Switzerland).

Cells were acquired on BD FACSAria II flow cytometer (Becton Dickinson, Mountain View, CA). FlowJo software (Tree Star Inc., Ashland, OR, USA) was used for analyzing flow cytometry data.

3.6 Antibodies for flow cytometry

3.6.1 Primary antibodies

mAb for EpCAM (clone G8.8), PDGFRa (APA5), CD45 (30-F11), Ter119 (TER-119), CD54 (YN1/1.7.4) and PECAM (390) were obtained from Biolegend. NKX2-1 (EP1584Y), Histone H3, H3K9ac, H3K9me3, HDAC1 (10E2) and HDAC2 (Y461) were obtained from Abcam. 5'-bromo-2'-deoxyuridine (BrdU) and 7-amino-actinomycin D (7-AAD) were obtained from BD Pharmingen (BD Pharmingen BrdU Flow kit).

3.6.2 Secondary antibodies

Goat anti rabbit or mouse anti rabbit antibodies conjugated with either A647 or A488 were obtained from Life technologies.

3.7 Absolute cell number calculation

To calculate the absolute cell numbers, all events acquired were first gated to remove cell debris by using forward-scattered light (FSC) and side-scattered light (SSC). Then, cell

doublets were removed by using SSC- height (SSC-H) and SSC- width (SSC-W). Erythroblasts/ Erythrocytes were further removed by gating out Ter119 positive cells. Organ cellularity was determined with a Z1 Coulter Counter (Beckman Coulter). The absolute cell number of each cell type was calculated by multiplying organ cellularity with the frequency of individual cell populations determined by flow cytometry.

3.8 Apoptosis

3.8.1 TUNEL assay

Terminal deoxynucleotidyl transferase dUTP nick end labeling (TUNEL) assay was performed on thyroid explants according to manufacture's instructions using In Situ Cell Death Detection Kit, Fluorescein (Roche, Mannheim, Germany).

3.8.2 Annexin V-PI staining

Frequencies of living and apoptotic cells of the thyroid explants were analyzed by an Apoptosis detection kit (Annexin V Apoptosis Detection Kit APC, eBioscience, San Diego, CA, USA). Briefly, thyroid explants were freshly harvested and digested with 1 mg/ml collagenase/dispase and 2 ug/ml DNase I (Roche Diagnostics, Switzerland) at 37^0 C for 20 minutes until single cell suspension was obtained. Cells were washed once in 1x binding buffer and were incubated for 15 min at RT with AnnexinV-APC. Cells were once again washed in 1x binding buffer and 5ul propidium iodide (PI) was added. Immediately cells were analyzed on BD FACSAria II flow cytometer (Becton Dickinson, Mountain View, CA, USA). Annexin V - positive/PI – negative cells were considered apoptotic, whereas annexin V - positive/PI - positive cells were considered (late apoptotic) necrotic cells.

3.9 Cell proliferation analysis with Bromodeoxyuridine

In vivo proliferations of embryonic and adult thyroid tissues and *ex vivo* proliferation of thyroid explants were performed using Bromodeoxyuridine (BrdU). In vivo BrdU labeling of mice was done by intraperitoneal (i.p.) injection of BrdU (BD Pharmingen; 1 mg/100 ul of PBS per mouse) for 2 h prior to tissue isolation. *Ex vivo* BrdU labeling of thyroid explants was done by adding BrdU (BD Pharmingen; final concentration of 10uM) for 2 h before

analysis. After digestion, fixation and permeabilization of the tissues/ explants as described before, these were further treated with 30ug of DNase I (BD Pharmingen) followed by anti-BrdU (BD Pharmingen) and 7-AAD (7-Aminoactinomycin D, BD Biosciences) staining. Cells were acquired immediately on BD FACSAria II flow cytometer.

3.10 Statistical analysis

All values are depicted as mean ± SD. Data represents at least 3 independent experiments. Differences in means between two groups were evaluated with unpaired 2-tailed Student t tests. For multiple group comparisons one-way ANOVA with Tukey's multiple comparison posttest was performed using GraphPad Prism version 5 for Mac OS X (GraphPad Software, San Diego California USA, www.graphpad.com). p values <0.05 were considered as significant.

4. RESULTS

The first part of the result is focused on the development of a new tool for thyroid research by using flow cytometry. This work is submitted for publication in journal 'Thyroid' and the manuscript for the same is in section 4.1. The second (4.2) and third sections (4.3) are focused on the role of HDACs and histone acetylation during thyroid development and are shown in detail in the respective sections.

4.1 New tools for thyroid research: Flow cytometry of the thyroid gland

Introductory notes

Thyroid is a heterogeneous organ whose parenchyma is composed of epithelial cells, endothelial cells, and fibroblasts. These data are based on immunohistochemical studies of the entire thyroid gland within the embryo. However, thyroid research is limited by the lack of a robust tool to identify and analyze the distinct cell types of the heterogenous organ separately. So far, flow cytometry is not established in the field.

To overcome this limitation and to analyze the role of histone acetylation in each cell type separately, we developed first a unique a robust flow cytometry protocol for identification of the distinct cell types and second, a protocol to quantify epigenetic changes for the embryonic as well as adult thyroid gland.

Flow cytometry protocol for the identification and quantification of distinct cell types in embryonic and adult thyroid is presented in a format as the submitted manuscript. Role of HDACs and of histone acetylation for the regulation of normal thyroid development is presented in section 4.2 and 4.3, see below.

Contribution

The work described below is submitted for publication in the Thyroid journal. The manuscript ID is THY-2015-0523. My contribution to this work was to establish the whole flow cytometry protocol for the identification and quantification of the discrete cell populations as well as establish protocol to study proliferation in these cells. I was responsible for the dissection of embryonic and adult thyroids from mice, for preparing single cell suspensions

from these heterogeneous murine thyroid tissues, for the labeling these cells with cell-type anti-mouse specific antibodies, for the acquisition of the cells on flow cytometer and the analysis of the data. These contributions were considered significant and I was acknowledged as first author of the work.

Submitted Manuscript

Cell growth dynamics in embryonic and adult mouse thyroid revealed by a novel approach to detect thyroid gland subpopulations

Gawade Sanjay MSc[1], Mayer Carlos PhD[1], Hafen Katrin[1], Barthlott Thomas PhD[1], Krenger Werner PhD[1], Szinnai Gabor MD, PhD[1,2]

[1] Pediatric Immunology, Department of Biomedicine, University of Basel, Basel, Switzerland; [2] Pediatric Endocrinology, University Children's Hospital Basel, University of Basel, Basel, Switzerland

sanjay.gawade@unibas.ch

carlos.mayer@unibas.ch

katrin.hafen@unibas.ch

thomas.barthlott@unibas.ch

werner.krenger@unibas.ch

gabor.szinnai@unibas.ch

Running Title: Thyroid cell analysis by flow cytometry

Key Words: flow cytometry, thyroid, development, organogenesis, cell populations, proliferation

Abstract word count: 347

Manuscript word count: 3116

Abstract (word count 347)

BACKGROUND: The thyroid is composed of endocrine epithelial cells, blood vessels and mesenchyme. However, no data exist thus far on absolute cell numbers, relative distribution, and proliferation of the different cell populations in the developing and mature thyroid. The aim of this study was therefore to establish a flow cytometry protocol that allows detection and quantification of discrete cell populations in embryonic and adult murine thyroid tissues.

METHODS: Cell-type anti-mouse specific antibodies were used for erythroid cells (Ter119), hematopoietic cells (CD45), epithelial cells (EpCam/CD326, E-cadherin/CD324), thyroid follicular cells and C-cells (Nkx2-1), endothelial cells (Pecam/CD31, Icam-1/CD54), fibroblasts (PDGFRa/CD140a). Proliferating cells were detected after labelling with 5-bromo-2'-deoxyuridine (BrdU). For flow cytometry analyses, micro-dissected embryonic (E) and adult thyroids were pooled (E13.5, n=25; E15.5, n=15; E17.5, n=15; adult n=4) in one sample.

RESULTS: The absolute parenchymal cell numbers per mouse thyroid (mean±SD), excluding the large number of $CD45^+$ and $Ter119^+$ cells, increased from 7'4250±1'338 at E13.5 to 271'561±22'325 in adult tissues. As expected, $Nkx2\text{-}1^+$ cells represented the largest cell population in adult tissues (61.2±1.1%). Surprisingly, at all three embryonic stages analyzed, thyroid follicular cells and C-cells accounted only for a small percentage of the total thyroid cell mass (between 4.7±0.4% and 9.4±1.6%). In contrast, the largest cell population at all three embryonic stages was identified as $PDGFRa/CD140a^+$ fibroblasts (61.4±0.4% to 77.3±1.1%) These cells represented, however, the smallest population in adult tissues (5.2±0.8%). $Pecam/CD31^+$ endothelial cells increased from E13.5 to E15.5 from 3.7±0.8% to 8.5±3.0%, then remained stable at E17.5 and adult tissues. Proliferation rates were sizable during

the entire organogenesis but differed between cell populations, with distinct proliferative peaks at E13.5 in epithelial cells (32.7±0.6% $BrdU^+$ cells), and at E15.5 in endothelial cells (22.4±2.4% $BrdU^+$ cells). Fibroblasts showed a constant proliferation rate in embryonic tissues. In adult tissues, $BrdU^+$ cells were between 0.1-0.4% in all cell types.

CONCLUSIONS: Using a novel flow cytometry-based method, we uncovered a previously not observed highly dynamic growth pattern of thyroid cell populations during embryogenesis. We believe that our approach will provide a useful new tool for cell function analyses in murine thyroid disease models.

Introduction

The thyroid gland is an endocrine organ composed of different cell types (1-3). The endocrine cell mass consists mainly of thyroid follicular cells (TFC) which are organized in the functional unit of the thyroid, the thyroid follicle. TFCs produce thyroid hormones T3 and T4 (1-3). The second endocrine cell type are parafollicular cells (C-cells) which represent a small population of the entire cell mass and secrete calcitonin (1-4). The thyroid also contains blood vessels, which form a dense capillary net around the thyroid follicles. This structure creates a close contact to the basal membrane of the TFCs to provide an optimal uptake of secreted thyroid hormones into the blood, the so-called angiofollicular unit (5). Finally, fibroblasts are interspersed between vessels and follicles (4).

At present, very few data are available, however, with regard to the precise cellular composition and cell growth dynamics of the developing thyroid due to lack of TFC-specific surface antigens and protocols for nuclear staining with TFC-specific transcription factors such as Nkx2-1. One previous study had quantified the different cell populations in the adult dog thyroid before flow cytometry was available by transmission electron microscopy. Here, 70% of thyroid cells were epithelial cells, 6% endothelial cells, and 24% fibroblasts (6). However, these results were never confirmed in other species.

Flow cytometry allows for a precise quantification of relative distributions of different cell types during various stages of differentiation. Using human thyroid tissues, endothelial cells were studied by flow cytometry using factor-VII related antigen (7). However, other thyroid cells were not analyzed in this study. In a second study, thyroglobulin and calcitonin antibodies were used to quantify TFC and C-cell mass in

adult rat thyroids. Here, 40% of the cells were thyroglobulin positive, thus representing TFCs, and 4% were calcitonin positive, representing C-cells (8).

To make available more precise data on thyroid cell populations both in adults and during thyroid development, we developed a straight forward flow cytometry protocol for quantification of the main cell populations in the murine thyroid gland and provide for the first time data on the developmental dynamics of growth of the embryonic thyroid gland at different consecutive stages. This protocol provides a new tool for future in-depth analyses of murine thyroid disease models.

5

Materials and Methods

Mice: Embryos from Swiss albino mice at embryonic day (E) 13.5, 15.5, 17.5 and adult female pregnant mice (age=8 weeks) were obtained from Janvier Labs (France). All experiments were performed in accordance with the federal regulations.

***In vivo* labeling of mice with Bromodeoxyuridine (BrdU):** Mice were injected intraperitoneally (i.p.) with 2mg 5-bromo-2'-deoxyuridine (BrdU; BD Biosciences; 1 mg/100 µl of PBS per mouse) 2 h prior to tissue isolation.

Cell suspension preparation: Embryonic thyroids from E13.5, E15.5, E17.5 embryos and thyroids from adult female pregnant mice were micro-dissected, cleaned of fat and connective tissue and placed on ice cold PBS 2%FCS (Phosphate buffer saline containing 2% fetal calf serum). Only entire bilobed thyroid glands with intact isthmus were used for experiments. Each experiment used pooled tissues to obtain sufficient cells for analysis: E13.5, n=25 pooled thyroids per sample; E15.5, n=15 pooled thyroids per sample; E17.5, n=15 pooled thyroids per sample; adult tissues n=4 thyroids per sample. To reduce experimental variation, all embryonic and adult thyroid tissues were micro-dissected on the same experimental day and all 4 stages were analyzed within the same experiment on the same day. Thyroids were enzymatically digested with 1 mg/ml collagenase/dispase and 2 ug/ml DNase I (Roche Diagnostics, Switzerland) at 37^0 C for 20 minutes until single cell suspension was obtained. Adult thyroids were first cut into small pieces using sterile scissors before enzymatic digestion. After obtaining the single cell suspension, cells were centrifuged with PBS 2%FCS for 5 minutes at 1500 rpm. Cells were then stained with cell surface markers for 20 min on ice. Prior to intracellular staining, cells were fixed

and permeabilized using the BD Cytofix/Cytoperm™ Fixation/Permeabilization solution kit (BD Biosciences, San Diego, CA, USA) according to the manufacturer's guidelines. Cells were then exposed to 10% goat serum for 45 min at room temperature. Intracellular staining with anti-Nkx2-1 antibody was done for 45 min at room temperature followed by secondary antibody for 30 min at room temperature. Non-nucleated cells were excluded by staining with DAPI; (4',6-Diamidine-2'-phenylindole dihydrochloride; Roche Diagnostics, Switzerland). To analyze cell proliferation, cells were also treated with 30ug of DNase I (BD Biosciences) followed by anti-BrdU staining and 7-AAD (7-Aminoactinomycin D, BD Biosciences) after the fixation and permeabilization step.

Flow cytometry analysis: Cells were acquired on BD FACSAria II flow cytometer (Becton Dickinson, Mountain View, CA). FlowJo software (Tree Star Inc., Ashland, OR, USA) was used for analyzing flow cytometry data. The following monoclonal antibodies were used: E-cadherin/CD324 (ECCD-2) from Invitrogen (Switzerland), EpCam/CD326 (G8.8), PDGFRa/CD140a (APA5), CD45 (30-F11), Ter119 (TER-119), Icam-1/CD54 (YN1/1.7.4), Pecam/CD31 (390), from Biolegend (San Diego, CA, USA), and Nkx2-1 (EP1584Y) from Abcam (Cambridge, UK). As secondary antibody, goat anti rabbit A647 was obtained from Life technologies (Eugene, OR, USA).

To calculate the absolute cell numbers, all events acquired were first gated to remove cell debris by using forward-scattered light (FSC) and side-scattered light (SSC; Figure 1A). Then, cell doublets were removed by using SSC-height (SSC-H) and SSC-width (SSC-W). Organ cellularity was determined with a Z1 Coulter Counter (Beckman Coulter, Brea, CA, USA). The absolute cell number of each cell type was calculated by multiplying organ cellularity with the frequency of individual cell populations determined by flow cytometry.

Statistical analysis: All values are given as mean ± SD. Data represents 3 independent experiments. For multiple group comparisons one-way ANOVA with Tukey's multiple comparison post test was performed using GraphPad Prism version 5 for Mac OS X (GraphPad Software, San Diego, CA, USA, www.graphpad.com).

P values <0.05 were considered as statistically significant.

Results

Establishment of a thyroid gland adapted combination of specific antibodies

In a first step, we established a protocol of intranuclear staining with Nkx2-1, a transcription factor expressed in TFCs and C-cells (9). Using this approach, we were able to identify the TFC / C-cell population (Figure 1A and 1B). In a second step, we validated the use of established surface markers to identify epithelial cells (EpCam/CD326$^+$, E-cadherin/CD324$^+$), endothelial cells (Pecam/CD31$^+$, Icam-1/CD54$^+$), fibroblasts (PDGFRa/CD140a$^+$), erythroid cells (Ter119$^+$), and hematopoietic cells (CD45$^+$) in the thyroid tissue (Figure 1A and 1B). The final gating strategy consisted of the combinatory use of Nkx2-1, CD45, Pecam, PDGFRa, EpCam and Ter119 (Figure 1A). Nkx2-1$^-$/EpCam$^+$ cells represented parathyroid cells (Figure 1A and 1B). The used gating strategy allowed to characterize between 82% to 92% of cells in the embryonic thyroid and 93% of cells in the adult murine thyroid gland (Figure 1A and Table 2). However, a population ranging from 8-20% of cells remained negative for all 6 antibodies in the different embryonic and adult tissues.

Assessment of absolute thyroid population cell numbers

Mean absolute total cell number (Table 1, Figure 2) of one thyroid gland was 7'425±1'338, 18'444±1259, 31'804±2'610, and 271'561±22'325 cells at E13.5, E15.5, E17.5, and in adult tissues, respectively. Different growth patterns were observed in endocrine cells, endothelial cells and fibroblasts. Firstly, Nkx2-1$^+$ TFC / C-cell and Nkx2-1$^-$/EpCam$^+$ parathyroid cell numbers were 684±91, and 109±33 cells/thyroid at E13.5, respectively, and increased 243-fold and 438-fold to adult stage (166'208±17'334, and 47'598±7008 cells/thyroid). Secondly, the cell number of Pecam$^+$ endothelial cells was 274±75 at E13.5 and reached 22'813±4027 in adult

tissues (83-fold increase with a peak between E13.5 and E15.5 during angiogenesis of the embryonic thyroid). Lastly, PDGFRa$^+$ fibroblasts showed highest cell numbers in embryonic tissues, however with only a slight increase from E13.5 to adult stage (2.0x), and surprisingly a decrease by 28% between E17.5 and the adult stage. Nkx2-1$^-$/CD45$^-$/Pecam$^-$/PDGFRa$^-$/EpCam$^-$/Ter119$^-$ cells showed a 34-fold increase from 609±154 cells/thyroid at E13.5 to 20'837±9'899 cells/thyroid in the adult. The absolute cell numbers of each cell type are summarized in Table 1 and Figure 2.

Relative frequencies of cell types

For calculation of relative frequencies of parenchymal cell populations, the number of Ter119$^+$ erythroid cells and CD45$^+$ hematopoietic cells were subtracted from the absolute total cell number of one thyroid gland. TFCs and C-cells (Nkx2-1$^+$ cells) were surprisingly low in relative frequency (4.7-9.4%) in embryonic tissues (Table 2, Figure 3 and Figure 5A). In contrast, in adult tissues they represented as expected the predominant population (61.2% of all cells). Parathyroid cells (Nkx2-1$^-$/EpCam$^+$ cells) were low (0.8-3.0%) in embryonic tissues, but increased to 17.8% in adult thyroid tissues. Endothelial cells (Pecam$^+$) doubled their frequency between E13.5 and E15.5 from 3.7% to 8.5% and remained 8.5% respectively 8.4% at E17.5 and adult stage. Fibroblasts (PDGFRa$^+$) were the predominant cell type in embryonic thyroid glands (61%-77%), while being the smallest cell population in adult tissues with 5.2% (Figure 3 and Figure 5A). Finally, the cell population negative for all used antibodies (Nkx2-1$^-$/CD45$^-$/Pecam$^-$/PDGFRa$^-$/EpCam$^-$/Ter119$^-$) increased from 8% at E13.5 to 20% and 19% at E15.5, and E17.5, respectively, but was low in adult tissues (8%). The origin of this cell population remains to be characterized.

Cell cycle analysis of discrete thyroid cell types

The different phases of the cell cycle in the identified cell populations were assessed by BrdU and 7-AAD labelling. Cells in G_0/G_1 phase were $BrdU^-/7\text{-}AAD^{2n}$, cells in S-phase were $BrdU^-/7\text{-}AAD^{2n/4n}$, and cells in G_2/M phase were $BrdU^-/7\text{-}AAD^{4n}$ (Figure 4A). Embryonic stage-specific frequencies of cells in S-phase were significantly different between E13.5-E15.5-E17.5 tissues for $EpCam^+$ epithelial cells ($P<0.01$) and $Pecam^+$ endothelial cells ($P<0.05$), while in $PDGFRa^+$ fibroblasts, values were not statistically different in embryonic stages ($P=0.07$). In contrast to epithelial cells, endothelial cells and fibroblasts, the unknown cell population ($Nkx2\text{-}1^-/CD45^-/Pecam^-/PDGFRa^-/EpCam^-/Ter119^-$) harbored markedly stable frequencies of $BrdU^+$ cells between E13.5 and E17.5 ($P=0.6$). Hence, we observed significant differences of the relative frequencies of cells in S-phase between the different cell types at each embryonic stage (E13.5 $P<0.01$; E15.5 $P<0.05$, E17.5 $P<0.05$), while BrdU-positive cell frequency did not differ in adult tissues between cell types ($P=0.55$).

Frequencies of proliferating cells among $EpCam^+$ epithelial cells were highest at E13.5 (32.7%±0.6). The fraction of proliferating cells then decreased to 13.6%±4.1 at E15.5 and to 6.7%±1.5 at E17.5 (Figure 4B and Figure 5B). In adult thyroid glands, the frequency of $BrdU^+$ cells was 0.1%±0.2%. In contrast, the fraction of proliferating cells among $Pecam^+$ endothelial cells increased in their proliferation from 17.2%±5.8 (E13.5) to 22.4%±2.4 at E15.5. Late in embryonic development (E17.5), a fraction (1.1%±0.4) of $Pecam^+/BrdU^+$ double positive cells was present. In adult tissues, the proliferation rate of $Pecam^+$ cells was 0.1±0.1%. Finally, $PDGFRa^+$ fibroblasts showed stable proliferation rates at E13.5 and E15.5 (9.0%±1.8, and 8.4%±2.1, respectively; Figure 4B and Figure 5B). They decreased to 3.0%±06 at E17.5, and to 0.4±0.3% in adult thyroids. The cell population negative for all used surface and intracellular markers ($Nkx2\text{-}1^-/CD45^-/Pecam^-/PDGFRa^-/EpCam^-/Ter119^-$) showed

proliferation rates of 14.8±1.9% at E13.5, of 16.8±5.5% at E15.5, and 11.4±9.1% at E17.5, and 0.0±0.1 in adult tissues.

Thus, our data indicated distinct cell population-specific proliferative waves during thyroid development with peak proliferation at E13.5 in the epithelial population, and at E15.5 in endothelial cells. In contrast, fibroblasts showed more stable proliferation rates during thyroid differentiation without clear peaks, and the unknown cell population was characterized by a markedly stable but high frequency of $BrdU^+$ cells in embryonic tissues.

Discussion

Improved tools for suitable cell analysis are required to obtain more in-depth knowledge with regard to thyroid development and disease. Flow cytometry has not been a standard protocol up to this date for thyroid research. By use of flow cytometry, we were able to quantify absolute cell numbers, relative frequencies, and proliferation rate of endocrine epithelial cells, endothelial cells, and fibroblasts in embryonic and adult murine thyroid tissues (summarized in Figure 5A and 5B). Our protocol provides a new tool for research in thyroid development and disease models in the mouse.

Until present, sorting of human thyroid endothelial cells and TFC precursors expressing green fluorescent protein (GFP) *in vitro* had been reported (7, 11). Both protocols did not allow analysis of the *in vivo* frequencies and cell growth dynamics of cell subpopulations in the developing thyroid. One study quantified TFCs in adult rat thyroids *in vivo* by flow cytometry (8). These authors used intracellular thyroglobulin (TG) and calcitonin staining to identify TFCs and C-cells. They observed 40% TG-positive TFCs, and 2-4% calcitonin-positive C-cells. The remaining cells were not characterized. In our study, the frequency of TFCs in adult tissues was higher (61%) (see Table 1 and Figure 2) which was likely explained by two technical differences: Firstly, we used the exclusively intranuclearly expressed TFC and C-cell transcription factor Nkx2-1 instead of TG to characterize TFCs. TG can be detected in the cytoplasm of TFCs, especially in embryonic tissues (12-14). But synthesized TG is excreted and accumulated within the follicular lumen and might be a less specific marker for TFCs than Nkx2-1. Secondly, Moerch et al used a much longer dissociation protocol of thyroid tissue compared to our protocol, possibly leading to a considerable loss of TFCs by dissociation (8).

Using morphological analysis of adult dog thyroids by transmission electron microscopy, Dow and co-workers quantified the different cell populations in the adult dog thyroid and found a frequency of 70% for TFCs, 26% of fibroblasts, and 6% of endothelial cells (6). These results were published in 1986, and are the only data characterizing all three main populations of the thyroid gland so far. Our results in the adult mouse thyroid are in accordance concerning percentage of Nkx2-1 positive TFCs (61% vs. 70% in the dog) and endothelial cells (8% vs. 6% in the dog) since these two cell types can be clearly differentiated from interstitial cells by morphological criteria. The relative abundance of fibroblasts was clearly lower in our study (Figure 3). We hypothesize that by morphological analysis, all interstitial cells were classified as fibroblasts, as morphological analysis might not be specific enough to differentiate between fibroblasts, C-cells and the population of unknown cells detected by flow cytometry in our study. Interspecies differences might be a further reason for differences with published data.

Quantitative data on the relative distribution in embryonic thyroids were not available thus far. We found a surprisingly low frequency of Nkx2-1-positive *bona fide* TFC / C-cells at all three embryonic stages analyzed ranging from 4.7-9.4% in contrast to their high abundance (61%) in adult tissues (Figure 3 and Figure 5A). These results in the embryonic tissues could have been limited by our gating strategy, only using Nkx2-1 and not adding further specific TFC markers such as Pax8. However, the epithelial origin and the low relative frequency of Nkx2-1^{+} cells was validated by double staining with EpCam, an epithelial surface marker known to be expressed on embryonic and adult TFCs (Figure 1B).

Importantly, our data indicate a switch of relative tissue composition between embryonic and adult tissues. The high percentage of mesenchyme at E13.5, E15.5 and E17.5 is in accordance with immunohistochemical data in the embryonic mouse

as well as human thyroid (10,12,14). In both species, Nkx2-1-positive TFCs form strands of epithelial cells embedded in or surrounded by mesenchyme. This close contact of mesenchyme and epithelial cells during development is in accordance with data from other endoderm derived organs, e.g. lung, and pancreas (15,16). The observation that mouse models with deletion of mesenchymal genes (e.g. *Fgf10*$^{-/-}$, or *Shh*$^{-/-}$) suffer from thyroid dysgenesis further supports the hypothesis of functional interaction between mesenchyme and epithelial cells (17,18). Finally, thyroidal fibroblasts showed growth promoting effects on a thyroid carcinoma cell line but not on differentiated FRTL-5 cells injected intrathyroidally, providing further arguments for epithelial-mesenchymal interactions in an undifferentiated state (19).

The mechanisms how the Nkx2-1-positive TFC / C-cell population becomes so predominant in the adult tissue remained unclear. The important switch between fibroblast and TFC populations (60-fold increase between E17.5 to adult) occurred after E17.5, the latest stage we analyzed. For better understanding developmental processes, late embryonic, neonatal and postnatal stages until the adult age need to be analyzed by the same approach. One key observation can be made between the E17.5 and the adult thyroid: the fibroblast population is the only cell population showing a significant decrease not only in relative frequency (61% to 4%) but also in absolute cell numbers (-28%) (Table 1, Figure 2). Whether this reduction in fibroblast/mesenchymal cell numbers could be explained by apoptosis or by processes of cell fate reprogramming or inter-lineage transdifferentiation, as described recently for cardiac endothelial cells, Schwann cells or hepatocytes, remains speculative (20-23).

In addition to phenotype data, our work provides information with regard to cell type-specific proliferation rates. We observed distinct cell type-specific proliferative waves during thyroid development with a highest and earliest peak in epithelial cells at

E13.5. A second but lower peak was observed in endothelial cells at E15.5. In contrast, mesenchymal cells showed rather stable proliferation throughout development (Figure 5B). So far, only few data on proliferation of Nkx2-1$^+$ cells during thyroid development are availabe (10,24). Our flow cytometry results (Figure 4B) are in general accordance with BrdU immunohistochemistry revealing high proliferation rate during thyroid morphogenesis as reported previously (E11.5: 23%/40%, E13.5: 40%, E15.4: 32%/32%)(10,24).

The observed proliferative wave of endothelial cells at E15.5 is in line with the strictly descriptive data without BrdU labelling of peak angiogenesis at E15.5 during folliculogenesis in the murine thyroid (10,25). Finally, the very low turnover rate in adult thyroid tissues in our study for all cell types is in accordance with the landmark data by Dumont's group in dog and human thyroids, suggesting about 5 renewals per lifetime (4,26).

We initially hypothesized that the thyroid is composed of three major cell populations: endocrine epithelial cells, endothelial cells and mesenchymal cells. However, even after exclusion of circulating Ter119$^+$ erythroid cells and CD45$^+$ hematopoietic cells a cell population ranging from 8% in adult tissues to 20% in embryonic tissues remained negative for all antibodies used in our protocol. Although our gating strategy does not use a second TFC specific marker, the negative staining for EpCam and for Nkx2-1 argue against epithelial or even TFC origin of these cells. Further, this cell population showed a clearly distinct proliferation pattern (constant high levels) compared to TFCs, endothelial cells and fibroblasts suggesting not being synchronized with the fundamental processes of angiogenesis and folliculogenesis of the differentiating thyroid.

“The presence of stem cells in the adult human and murine thyroid at very low frequency (0.3-1.4%) has been suggested recently (28-31). This percentage is clearly

lower than the relative distribution of the uncharacterized cell population in our experiments (8%) (Figure 3). It remains therefore to be determined, whether 1) the Nkx2-1$^-$/CD45$^-$/Pecam$^-$/PDGFRa$^-$/EpCam$^-$/Ter119$^-$ cell population represents a homogenous population or several yet unidentified cell populations and whether 2) they would stain positive for stem cell markers.

In conclusion, we provide a novel validated protocol for flow cytometric analysis of the different cell populations of the thyroid gland. Our results add to current knowledge quantitative data on *in vivo* frequencies and cell growth dynamics during normal murine thyroid development. Finally, we identified a relevant cell population besides epithelial, endothelial and mesenchymal cells that needs to be further characterized. We believe that our approach will provide a useful tool for cell function analysis in murine thyroid disease models.

Acknowledgements

The project was supported by a research grant from the Swiss National Science Foundation (31003A-130458), and a grant from the Gedächtnisstiftung Suzy Rückert zur Krebsbekämpfung.

Disclosure Statement

No competing financial interests exist.

Corresponding Author

Gabor Szinnai, MD, PhD; Pediatric Endocrinology, University Children's Hospital Basel, and Department of Biomedicine, University of Basel, Spitalstrasse 33, CH-4031 Basel, Switzerland, Phone: +41-61-704-2922, Fax: +41-61-704-1213, e-mail: gabor.szinnai@unibas.ch

References

1. De Felice M, Di Lauro R 2003 Thyroid development and its disorders: genetics and molecular mechanisms. Endocr Rev 25:722-746.
2. Nilsson M, Fagman H 2013 Mechanisms of thyroid development and dysgenesis: an analysis based on developmental stages and concurrent embryonic anatomy. Curr Top Dev Biol 106:123-170.
3. Szinnai G 2014 Genetics of normal and abnormal thyroid development in humans. Best Pract Res Clin Endocrinol Metab 28:133-150.
4. Dumont JE, Lamy F, Roger P, Maenhaut C 1992 Physiological and pathological regulation of thyroid cell proliferation and differentiation by thyrotropin and other factors. Physiol Rev 72:667-697.
5. Colin IM, Denef JF, Lengelé B, Many MC, Gérard AC 2013 Recent insights into the cell biology of thyroid angiofollicular units. Endocr Rev 34:209-238.
6. Dow CJ, Dumont JE, Ketelbant P 1986 Percentage of epithelial cells, fibroblasts and endothelial cells in the dog thyroid. C R Seances Soc Biol Fil 180:629-632.
7. Patel VA, Logan A, Watkinson JC, Uz-Zaman S, Sheppard MC, Ramsden JD, Eggo MC 2003 Isolation and characterization of human thyroid endothelial cells. Am J Physiol Endocrinol Metab 284:E168-176.
8. Moerch U, Nielsen HS, Lundsgaard D, Oleksiewicz MB 2007 Flow sorting from organ material by intracellular markers. Cytometry A 71:495-500.
9. Kusakabe T, Hoshi N, Kimura S 2006 Origin of the ultimobranchial body cyst: T/ebp/Nkx2.1 expression is required for development and fusion of the ultimobranchial body to the thyroid. Dev Dyn 235:1300-1309.

10. Fagman H, Andersson M, Nilsson M 2006 The developing mouse thyroid: embryonic vessel contacts and parenchymal growth pattern during specification, budding, migration, and lobulation. Dev Dyn 235:444-455.
11. Arufe MC, Lu M, Kubo A, Keller G, Davies TF, Lin RY 2006 Directed differentiation of mouse embryonic stem cells into thyroid follicular cells. Endocrinology 147:3007-3015.
12. Shepard TH, Andersen HJ, Andersen H 1964 Histochemical studies of the human fetal thyroid during the first half of fetal life. Anat Rec 149:363-379.
13. Olin P, Ekholm R, Almquist S 1970 Biosynthesis of thyroglobulin related to the ultrastructure of the human fetal thyroid gland. Endocrinology 87:1000-1014.
14. Szinnai G, Lacroix L, Carré A, Guimiot F, Talbot M, Martinovic J, Delezoide AL, Vekemeans M, Michiels S, Caillou B, Schlumberger M, Bidart JM, Polak M 2007 Sodium/iodide symporter (NIS) gene expression is the limiting step for the onset of thyroid function in the human fetus. J Clin Endocrinol Metab 92:70-76.
15. Serup P 2012 Signaling pathways regulating murine pancreatic development. Semin Cell Dev Biol 23:663-672.
16. McCulley D, Wienhold M, Sun X 2015 The pulmonary mesenchyme directs lung development. Curr Opin Genet Dev 32:98-105.
17. Ohuchi H, Hori Y, Yamasaki M, Harada H, Sekine K, Kato S, Itoh N 2000 FGF10 acts as a major ligand for FGF receptor 2 IIIb in mouse multiorgan development. Biochem Biophys Res Commun 227:643-649.
18. Fagman H, Grände M, Gritli-Linde A, Nilsson M 2004 Genetic deletion of sonic hedgehog causes hemiagenesis and ectopic development of the thyroid in mouse. Am J Pathol 164:1865-1872.

19. Saitoh O, Mitsutake N, Nakayama T, Nagayama Y 2009 Fibroblast-mediated in vivo and in vitro growth promotion of tumorigenic rat thyroid carcinoma cells but not normal Fisher rat thyroid follicular cells. Thyroid 19:735-742.
20. Crespo I, Del Sol A 2013 A general strategy for cellular reprogramming: the importance of transcription factor cross-repression. Stem Cells 31:2127-2135.
21. Ubli E, Duan J, Pillai IC, Rosa-Garrido M, Wu Y, Bargiacchi F, Lu Y, Stanbouly S, Huang J, Rojas M, Vondriska TM, Stefani E, Deb A 2014 Mesenchymal-endothelial transition contributes to cardiac neovascularization. Nature 514:585-590.
22. Thoma EC, Merkl C, Heckel T, Haab R, Knoflach F, Nowaczyk C, Flint N, Jagasia R, Jensen Zoffmann S, Truong HH, PEtitjean P, Jessberger S, Graf M, Iacone R 2014 Chemical conversion of human fibroblasts into functional Schwann cells. Stem Cell Reports 3:539-547.
23. Zhu S, Wang H, Ding S 2015 Reprogramming fibroblasts toward cardiomyocytes, neural stem cells and hepatocytes by cell activation and signal-directed lineage conversion. Nat Protoc 10:959-973.
24. Carré A, Rachdi L, Tron E, Richard B, Castanet M, Schlumberger M, Bidart JM, Szinnai G, Polak M 2011 Hes1 is required for appropriate morphogenesis and differentiation during mouse thyroid gland development. PLoS One 6:e16752.
25. Hick AC, Delmarcelle AS, Bouquet M, Klotz S, Copetti T, Forez C, Van Der Smissen P, Sonveaux P, Collet JF, Feron O, Courtoy PJ, Pierreux CE 2013 Reciprocal epithelial:endothelial paracrine interactions during thyroid development govern follicular organization and C-cells differentiation. Dev Biol 381:227-240.

26. Coclet J, Foureau F, Ketelbant P, Galand P, Dumont JE 1989 Cell population kinetics in dog and human adult thyroid. Clin Endocrinol 31:655-665.
27. Thomas T, Nowka K, Lan L, Derwahl M 2006 Expression of endoderm stem cell markers: evidence for the presence of adult stem cells in human thyroid glands. Thyroid 16:537-544.
28. Lan L, Cui D, Nowka K, Derwahl M 2007 Stem cells derived from goiters in adults form spheres in response to intensive growth stimulation and require thyrotropin for differentiation into thyrocytes. J Clin Endocrinol Metab 92:3681-3688.
29. Zane M, Scavo E, Catalano V, Bonanno M, Todaro M, De Maria R, Stassi G 2015 Normal vs cancer thyroid stem cells: the road to transformation. Oncogene doi:10.1038/onc.2015.138.
30. Hoshi N, Kusakabe T, Taylor BJ, Kimura S 2007 Side population cells in the mouse thyroid exhibit stem/progenitor cell-like characteristics. Endocrinology 148:4251-4258.

Figures

Fig1

A Gating strategy for flow cytometry analysis

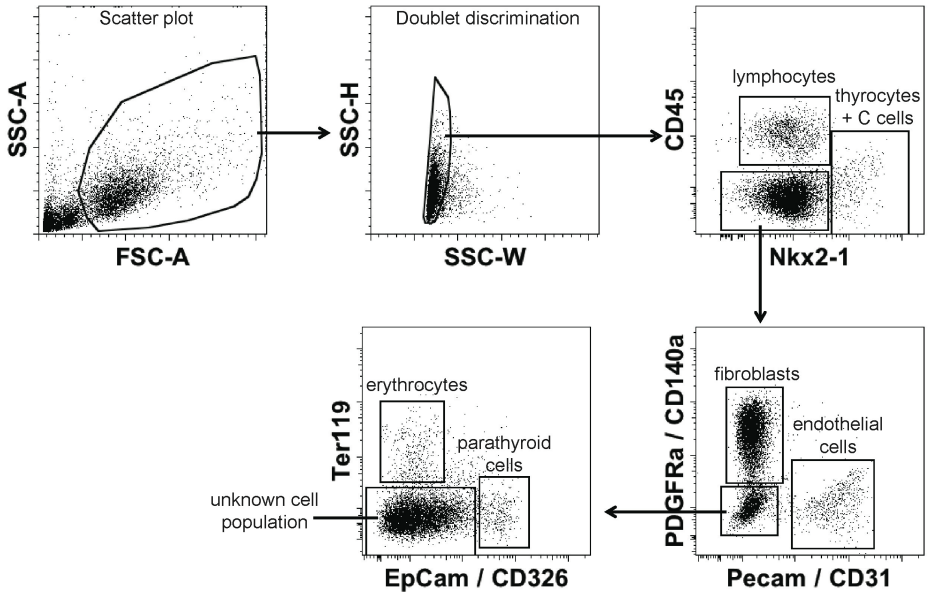

B Double staining for validation of the antibodies

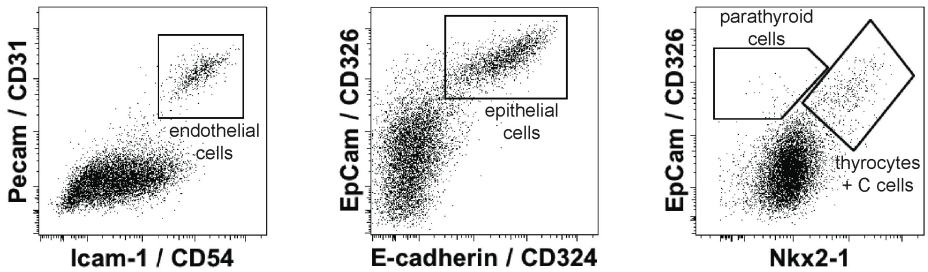

Fig2

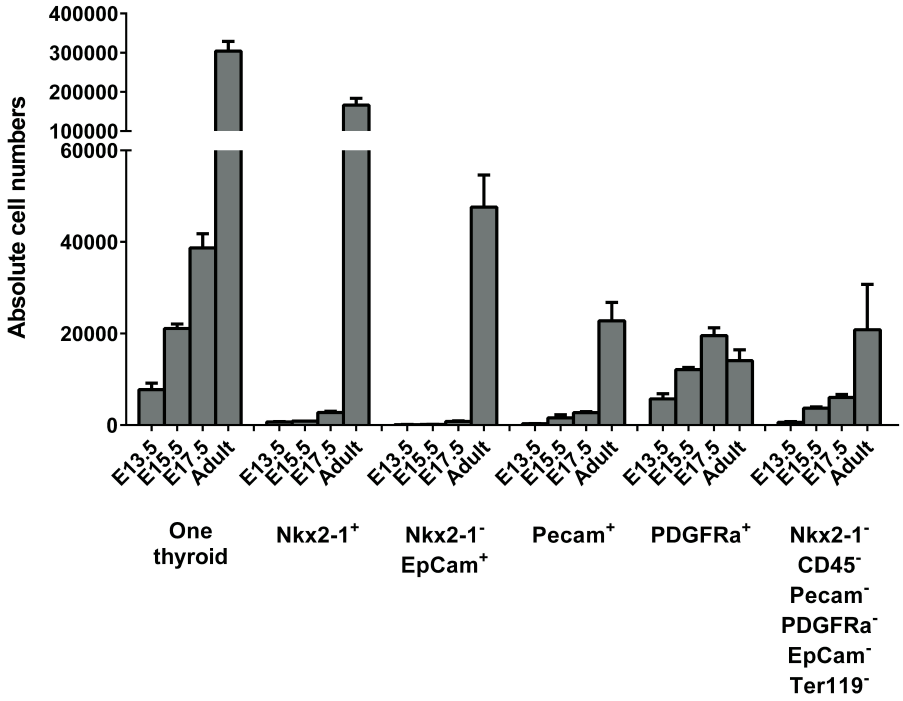
Absolute cell numbers
400000
300000
200000
100000
60000
40000
20000
0
E13.5
E15.5
E17.5
Adult
One thyroid
Nkx2-1+
Nkx2-1- EpCam+
Pecam+
PDGFRa+
Nkx2-1- CD45- Pecam- PDGFRa- EpCam- Ter119-

Fig3

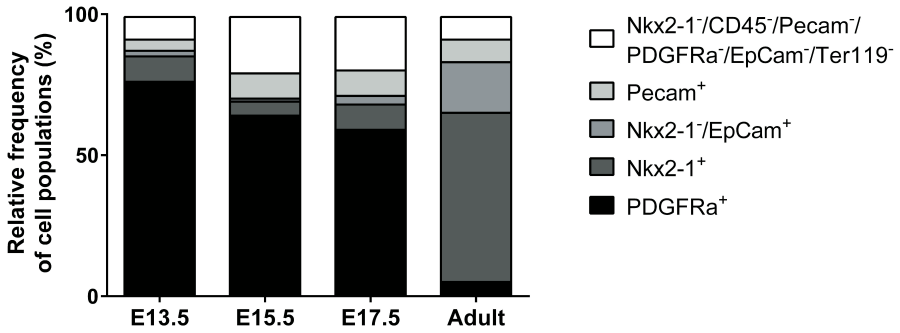
Relative frequency of cell populations (%)
100
50
0
E13.5
E15.5
E17.5
Adult
Nkx2-1-/CD45-/Pecam-/ PDGFRa-/EpCam-/Ter119-
Pecam+
Nkx2-1-/EpCam+
Nkx2-1+
PDGFRa+

Fig4

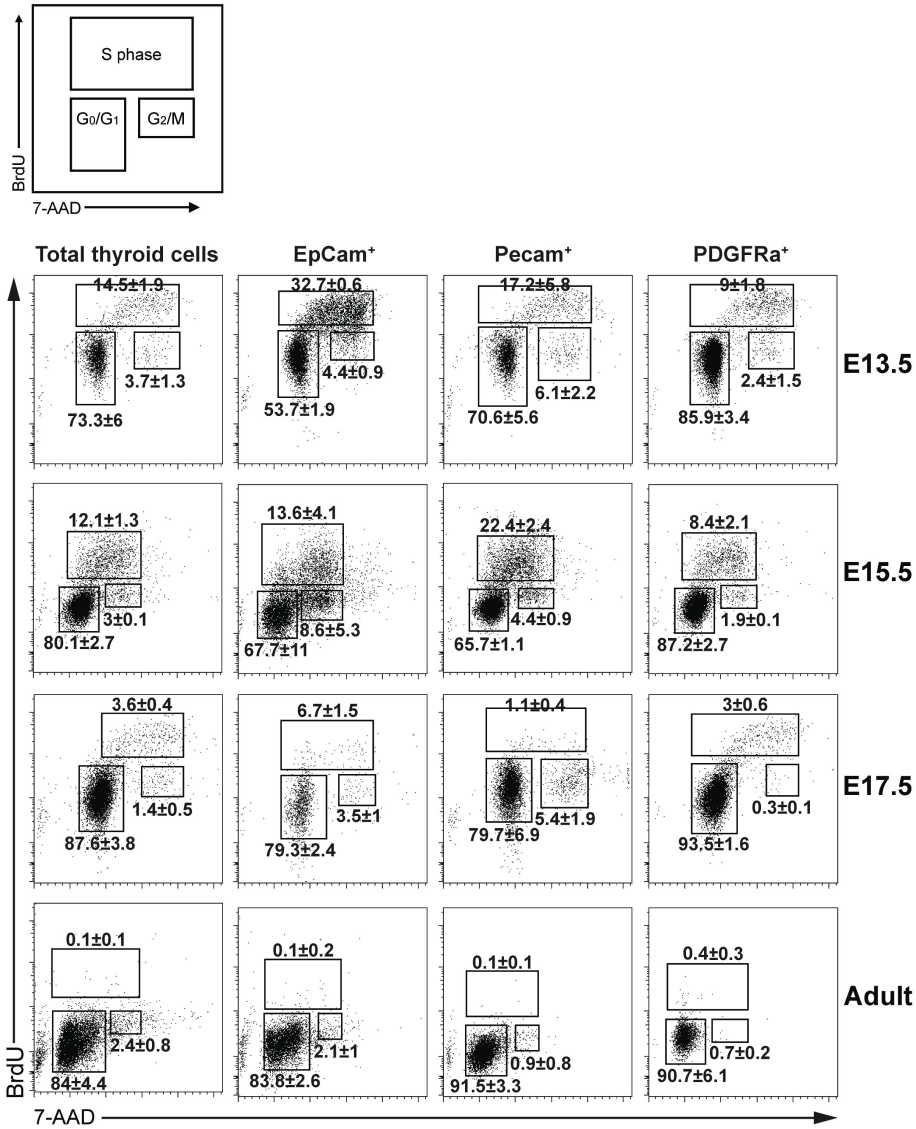
S phase
G0/G1
G2/M
BrdU
7-AAD
Total thyroid cells
EpCam+
Pecam+
PDGFRa+
E13.5
E15.5
E17.5
Adult
14.5±1.9
3.7±1.3
73.3±6
32.7±0.6
4.4±0.9
53.7±1.9
17.2±5.8
6.1±2.2
70.6±5.6
9±1.8
2.4±1.5
85.9±3.4
12.1±1.3
3±0.1
80.1±2.7
13.6±4.1
8.6±5.3
67.7±11
22.4±2.4
4.4±0.9
65.7±1.1
8.4±2.1
1.9±0.1
87.2±2.7
3.6±0.4
1.4±0.5
87.6±3.8
6.7±1.5
3.5±1
79.3±2.4
1.1±0.4
5.4±1.9
79.7±6.9
3±0.6
0.3±0.1
93.5±1.6
0.1±0.1
2.4±0.8
84±4.4
0.1±0.2
2.1±1
83.8±2.6
0.1±0.1
0.9±0.8
91.5±3.3
0.4±0.3
0.7±0.2
90.7±6.1

Fig5

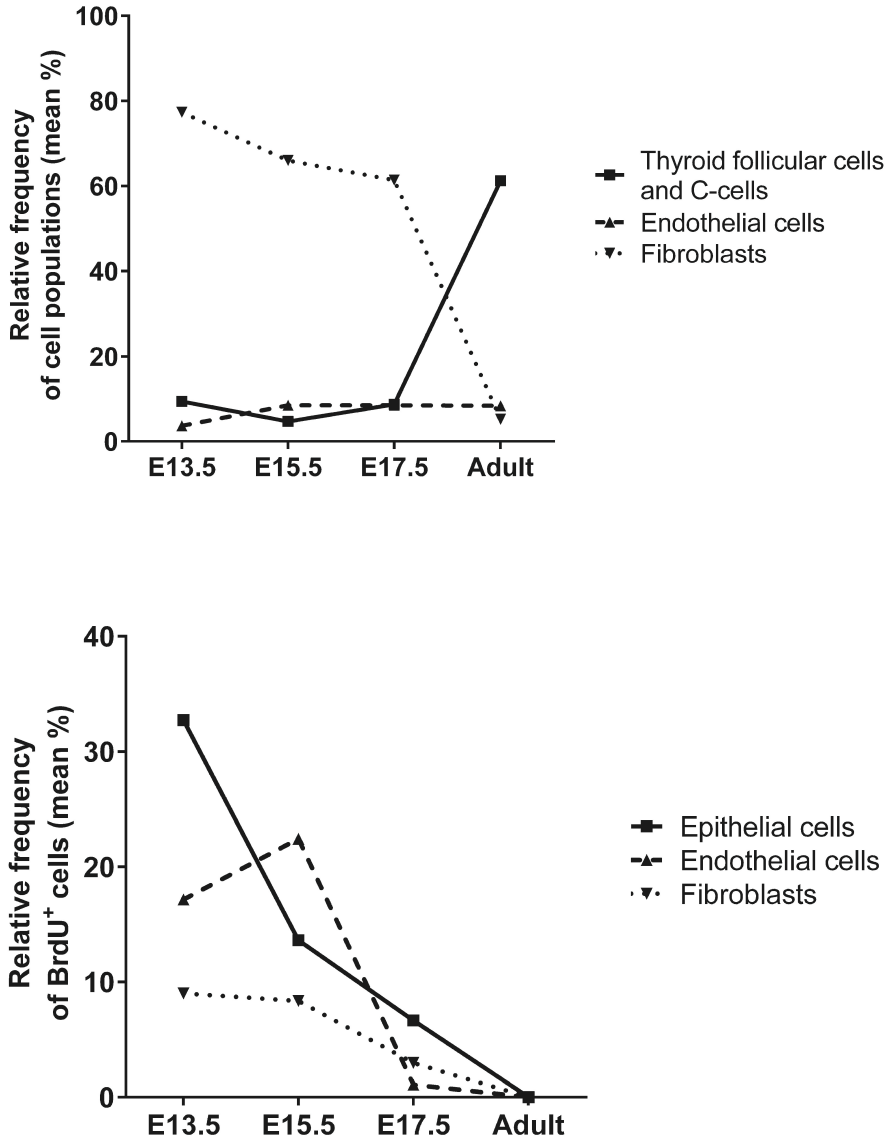
Relative frequency of cell populations (mean %)
100
80
60
40
20
0
E13.5
E15.5
E17.5
Adult
Thyroid follicular cells and C-cells
Endothelial cells
Fibroblasts
Relative frequency of BrdU+ cells (mean %)
40
30
20
10
0
E13.5
E15.5
E17.5
Adult
Epithelial cells
Endothelial cells
Fibroblasts

Figure legends

Figure 1. Gating strategy for flow cytometric analysis of thyroid glands.

A) Representative FACS plot of pooled and fixed E15.5 thyroids demonstrating the gating strategy used for the identification of thyroid cell populations. CD (Cluster of differentiation) numbers are indicated for each antibody, when appropriate, following the original name (e.g. Pecam / CD31). Numbers represent frequencies of cell populations in percent within each panel (and not of the total thyroid). Arrows indicate which gated population is analyzed in the next panel.

Top left panel: Scatter plot: SSC-A (side-scattered area) and FSC-A (forward-scattered area) gate. All events outside this gate are debris. **Top middle panel:** Doublet discrimination: SSC-H (side-scattered height) and SSC-W (side-scattered width) gate, defining singlets. All events outside this gate are doublets or aggregates. **Top right panel:** Right gate represents events that are Nkx2-1$^+$ thyrocytes and C-cells, upper left gate represents events that are CD45$^+$ lymphocytes and lower left gate represents remaining cell populations, that were further analyzed in the next panel**. Bottom right panel:** Right gate represents events that are Pecam$^+$ endothelial cells, upper left gate represents events that are PDGFRa$^+$ fibroblasts and lower left gate represents remaining cell population, that were further analyzed in the next panel**. Bottom middle panel:** Right gate represents events that are EpCam$^+$ epithelial cells, that were Nkx2-1$^-$ in the top right panel, thus representing parathyroid cells, upper left gate represents events that are Ter119$^+$ erythrocytes and lower left gate represents the remaining unknown cell population(s) that is/are characterized as Nkx2-1$^-$/CD45$^-$/Pecam$^-$/PDGFRa$^-$/EpCam$^-$/Ter119$^-$.

B) Validation of cell types by co-labelling with two different antibodies specific for the same cell population. **Left panel:** Top right gate represents events that are co-labeled with Pecam and Icam-1, representing endothelial cells. Events outside the gate represent all other cell populations**. Middle panel:** Top right gate represents events that are $EpCam^+$/E-$cadherin^+$ epithelial cells. All events outside the gate represent all other cell populations**. Right panel:** Top right gate represents events that are $EpCam^+$/$Nkx2\text{-}1^+$ thyrocytes and C-cells, top left gate represents events that are $Epam^+$/$Nkx2\text{-}1^-$ parathyroid cells. All events outside the gate represent all other cell populations**.**

Figure 2. Comparison of absolute cell numbers of the whole thyroid and of each subpoulation at embryonic stages and in adult tissues. One thyroid; data are representative for the whole cell mass of one entire bilobed thyroid gland after exclusion of $Ter119^+$ erythroid cells and $CD45^+$ hematopoietic cells; $Nkx2\text{-}1^+$ cells, thyroid follicular cells and C-cells; $Nkx2\text{-}1^-$/$EpCAM^+$ cells, parathyroid cells; $Pecam^+$ cells, endothelial cells; $PDGFRa^+$ cells, fibroblasts; $Nkx2\text{-}1^-$/$CD45^-$/$Pecam^-$/ $PDGFRa^-$ /$EpCam^-$/$Ter119^-$ cells, unknown cell type. Data represent results from 3 independent experiments (mean±SD) with pools of n=25 bilobed thyroids at E13.5, n=15 bilobed thyroids at E15.5 and E17.5 and n=4 thyroids in adult samples for each experiment.

Figure 3. Relative frequencies of cell populations characterized by flow cytometry in embryonic and adult thyroid tissues. Relative frequencies were calculated after exclusion of erythyroid ($Ter119^+$) and hematopoietic cells ($CD45^+$). Results represent data from 3 independent experiments (mean±SD) with pooled thyroid tissues (n=25 bilobed thyroids at E13.5, n=15 bilobed thyroids at E15.5 and E17.5 and n=4 thyroids in adult samples for each experiment).

Figure 4. Cell cycle analysis at all stages in cell populations. A) Analysis of BrdU incorporation 2 hours after i.p. injection of pregnant mice. Flow cytometry plots depict intracellular expression of BrdU and 7-AAD (7-Aminoactinomycin D), which marks the 2n or 4n DNA. B) The numbers represent frequencies of cells in $G_{0/1}$ phase ($BrdU^-/7\text{-}AAD^{2n}$), S-phase ($BrdU^+/7\text{-}AAD^{2n/4n}$), and G_2/M phase ($BrdU^-/7AAD^{4n}$). Flow cytometry plots depict one representative experiment. The frequencies represent data from 3 independent experiments (mean±SD) with pooled thyroid tissues (n=25 bilobed thyroids at E13.5, n=15 bilobed thyroids at E15.5 and E17.5 and n=4 thyroids in adult samples for each experiment).

Figure 5. Summary of cell growth dynamics of the three main populations of the thyroid gland during late embryonic stages and in adult tissues. A) Representation of the fundamental switch from the fibroblast to the TFC / C-cell population between embryonic and adult stage. B) Cell type-specific distinct proliferative waves during embryonic development.

Tables

Table 1. Absolute cell numbers of the different cell populations in the developing and adult thyroid organ.

Cell populations	**E13.5**	**E15.5**	**E17.5**	**Adult**
Nkx2-1$^+$ cells: Thyroid follicular cells and C-cells	684±91	865±28	2'746±290	166'208±17'334
Nkx2-1$^-$/EpCAM$^+$ cells: Parathyroid cells	109±33	152±27	784±138	47'598±7'008
Pecam$^+$ cells: Endothelial cells	274±75	1'582±663	2'704±238	22'813±4'027
PDGFRa$^+$ cells: Fibroblasts	5'748±1'107	12'151±453	19'541±1'744	14'104±2'346
All$^-$ unknown cells: (Nkx2-1$^-$/CD45$^-$/Pecam/ PDGFRa$^-$/EpCam/Ter119$^-$)	609±154	3'694±291	6'028±670	20'837±9'899
CD45$^+$ cells: Hematopoietic cells	329±58	2'518±314	6'353±442	31'330±12'808
Ter119$^+$ cells: Erythroid cells	28±14	156±29	523±100	1'442±500
Total cell number of one thyroid gland	7'782±1'395	21'118±983	38'681±3'093	304'333±24'732
Total cell number of one thyroid gland without Ter119$^+$ and CD45$^+$ cells	7'425±1'338	18'444±1259	31'804±2'610	271'561±22'325

E, Embryonic day. Data represent results from 3 independent experiments (mean±SD) with pooled tissues (n=25 bilobed thyroids at E13.5, n=15 bilobed thyroids at E15.5 and E17.5 and n=4 thyroids in adult samples for each experiment).

Table 2. Relative frequencies of cell populations in the developing and adult thyroid organ after exclusion of erythroid ($Ter119^+$) and hematopoietic cells ($CD45^+$).

	E13.5	**E15.5**	**E17.5**	**Adult**
$Nkx2\text{-}1^+$ cells: Thyroid follicular cells and C-cells	9.4±1.6%	4.7±0.4%	8.7±0.9%	61.2±1.1%
$Nkx2\text{-}1^-/EpCam^+$ cells: Parathyroid cells	1.5±0.4%	0.8±0.2%	2.5±0.6%	17.8±3.9%
$Pecam^+$ cells: Endothelial cells	3.7±0.8%	8.5±3.0%	8.5±0.2%	8.4±1.1%
$PDGFRa^+$ cells: Fibroblasts	77.3±1.1%	66.0±2.5%	61.4±0.4%	5.2±0.8%
All^- unknown cells: ($Nkx2\text{-}1^-/CD45^-/Pecam^-/PDGFRa^-/EpCam^-/Ter119^-$)	8.2±0.9%	20.0±0.7%	18.9±1.0%	7.5±2.9%

E, Embryonic day. Data represent results from 3 independent experiments (mean±SD) with pooled tissues (n=25 bilobed thyroids at E13.5, n=15 bilobed thyroids at E15.5 and E17.5 and n=4 thyroids in adult samples for each experiment).

4.2 Epigenetic changes during thyroid development *in vivo*.

In a first line of research, we decided to investigate the possible epigenetic changes associated with histone acetylation during thyroid development *in vivo* at three levels. We analyzed, whether HDAC expression, HDAC activity and histone acetylation was dynamically changed during thyroid development.

4.2.1 General HDAC activity

In order to investigate the changes in HDAC activity during mouse thyroid development, total HDAC activity assay was carried out in TFC precursors (E13.5), in differentiating TFCs (E15.5), and in adult TFCs. Total HDAC activity decreased by 28% from E13.5 to E15.5 developmental stage and by 60% between E13.5 and adult stage (Figure 10).

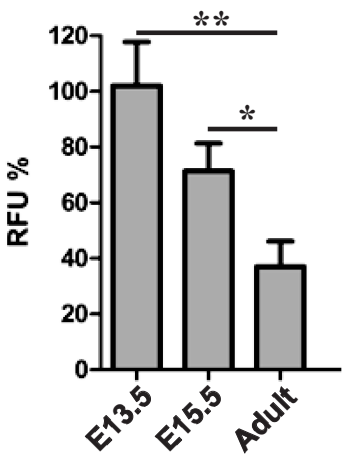

Figure 10. HDAC activity at different stages of TFC differentiation. Total HDAC enzymatic activity was measured from E13.5 (set to 100%) to adult thyroids. Each column represents triplicates of n=16 pooled embryonic thyroids at E13.5 and E15.5, and n= 3 at adult stage. RFU, Reference Fluorescence Units. Bar diagrams display the mean, SD and one-way ANOVA with Tukey's Multiple Comparison post test (*P < 0.05, **P < 0.01, ***P< 0.001, n = 3).

4.2.2 Expression of HDAC1 and HDAC2

The histone deacetylases HDAC1 and HDAC2 play a very important role in developmental processes and exhibit developmental stage and lineage-specific expression patterns. To examine the individual contribution of these deacetylases during thyroid development, we measured the expression levels of HDAC1 and HDAC2 using flow cytometry at E13.5, E15.5, E17.5 and adult thyroid. Cells were first labeled with antibodies for respective cell type: anti-EpCAM for epithelial cells, anti-PECAM for endothelial cells and anti-PDGFRa for fibroblasts and later labeled with HDAC1 or HDAC2. Differences in the levels of HDACs in total thyroid cells, and in epithelial cells, endothelial cells and fibroblasts at E13.5, E15.5,

E17.5 and adult thyroid are shown in a representative Figure 11A for HDAC1 and Figure 12A for HDAC2. For quantification, HDAC levels were measured as geometric mean fluorescence units (MFIs).

The level of HDAC1 in total thyroid cells was highest at E13.5 and at E15.5 (Figure 11B). Significant decrease by 28% was observed between E13.5 and E17.5, and further decrease by 28% in adult thyroid. In epithelial cells, the HDAC1 levels are highest at E13.5 and in adult, and significant decrease by 41% was observed at E15.5 and E17.5. In endothelial cells, the HDAC1 levels are highest in E13.5 and significant decrease by 23% was observed at E15.5, further decrease by 30% at E17.5. Fibroblasts had highest HDAC1 levels at E13.5 and at E15.5, and significant decrease by 26% is observed at E17.5. No change was observed between E17.5 and adult thyroid.

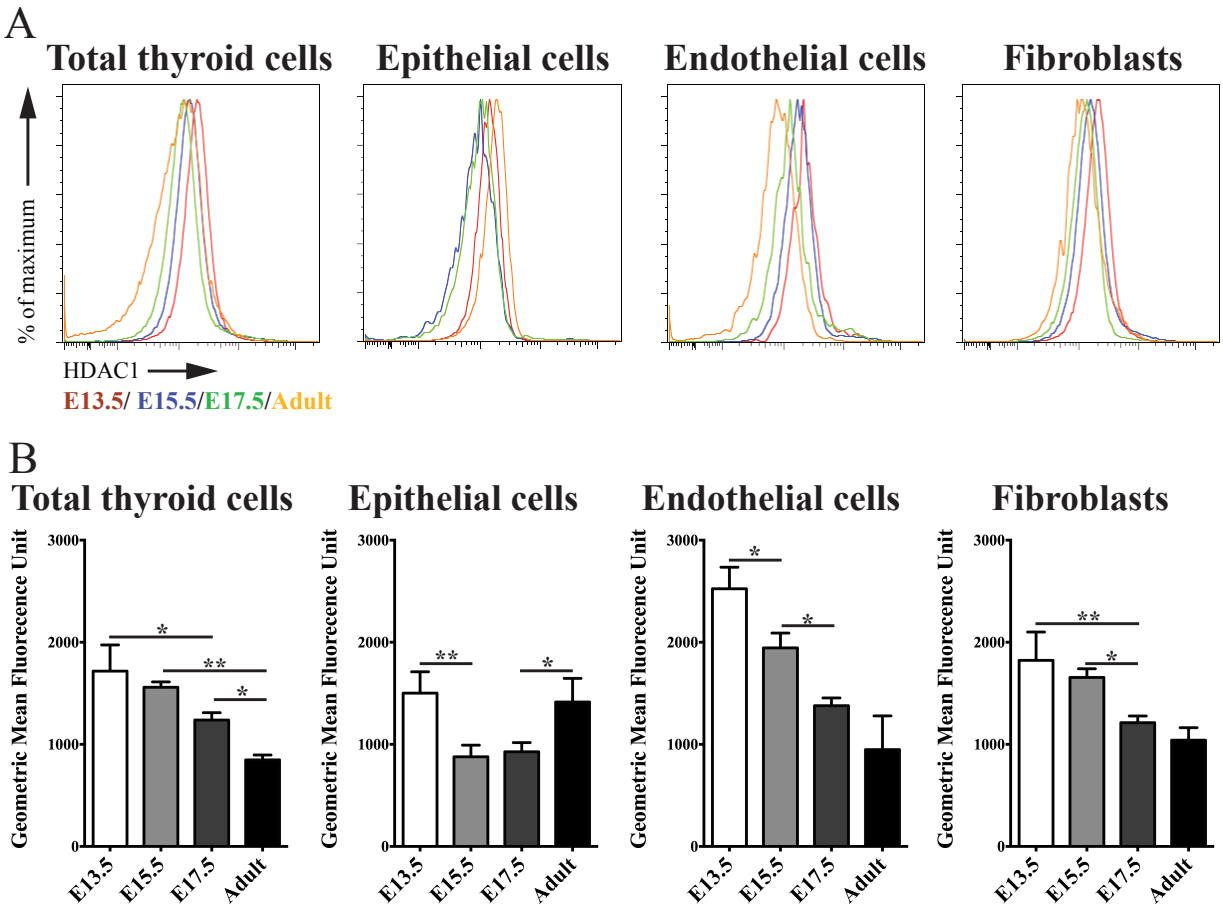

Figure 11. Chromatin flow cytometry quantitates HDAC1 levels in developing and adult thyroid. A flow cytometry plot representation of HDAC1 levels in E13.5 (red peak), E15.5 (blue peak), E17.5 (green peak) and in adult thyroid (orange peak) after immunofluoroscently staining various thyroid cell types with HDAC1 antibody (A). Geometric mean florescence intensity (MFI) of HDAC1 in total thyroid cells, epithelial cells, endothelial cells and fibroblasts of E13.5, E15.5, E17.5 and adult thyroid (B). Bar diagrams display the mean, SD and one-way ANOVA with Tukey's Multiple Comparison post test (*$P < 0.05$, **$P < 0.01$, ***$P < 0.001$, n =3).

The level of HDAC2 in total thyroid cells was highest at E13.5 and significant decrease by 53% was observed at E15.5 and further decrease by 43% at E17.5 (Figure 12B). In epithelial cells, the HDAC2 levels are highest in E13.5 and significant decrease by 38% was observed at E15.5. In endothelial cells, the HDAC2 levels are highest at E13.5 and at E15.5, and significant decrease by 45% was observed at E17.5, and further significant decrease by 51% in adult thyroid. Fibroblasts have highest HDAC2 levels at E13.5 and significant decrease by 53% was observed at E15.5, and further significant decrease by 41% at E17.5. No change is observed between E17.5 and adult thyroid.

Thus, HDAC1 and HDAC2 levels shown dynamic pattern during mouse thyroid development and can be measured with flow cytometry.

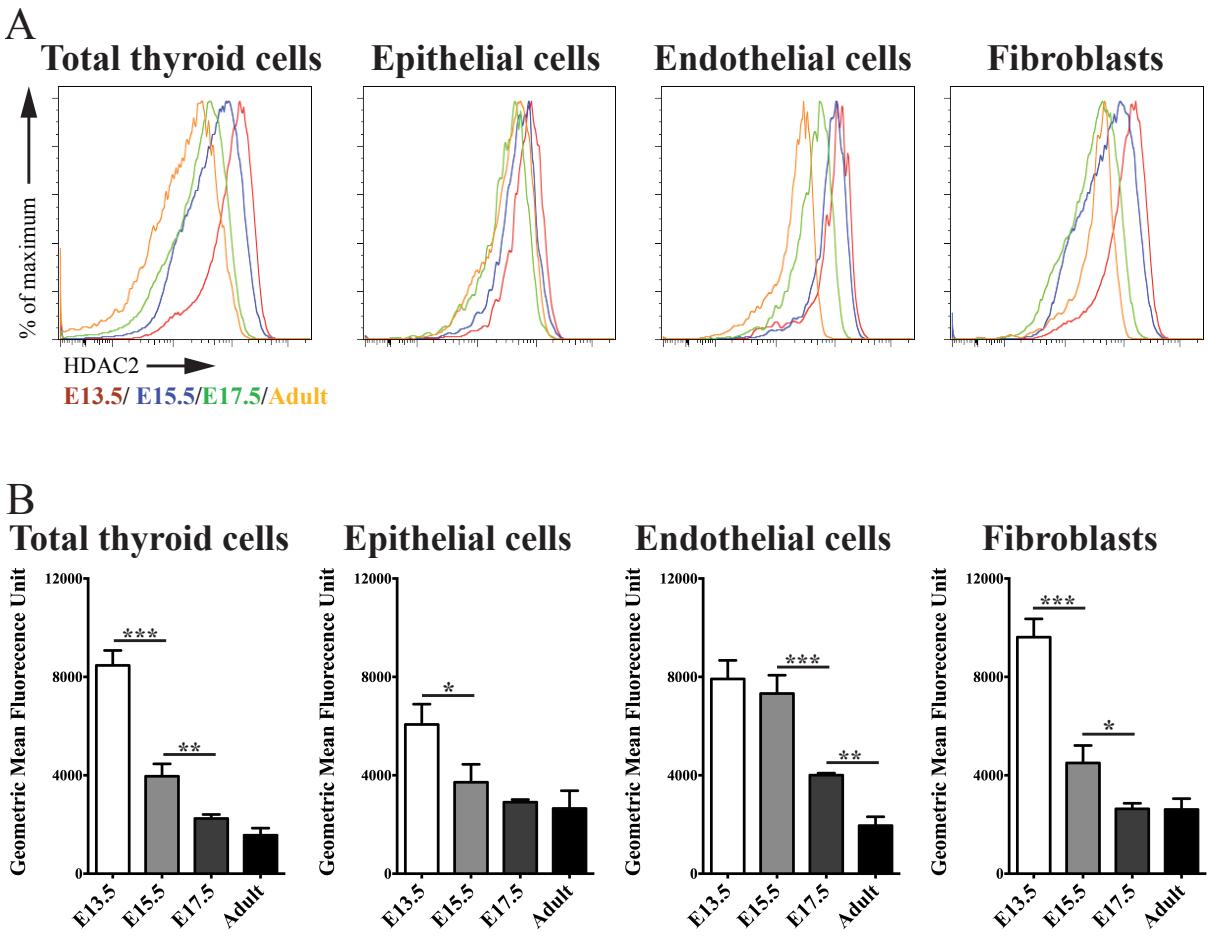

Figure 12. Chromatin flow cytometry quantitates HDAC2 levels in developing and adult thyroid. A flow cytometry plot representation of HDAC2 levels in E13.5 (red peak), E15.5 (blue peak), E17.5 (green peak) and in adult thyroid (orange peak) after immunofluoroscently staining various thyroid cell types with HDAC2 antibody (A). Geometric mean florescence intensity (MFI) of HDAC2 in total thyroid cells, epithelial cells, endothelial cells and fibroblasts of E13.5, E15.5, E17.5 and adult thyroid (B). Bar diagrams display the mean, SD and one-way ANOVA with Tukey's Multiple Comparison post test (*$P < 0.05$, **$P < 0.01$, ***$P < 0.001$, n = 3)

4.2.3 Expression of H3K9acetylation

Since the acetylation state of histones modulates chromatin structure and epigenetically regulates gene expression, we first checked the levels of histone H3K9ac in mouse thyroid by flow cytometry.

Cells were first labeled with antibodies for respective cell type: anti-EpCAM for epithelial cells, anti-PECAM for endothelial cells and anti-PDGFRa for fibroblasts and later labeled with H3K9ac. Differences in the levels of H3K9ac in total thyroid cells, and in epithelial cells, endothelial cells and fibroblasts at E13.5, E15.5, E17.5 and adult thyroid are shown in a representative Figure 13A. For quantification, H3K9ac levels obtained in adult were kept as 1 and fold change to adult was calculated as shown for E13.5, E15.5 and E17.5 (Figure 13B). The level of H3K9ac in total thyroid cells was increased by 5-fold at E13.5 and E15.5, and 3.5-fold at E17.5. In epithelial cells, 2.5-fold increase was observed at E13.5, and 1.5-fold at E15.5 and at E17.5. In endothelial cells, 4-fold increase was observed at E13.5, E15.5 and at E17.5. In fibroblasts, 5-fold increase was observed at E13.5, E15.5 and 3-fold at E17.5. In aggregate, acetylation of histone H3K9 shows dynamic pattern in different cell types at various developmental stages during mouse thyroid development.

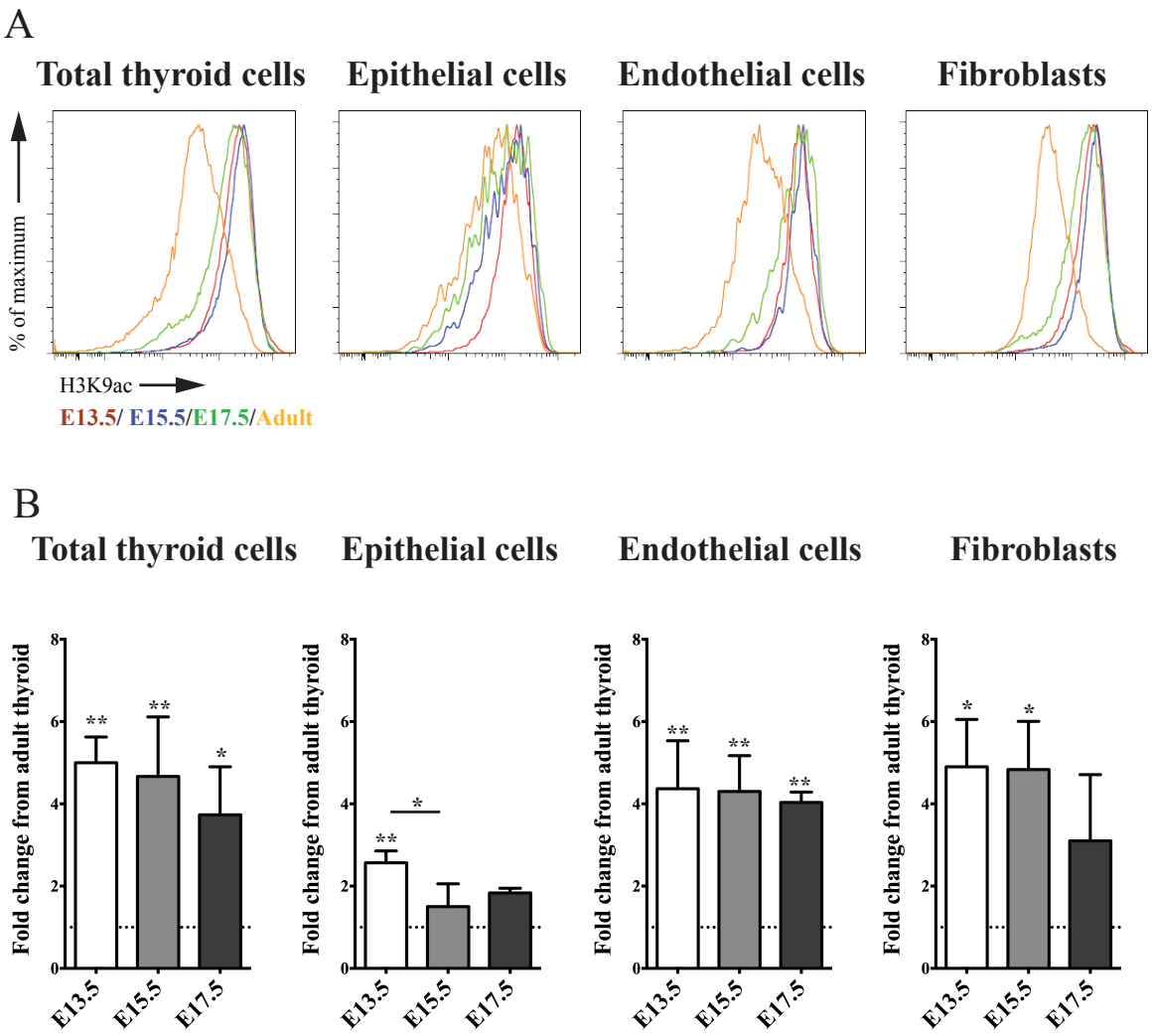

Figure 13. Chromatin flow cytometry quantitates histone H3K9ac levels in developing and adult thyroid. A flow cytometry plot representation of H3K9ac levels in E13.5 (red peak), E15.5 (blue peak), E17.5 (green peak) and in adult thyroid (orange peak) after immunofluoroscently staining various thyroid cell types with H3K9ac antibody (A). Geometric mean florescence intensity (MFI) of H3K9ac in total thyroid cells, epithelial cells, endothelial cells and fibroblasts was calculated and the MFI of adult thyroid was set to 1, as indicated by dotted line, and the fold response to adult was calculated. Bar diagrams display the mean, SD and one-way ANOVA with Tukey's Multiple Comparison post test (*P < 0.05, **P < 0.01, ***P< 0.001, n = 3).

4.3 Effect of HDAC inhibition on thyroid development *ex vivo*.

In a second line of research, we decided to modify HDAC activity pharmacologically in an *ex vivo* culture model of the developing thyroid and to analyze the effect of HDAC inhibition on key steps of thyroid development.

4.3.1 Effect of HDAC inhibition on epigenetic markers

To quantify the effect of HDAC inhibition on epigenetic parameters, we chose to quantify; 1) changes in total HDAC enzymatic activity, 2) changes in acetylation of a specific histone mark H3K9 by immunohistochemistry and flow cytometry, and 3) to provide evidence of change at H3K9 by HDACi, we were able to quantify for the first time by flow cytometry the epigenetic switch from methylated to acetylated state at H3K9.

General HDAC activity in our *ex vivo* culture model

In order to validate our *ex vivo* culture model for epigenetic research, we investigated the changes in HDAC activity in our *ex vivo* model during mouse thyroid development. Total HDAC activity assay was carried out in TFC precursors (E13.5), in differentiating TFCs (E13.5 + 3d), and in adult thyroids (Adult + 7d). Total HDAC activity decreased by 40% from E13.5 to E13.5 + 3d developmental stage and by 80% between E13.5 and adult thyroid (Figure 14). These results provided evidence that developmental changes of total HDAC activity in our culture model recapitulated HDAC activity levels *in vivo* (Figure 10).

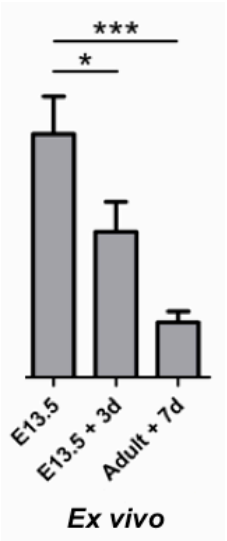

Figure 14. HDAC activity measured *ex vivo*. Total HDAC enzymatic activity was measured at E13.5 (set to 100%), at E13.5 +3d and at Adult +7d stages. Each column represents triplicates of n=16 pooled embryonic thyroids at E13.5 and at E13.5 + 3d, and n= 3 at adult stage. RFU, Reference Fluorescence Units. Bar diagrams display the mean, SD and one-way ANOVA with Tukey's Multiple Comparison post test (**P* < 0.05, ***P* < 0.01, ****P*< 0.001, n = 3).

General HDAC activity after HDAC inhibition

In order to investigate the changes in HDAC activity in our *ex vivo* model after HDACi during mouse thyroid development, total HDAC activity assay was carried out in E13.5 + 3d thyroid explants without any treatment (Control), and with HDAC inhibitors VPA 1mM and TSA 5uM, and with HATi Curcumin 10uM. Total HDAC activity decreased by 50% after HDACi by VPA and TSA and no change was observed after HATi by curcumin as expected (Figure 15). Thus, pharmacological modulation of HDAC activity by VPA and TSA was effective in our model.

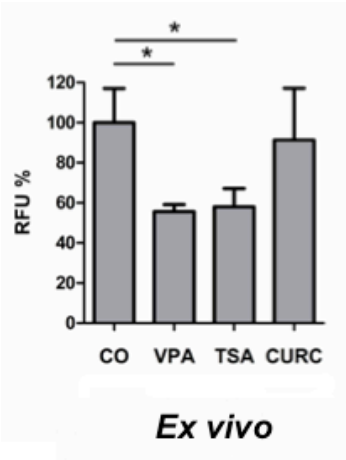

Figure 15. HDAC activity measured *ex vivo* after HDACi. Total HDAC enzymatic activity was measured at E13.5 +3d, control (set to 100%), and after treatment with HDACi VPA 1mM and TSA 5uM, and HATi Curcumin 10uM. Each column represents triplicates of n=16 pooled embryonic thyroids at E13.5 and at E13.5 + 3d, and n= 3 at adult stage. RFU, Reference Fluorescence Units. Bar diagrams display the mean, SD and one-way ANOVA with Tukey's Multiple Comparison post test (**P* < 0.05, ***P* < 0.01, ****P*< 0.001, n = 1).

H3K9acetylation/trimethylation after HDAC inhibition

To investigate whether an epigenetic switch occurs in a spatiotemporal manner between two histone marks on the same specific residue, one mark that is usually associated with gene activation and other usually with gene repression, we first measured the pattern of H3K9ac (mark for gene activation) and H3K9me3 (mark for gene repression) by immunohistochemistry. E13.5 thyroids were cultured for 3 days and 7 days, without (control) and with HDACi (VPA 1mM), and were immunostained for H3K9 acetyl or H3K9 tri-methyl histone marks (Figure 16A- 16D). The fluorescence intensity for H3K9ac after 3 days of culture in control was higher in the periphery than in the center whereas in VPA 1mM treated explants, it was heterogenous throughout the explant (Figure 16A). After 7 days of culture, fluorescence intensity for H3K9ac was higher throughout the VPA 1mM treated explants than in control (Figure 16B). The fluorescence intensity for H3K9me3 after 3 days of culture in control was higher in the center than in the periphery whereas it was higher in the periphery in VPA 1mM treated explants (Figure 16C). After 7 days of culture, fluorescence intensity for

H3K9me3 was higher throughout the VPA 1mM treated explant and was higher in the periphery in the control explant (Figure 16D). In summary, an inverse spatial distribution of H3K9ac vs. H3K9me3 was observed in control tissues at day 3 and day 7. In VPA treated tissues, no clear pattern was detected.

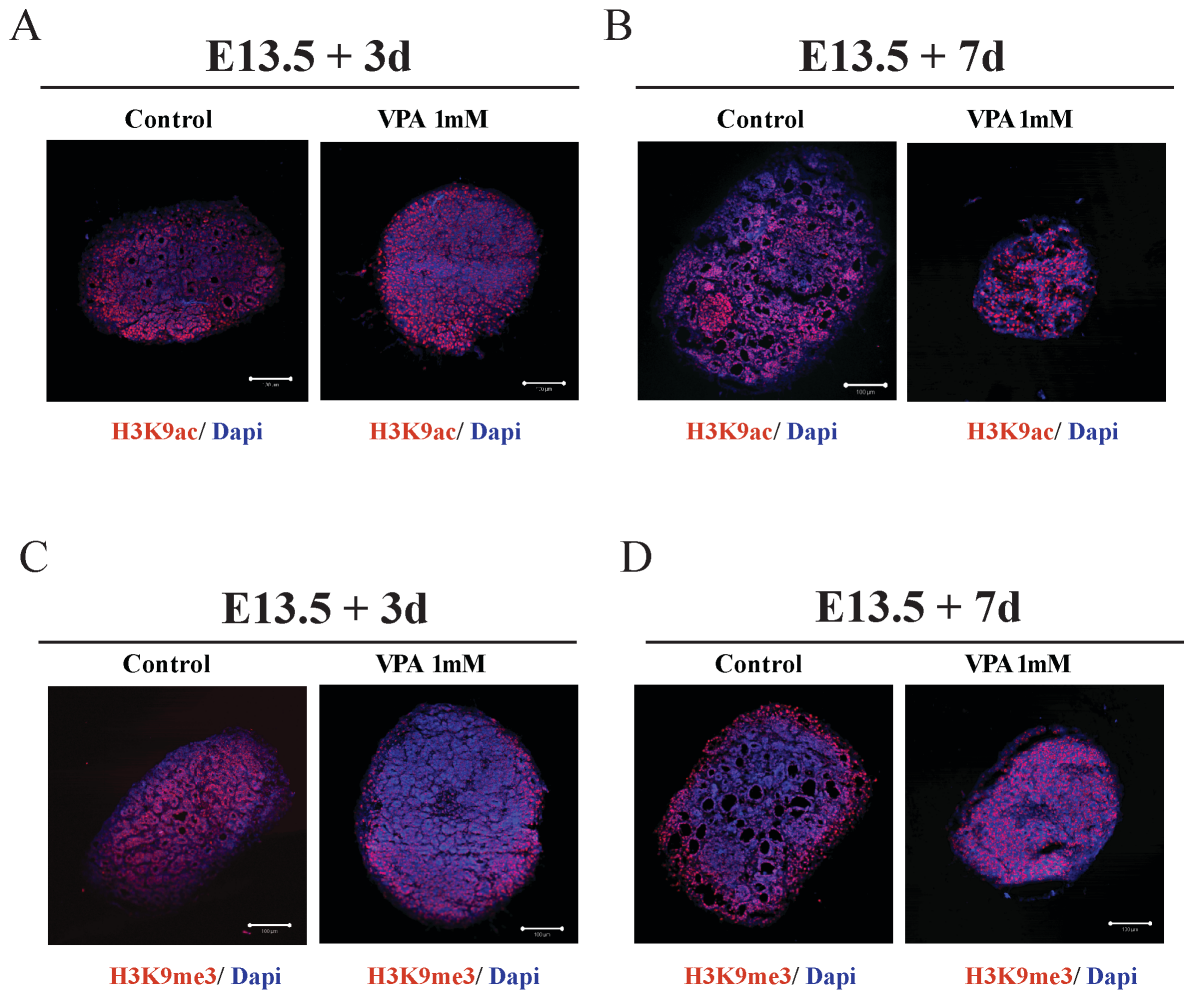

Figure 16. H3K9 acetylation and H3K9 tri-methylation after HDAC inhibition ex vivo. OCT embedded thyroid cultures with and without VPA 1mM treatment for 3 days (Figure A and C) and 7 days (Figure B and D) were cut in sections and analyzed by immunofluorescence microscope (A-D). Sections were stained for Dapi (blue), H3K9ac (red) (A-B) and H3K9me3 (red) (C-D) Scale bar = 100 uM.

Next, as observed spatial labeling patterns of H3K9ac and H3K9me3 did not provide detailed information on changes in individual cell types after HDAC inhibition, we then quantified the levels of acetylation (H3K9ac) and tri-methylation (H3K9me3) at H3K9 residue by flow cytometry in all thyroid cells as well as in each individual thyroid cell populations. Cells were first labeled with antibodies for respective cell type: anti-EpCAM for epithelial cells, anti-PECAM for endothelial cells and anti-PDGFRa for fibroblasts and later labeled with H3K9ac.

Differences in the levels of H3K9ac in epithelial cells, endothelial cells, fibroblasts, and total thyroid cells and at E13.5+3d are shown in a representative Figure 17A. H3K9ac levels obtained after HDACi in control explants are kept at 1 and fold change from control are calculated. Significant changes were observed in the levels of H3K9ac after 3 days of culture (Figure 17B). 2-fold increase in H3K9ac levels was observed on HDACi in total thyroid cells, epithelial cells, endothelial cells and fibroblasts respectively. Significant 1.5-fold increase in H3K9ac levels was observed in epithelial cells and total thyroid cells after 7 days of culture (Figure 17C). This suggested that HDAC inhibition caused increased H3K9 acetylation in all cell types after 3 days. This effect was only maintained over 7 days in epithelial cells.

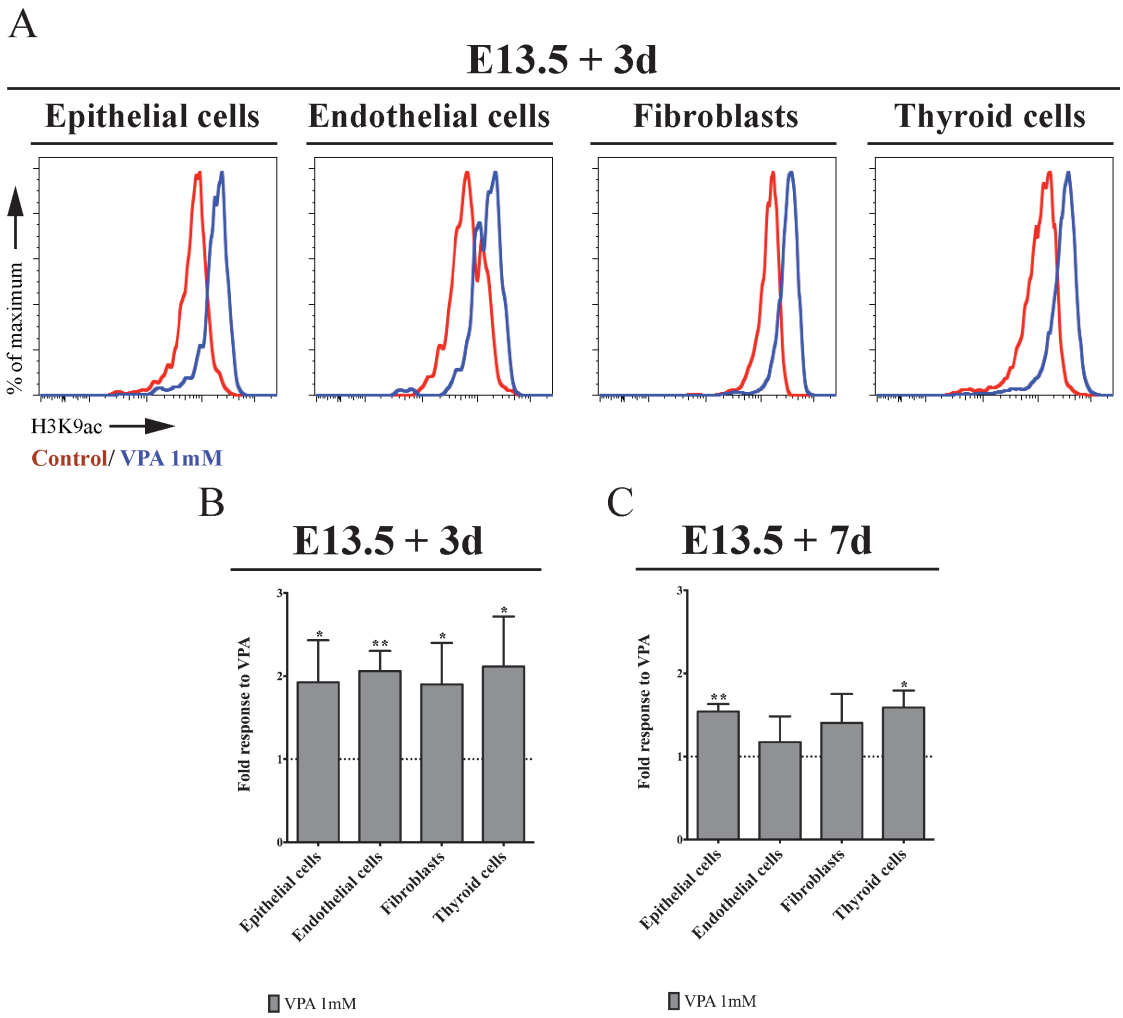

Figure 17. Flow cytometry changes in H3K9 acetylation after HDAC inhibition *ex vivo*. A representative flow cytometry plot of H3K9ac levels in control (red peak) and with VPA 1mM treatment (blue peak) after 3 days of culture (A). Changes in H3K9ac levels in control and VPA 1mM treated explants as measured by flow cytometry after immunofluoroscently staining with H3K9ac antibody after 3 days (B) and 7 days (C). Geometric mean florescence intensity (MFI) of H3K9ac in each cell type was calculated and the MFI of control was set to 1, as indicated by dotted line, and the fold response to VPA was calculated. Bar diagrams display the mean, SD and t test statistics (*$P < 0.05$, **$P < 0.01$, ***$P < 0.001$, unpaired t test, n = at least 3).

To observe an epigenetic switch, H3K9ac and H3K9me3 levels obtained after 3 days of culture were further measured in HDACi treated and non treated (control) explants and their MFI was calculated. Levels in control explants are kept at 1 and fold change from control are calculated. Significant changes were observed in the levels of H3K9ac and H3K9me3 (Figure 18). 2 fold increase in H3K9ac and 0.5 fold decrease in H3K9me3 was observed in total thyroid cells, endothelial cells and fibroblasts respectively, whereas in epithelial cells, significant 2 fold increase was seen in H3K9ac and no significant change was seen in H3K9me3 levels. Thus an epigenetic switch occurred at histone H3K9 residue on HDACi between the transcription activating mark (H3K9ac) and transcription repressive mark (H3K9me3).

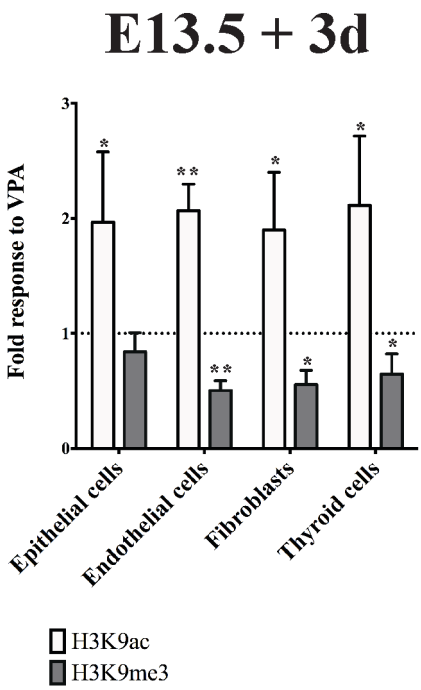

Figure 18. Epigenetic switch at H3K9 residue as analyzed by flow cytometry. Changes in H3K9ac and H3K9me3 levels in control and VPA 1mM treated cultures as measured by FACS after 3 days. Geometric mean florescence intensity (MFI) of H3K9ac or H3K9me3 in each cell type was calculated and the MFI of control was set to 1, as indicated by dotted line, and the fold response to VPA was calculated. Bar diagrams display the mean, SD and t test statistics (**P* < 0.05, ***P* < 0.01, ****P*< 0.001, unpaired t test, n = at least 3).

4.3.2 Effect of HDAC inhibition on thyroid development

After having provided proof of significant changes of HDAC activity and as a consequence an increased level of H3K9 acetylation associated with concomitant decrease in H3K9 tri-methylation, we analyzed the effect of the disordered histone code on thyroid development. To do so we analyzed the effect of HDACi on folliculogenesis, angiogenesis, proliferation and gene expression.

HDACi treatment suppresses follicle formation

We first analyzed the effect of HDAC inhibition during mouse thyroid development with HDAC inhibitor Valproic acid (VPA) on the formation of thyroid follicles. Thyroid follicle is the functional unit of thyroid gland and proper formation of thyroid follicle is one of the final key steps of thyroid development and lack of follicles is a hallmark of TD. E13.5 thyroids were cultured on floating filters at the air-medium interface for 3 and 7 days. Under control conditions, the TFCs start to form thyroid follicles after 3 days and complete follicle formation occurs after 7 days, thus replicating the thyroid development process *in vivo*. Effect of HDACi on structural differentiation of these explants was analyzed in presence and absence (control) of increasing dose of VPA from 0.5 mM to 1.5 mM.

First, hematoxylin/eosin staining of the explants revealed that in the absence of VPA treatment, thyroid follicles start to form at day 3 (Figure 19A, shown with an arrow) and folliculogenesis with enlargement of the follicle surface is ongoing at day 7 of culture (whole process of folliculogenesis was completed by day 7) (Figure 19B, shown with an arrow). In contrast, with VPA treatment, drastic clear decrease in follicle number and follicle surface formation was observed at day 3 and day 7 (Figure 19A and 19B).

Secondly, morphometric analyses of HE stained sections was done to quantify 1) the total number of follicles per section and 2) - to compensate for decreased tissue size after VPA treatment - the total follicle surface per tissue surface for each treatment condition. Significant dose dependent decrease in the total number of follicles formed (day 3 and 7) as well as the total follicle surface per tissue surface (day 7) was observed after HDAC inhibition by VPA (Figures 19C and 19D, and Table 3). Thus, HDAC inhibition by VPA inhibited follicle formation.

Table 3. Total follicle surface at E13.5+7 in control and VPA treated thyroids. Results represent analysis of 10 tissues for each condition *** $P<0.001$

Mean follicle surface /tissue surface (um^2/um^2)	Control	VPA 0.5mM	VPA 0.75mM	VPA 1.0mM	VPA 1.5mM
mean	0.038	0.006 ***	0.005 ***	0.004 ***	0.002 ***
SD	0.016	0.003	0.002	0.003	0.001

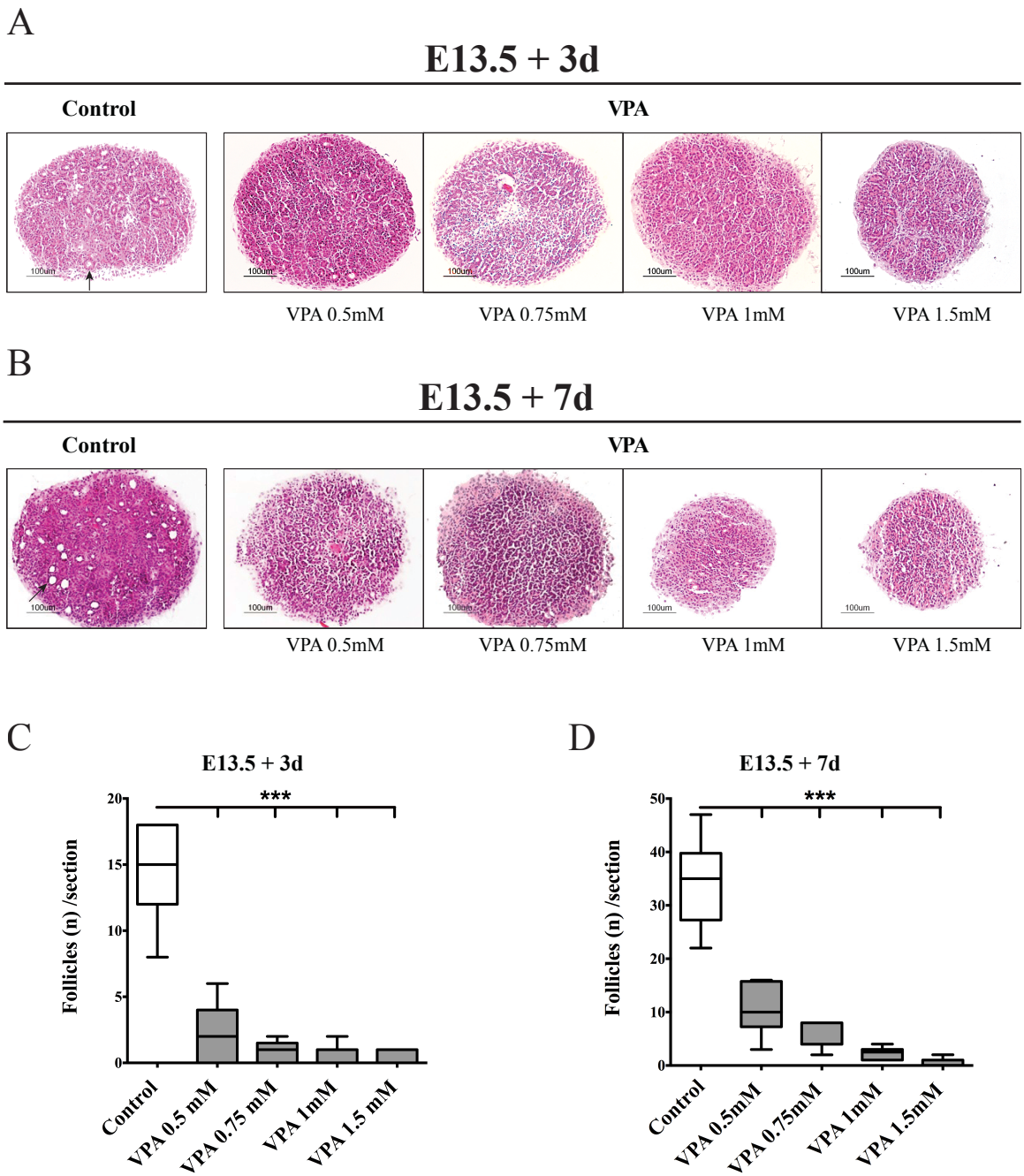

Figure 19. Dose dependent decrease in follicle numbers. E13.5 mouse thyroids were cultured at the air-medium interface for 3 and 7 days, with or without HDACi VPA. VPA was added at increasing doses from 0.5 mM to 1.5 mM. Untreated cultures were analyzed as control tissues. Representative images of hematoxylin/eosin staining after 3 (A) and 7 (B) days in culture are shown. An arrow indicates a thyroid follicle formed at day 3 (A) and day 7 (B) in control culture. Fewer follicles were observed with VPA treatment than in the control at day 3 and 7. Morphometric analysis revealed dose dependent significant decrease in the total follicles formed after VPA treatment at day 3 (C) and 7 (D) than in the control. Scale bar, 100 um. Bar diagrams display the mean, SD and t test statistics. Each column represents analysis of at least 5 cultures. Each section of the culture was measured twice (***$P< 0.001$, unpaired t test, n = 3).

Morphometric analyses of surface area of the explants were done to quantify change in surface area after HDACi. Significant dose dependent decrease in the surface area at day 3 was observed after HDAC inhibition by VPA (Figure 20). Thus, HDAC inhibition by VPA

suggested disturbed growth of the explants. Since we observed smaller explant surface by hematoxylin and eosin stain, we quantified the difference in surface area between control and the four applied VPA doses.

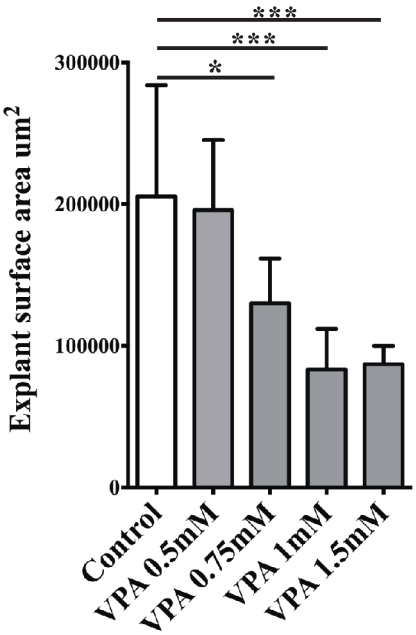

Figure 20. Dose dependent decrease in surface area of the explants. E13.5 mouse thyroids were cultured at the air-medium interface for 7 days, with or without HDACi VPA. VPA was added at increasing doses from 0.5 mM to 1.5 mM. Untreated explants were analyzed as control tissues. Morphometric analysis revealed dose dependent significant decrease in the explant surface area formed after VPA treatment at day 3 than in the control. Bar diagrams display the mean, SD and t test statistics. Each column represents analysis of at least 5 explants. Each section of the explant was measured twice (***P< 0.001, unpaired t test, n = 3).

HDACi disturbs angiogenesis

To assess whether HDACi has an effect on angiogenesis during thyroid development, E13.5 thyroids were cultured for 3 and 7 days, without (control) and with (VPA 1mM). Explants were then immunostained with endothelial cell specific antibody anti-PECAM and thyrocyte specific antibody anti-NKX2-1 (Figure 21A and 21B). In control explants, abundant network of blood vessels surrounding the thyroid follicle was observed after 3 and 7 days of culture. However, decreased network of blood vessels was observed after VPA treatment after 3 and 7 days of culture suggesting disturbance in angiogenesis in these explants.

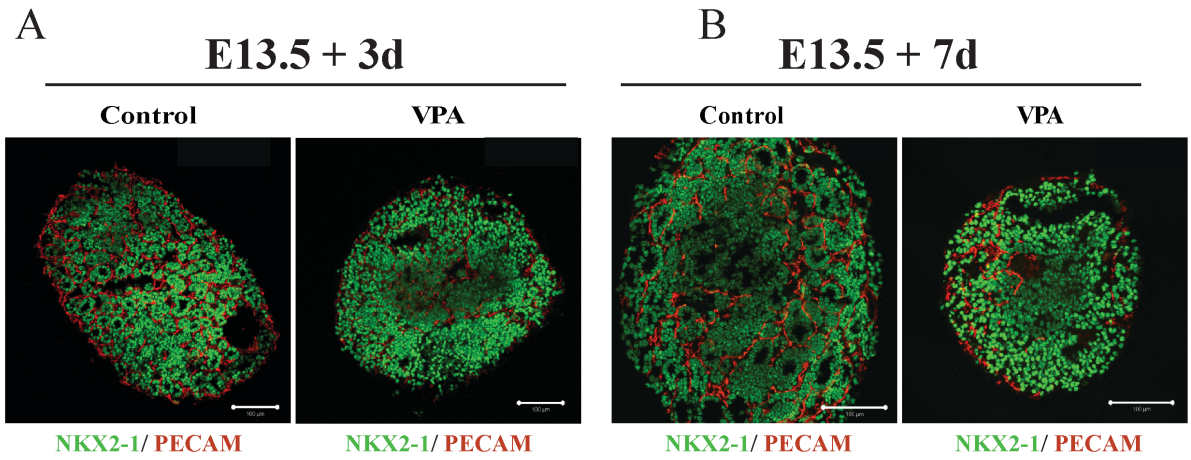

Figure 21. HDAC inhibition inhibits angiogenesis. OCT embedded thyroid cultures with and without VPA 1mM treatment for 3 days (A) and 7 days (B) and analyzed by confocal microscope. Sections were stained for NKX2-1 (green; thyrocytes and C-cells) and PECAM (red; endothelial cells). Scale bar = 100 uM.

HDACi treatment does not induce apoptosis

To investigate whether apoptosis is induced after HDACi on E13.5 thyroids cultured for 3 and 7 days, we performed Terminal deoxynucleotidyl transferase (TdT) dUTP Nick-End Labeling assay (TUNEL) on the explants. Using TUNEL assay, we found out that VPA treatment after 3 and 7 days did not modify the number of apoptotic cells (Figure 22A). This was confirmed by performing Annexin V- Propidium iodide (PI) staining on these explants and no significant difference was observed in HDACi treated explants as compared to control, either after 3 or 7 days (Figure 22B). These results show that HDACi treatment does not modify apoptosis and further suggests that the effects of HDACi on thyroid differentiation and development are direct.

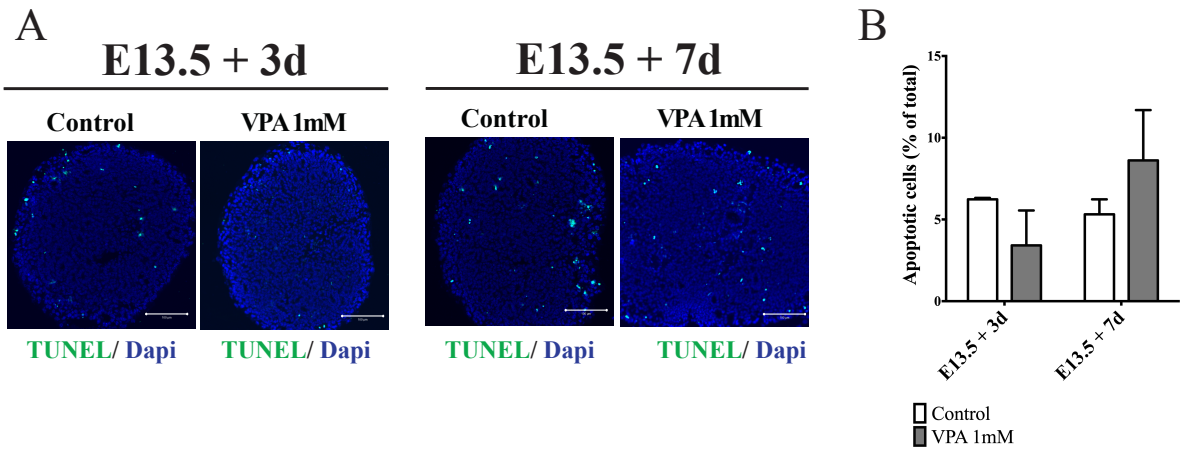

Figure 22. HDACi treatment does not induce apoptosis. Immunohistochemical staining of thyroid cultures treated with HDACi VPA 1mM for 3 and 7 days (A). TUNEL positive cells are shown in green color and nuclei of all the cells were stained with Dapi, shown in blue. Scale bar = 100 uM. Annexin V – Propidium iodide (PI) staining by flow cytometry on the explants in column graphs (B).

Direct effect of HDACi on follicle formation

So far, decreased follicle formation and angiogenesis was observed in HDACi treated tissues. (Figures 19 and 21, respectively). To assess whether HDACi inhibits follicle formation and angiogenesis both directly, or decreased follicle formation would be a consequence of decreased angiogenesis, we used an angiogenesis inhibitor Sunitinib. E13.5 thyroids were treated without (control) and with the angiogenesis inhibitor Sunitinib 1uM for 3 and 7 days. Explants were immunostained with endothelial cell specific antibody anti-PECAM and thyrocyte specific antibody anti-NKX2-1 (Figures 23A and 23B). Huge network of blood vessels was observed around thyroid follicles in control tissues after 3 and 7 days, however it was completely absent in Sunitinib treated explants. Absence of endothelial cells was also confirmed by performing flow cytometry on these explants as no CD31 (PECAM) positive cells are seen (Figures 23C and 23D). However, in spite of no angiogenesis, we still observed some but reduced follicle formation compared to control, suggesting that HDAC inhibition has direct effects on both, follicle formation and angiogenesis.

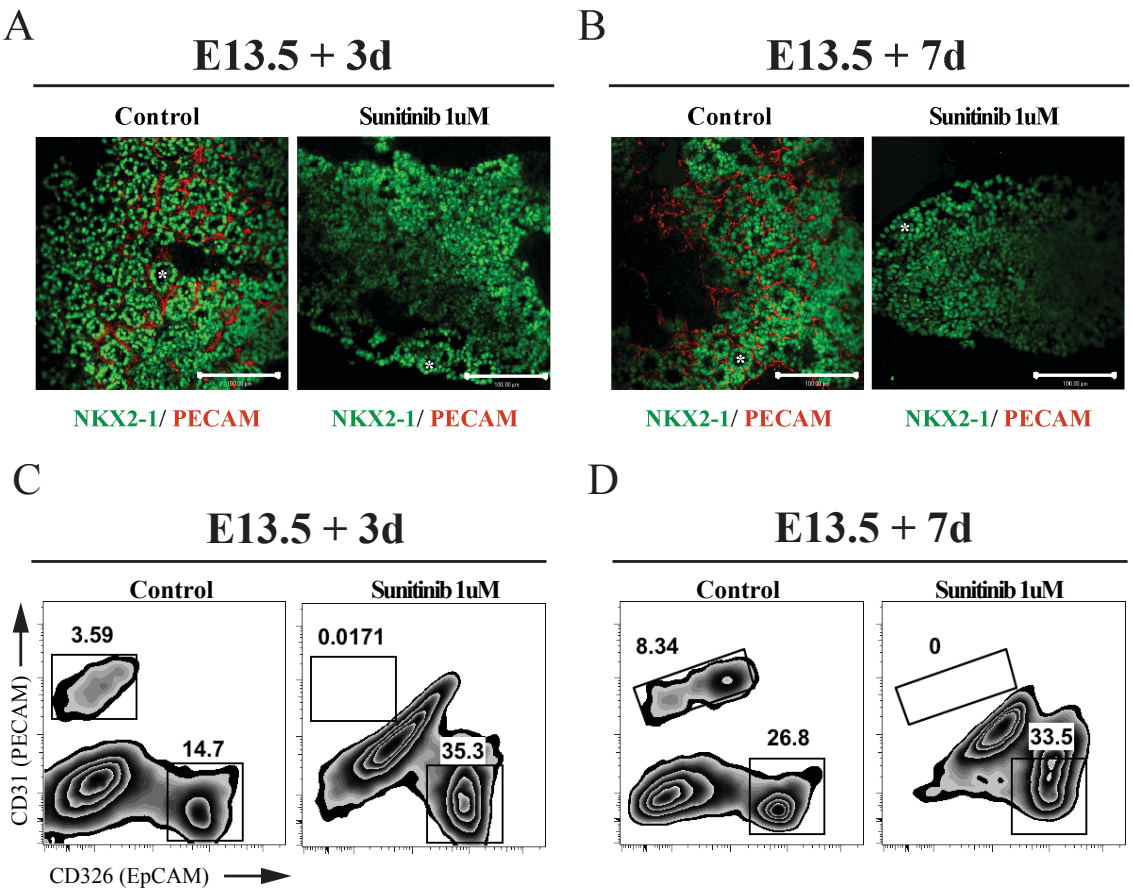

Figure 23. Direct effect of HDACi on angiogenesis. OCT embedded thyroid explants with and without Sunitinib 1uM treatment at 3 (A) and 7 (B) days were cut in sections and analyzed by confocal microscope. Sections were stained for NKX2-1 (green; thyrocytes and C-cells) and PECAM (red; endothelial cells). Scale bar = 100 uM. Flow cytometry plots of thyroid explants without (control) or with Sunitinib 1uM for 3 (C) and 7 (D) days.

HDACi decreases proliferation of epithelial and endothelial cells

To investigate the effect of HDACi on proliferation of thyroid cell populations during thyroid development, we analyzed BrdU incorporation by immunohistochemistry and flow cytometry. E13.5 thyroids cultured for 3 and 7 days, without (control) and with (VPA 1mM) were incorporated with BrdU for 2 hours prior to removing the explants from the culture conditions. Immunohistochemical staining of the explants shows few cells that are BrdU positive after VPA treatment as compared to control, both at 3 (Figure 24A) and 7 (Figure 24B) days. Since, it was not able to confirm and quantify that in which cell type this decreased proliferation occurred, we analyzed the explants by flow cytometry. BrdU was incorporated into explants for 2 hours before removing them for flow cytometry analysis. They were labeled with antibodies for respective cell type: anti-EpCAM for epithelial cells, anti-PECAM for endothelial cells and anti-PDGFRa for fibroblasts, and further with anti-BrdU and 7-AAD that marks the DNA. Cell proliferation in respective cell type, at 3 and 7 days of culture, either without (Control) or with (VPA 1mM) is seen in representative plots from one of the experiment (Figure 24C and 24D). On HDACi with VPA 1mM, significant reduction in absolute numbers of BrdU positive cells after 3 days of culture was observed in total thyroid cells (60%), epithelial cells (95%) and endothelial cells (90%) (Figure 24E). After 7 days of culture, significant reduction in absolute numbers of BrdU positive cells was observed in total thyroid cells (50%), epithelial cells (75%) and endothelial cells (97%) (Figure 24F), whereas no difference was observed in fibroblasts at either after 3 or 7 days of culture (Figure 24E and 24F).

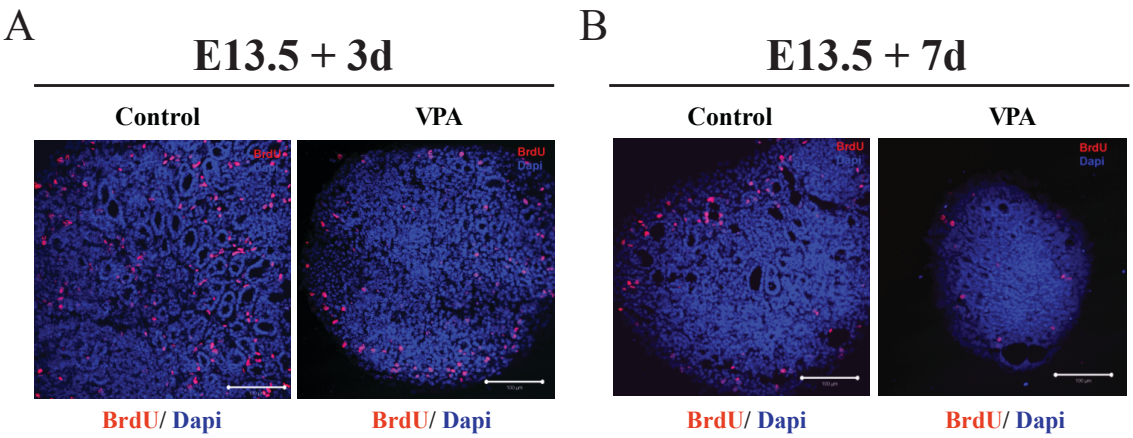

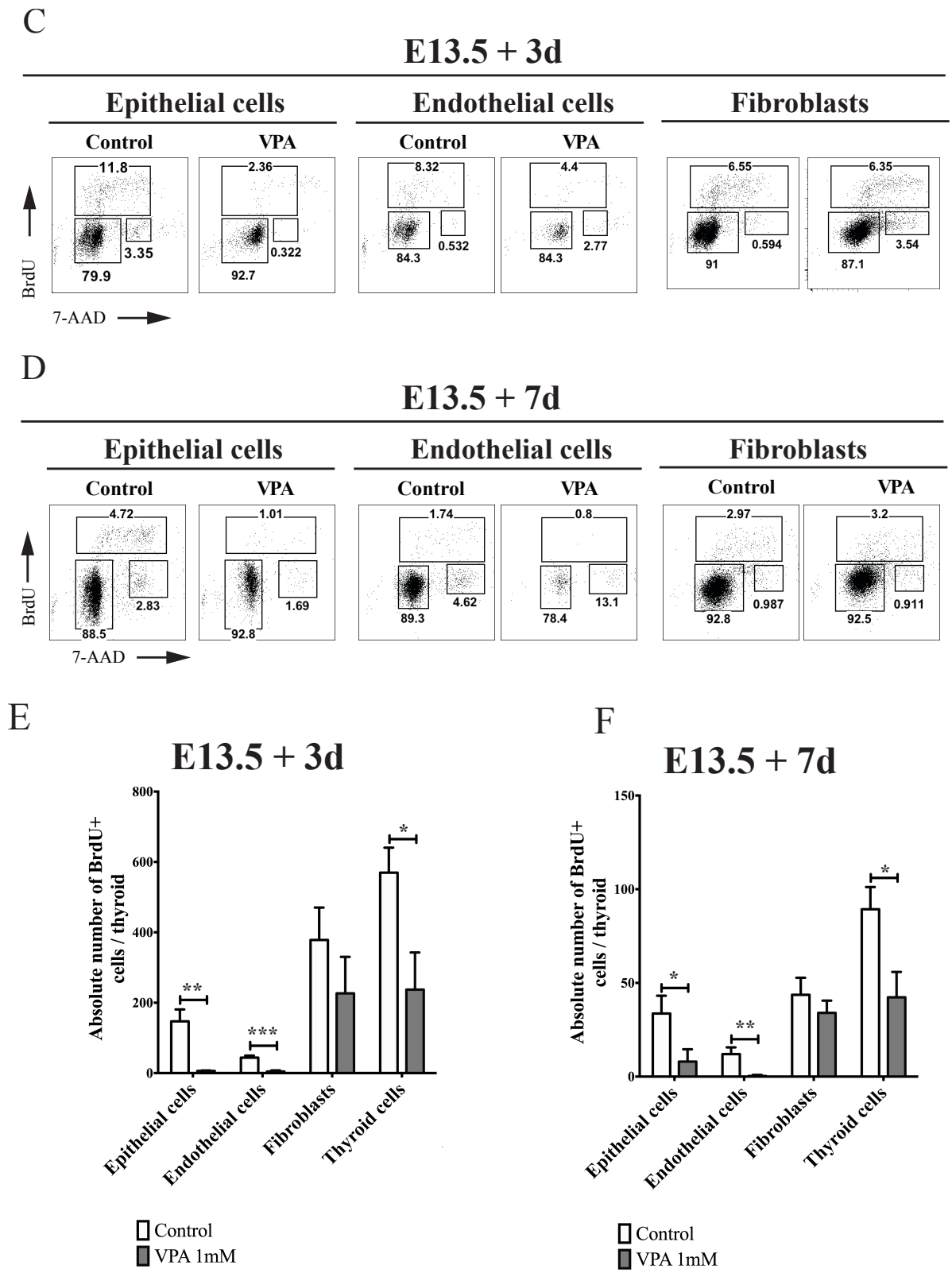

Figure 24. Analysis of proliferation after HDACi. Immunohistochemistry for BrdU performed on control (untreated) and VPA 1mM treated cultures for 3 (A) and 7 (B) days. Thyroid cultures were labeled with BrdU for 2 hours. Scale bar = 100 uM. Cell cycle analysis of individual cell types after 2 hours BrdU labeling at day 3 (C) and day 7 (D). Flow cytometry plots depict intracellular expression of BrdU and 7-AAD (7-Aminoactinomycin D), which marks the DNA. The numbers represent frequencies of cells in G0/G1 ($BrdU^-$ $7\text{-}AAD^-$), S ($BrdU^+$ $7\text{-}AAD^{-/+}$) and G2/M phase ($BrdU^-$ $7\text{-}AAD^+$). Absolute number of BrdU positive cells obtained by FACS analysis after VPA 1mM treatment for 3 (E) and 7 (F) days. Bar diagrams display the mean, SD and t test statistics (*$P < 0.05$, **$P < 0.01$, ***$P< 0.001$, unpaired t test, n = at least 3).

HDACi decreases cellularity of epithelial and endothelial subpopulations of thyroid

To investigate the effect of HDACi on thyroid cell populations during thyroid development, we analyzed the total thyroid cellularity as well as individual thyroid cell populations by flow cytometry. E13.5 thyroids after 3 and 7 days of culture, without (control) and with (VPA 1mM) were labeled with antibodies for respective cell type: anti-EpCAM for epithelial cells, anti-PECAM for endothelial cells and anti-PDGFRa for fibroblasts (Figure 25A and 25C). On HDACi with VPA 1mM, total and individual cell type specific cellularity in absolute numbers did not change significantly after 3 days (Figure 25B), however significant decrease was observed after 7 days in total thyroid cells (60%), epithelial cells (50%) and endothelial cells (80%), whereas no difference was observed in fibroblast population (Figure 25D). After both, 3 and 7 days of culture in either presence or absence of VPA, fibroblasts were the major population followed by epithelial cells and the smallest were endothelial cells. Thus, HDACi treatment caused decrease in total thyroid cells, epithelial cells and endothelial cells after 7 days of culture, whereas fibroblast population remained unchanged. In summary, HDACi caused decreased endocrine cell mass, a phenotype reminiscent of thyroid hypoplasia in patients with TD.

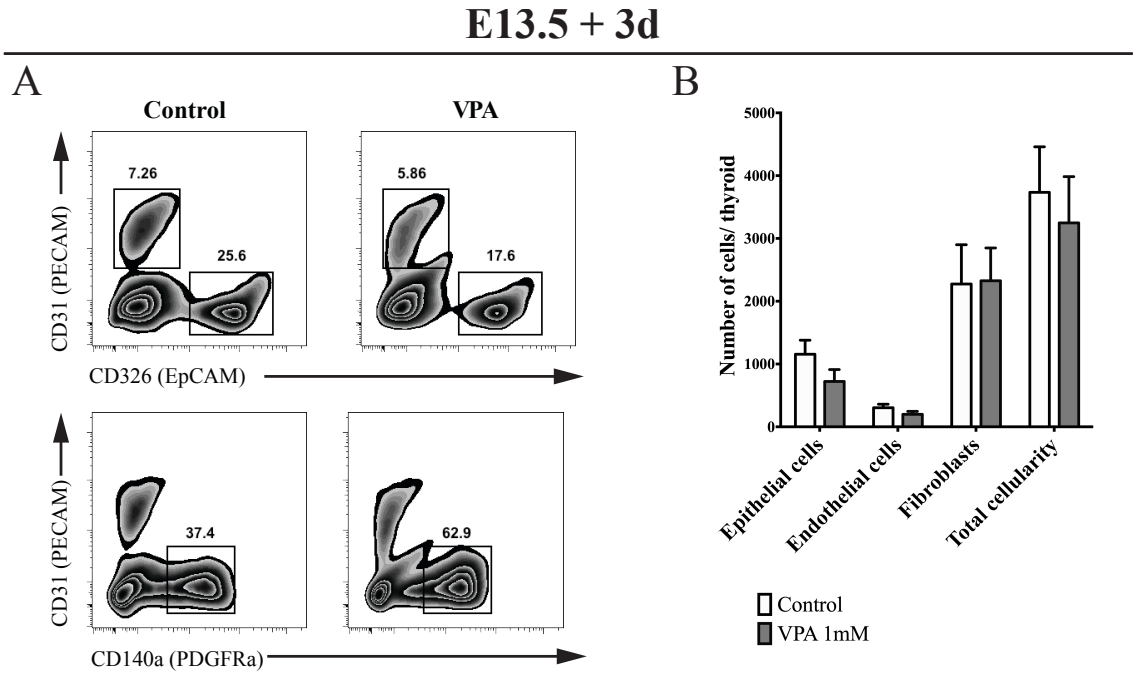

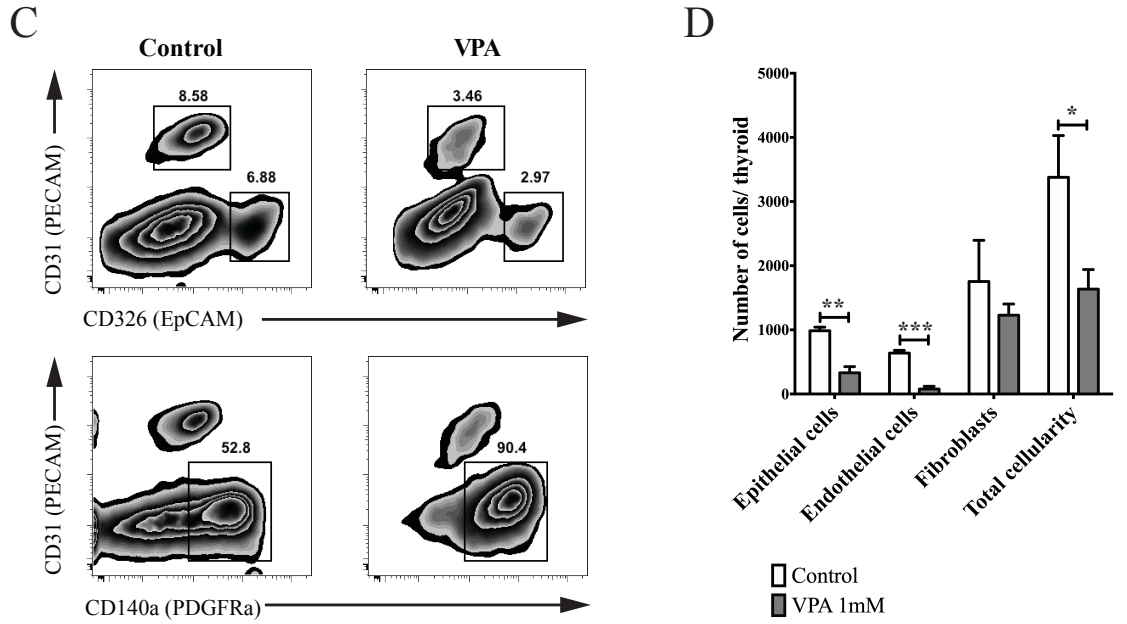

Figure 25. Analysis of cellularity after HDACi. Flow cytometry plots of thyroid cultures after HDACi of all epithelial cells (EpCAM+), endothelial cells (PECAM+) and fibroblasts (PDGFRa+) are indicated in zebra plots for 3 (A) and 7 (C) days. Comparative cellularity of epithelial, endothelial, fibroblasts and total thyroid cellularity after 3 (B) and 7 (D) days of VPA treatment. Each column represents pool of at least 10 thyroids (*P < 0.05, **P < 0.01, *** P< 0.001, unpaired t test, n = 3).

HDACi alters thyroid specific gene expression

Besides structural differentiation of an organ, its function is dependent on proper gene expression of tissue specific set of functional gene. Expression of genes involved in thyroid development, such as *Pax8,* genes encoding proteins involved in thyroid hormone synthesis such as *Nis, Tg, Tpo,* and genes encoding cell adhesion molecules involved in folliculogenesis and angiogenesis such as *Cdh16*, *Pecam* and *EpCAM,* was done by using real-time PCR. After 3 days of culture with HDACi VPA 1mM, expression of *Pax8* was increased, whereas expression of *Nis*, *Tpo* and *Cdh16* is significantly decreased. No significant changes are seen in the expression of Tg, Pecam and EpCAM (Figure 26A). After 7 days of culture with HDACi VPA 1mM, expression of functional genes such as *Nis*, *Tg* and *Tpo* was significantly increased, whereas expression of *Cdh16* and *Pecam* was significantly decreased (Figure 26B). Thus HDAC inhibition profoundly altered gene expression during thyroid development.

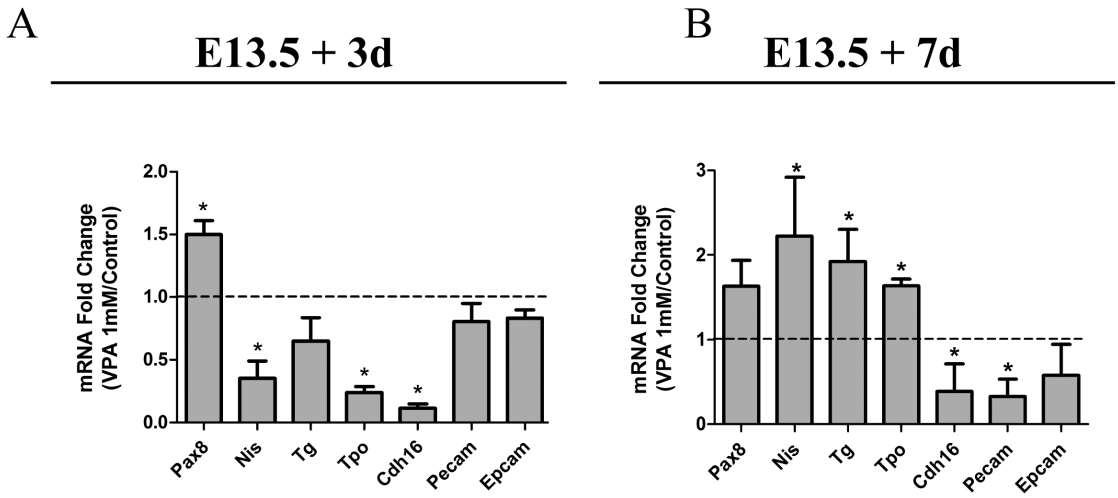

Figure 26. Thyroid specific gene expression after HDACi. Real time PCR quantification of *Pax8*, *Nis*, *Tg*, *Tpo*, *Cdh16*, *Pecam* and *EpCam* after 3 (A) and 7 (B) days of HDACi with VPA 1mM. Values obtained from control are set to 1 as shown in the dotted line and mRNA fold change to VPA 1mM was calculated. Bar diagrams display the mean, SD and t test statistics (*$P < 0.05$, unpaired t test, n = at least 3).

5. DISCUSSION

Focusing on molecular mechanisms of normal and abnormal thyroid development, this work had two main aims:

First, to establish a flow cytometry protocol for the thyroid gland and provide a new research tool for detailed quantification of the different cell populations and their growth dynamics during normal murine thyroid development, and in murine models of thyroid disease.

Second, to investigate the role of HDACs and of histone acetylation for regulation of thyroid development and to investigate whether disordered histone acetylation might cause disturbed thyroid development reminiscent of thyroid dysgenesis in patients with congenital hypothyroidism.

5.1. Cell growth dynamics in embryonic and adult mouse thyroid revealed by a novel approach to detect thyroid gland subpopulations

The thyroid is composed of endocrine epithelial cells, blood vessels and mesenchyme. Fluorescence-activated cell sorting (FACS) provides a tool for quantification of distinct cell populations. However, flow cytometry has not been a standard protocol up to this date for thyroid research. Thus, in the absence of an established tissue-specific protocol, no data exist on absolute cell numbers, relative distribution, and proliferation of the different cell populations in the developing and mature thyroid. The aim of this study was to establish a flow cytometry protocol allowing quantification of cell populations in murine embryonic (E13.5, E15.5, and E17.5) and adult thyroid tissues. These time points were chosen as structural and functional differentiation of TFCs occurs between E14.5-E16.5. Structural differentiation is characterized by follicle formation, angiogenesis and growth of the tissue. Functional differentiation is characterized by onset of thyroid hormone synthesis. Thus, if reliable, a flow cytometry protocol should detect major changes in absolute cell number and relative frequency of cell populations during this time window of morphogenesis and differentiation.

A gating strategy and the use of antibodies for flow cytometry were established allowing characterization of TFCs and C-cells ($EpCam^+/Nkx2\text{-}1^+$ cells), parathyroid cells ($EpCam^+/Nkx2\text{-}1^-$ cells), endothelial cells ($Pecam^+$ cells), fibroblasts ($PDGFRa^+$ cells) after

exclusion of Ter119$^+$ erythrocytes and CD45$^+$ hematopoietic cells. Specificity of antibodies was validated whenever available by a second cell type specific marker: epithelial cells (EpCam, E-cadherin, Nkx2-1) and endothelial cells (Pecam, Icam-1).

For the first time, our study provided quantitative data on the absolute parenchymal cell number per thyroid (mean±SD): it increased from 7300±1300 at E13.5 to 190000±20000 in adult tissues. As expected, Nkx2-1$^+$ cells represented the largest cell population in adult tissues. Surprisingly, at all three embryonic stages thyrocytes accounted only for a small percentage of the total thyroid cell mass. In contrast, the largest cell population at all three embryonic stages were PDGFRa$^+$ fibroblasts, while representing the smallest cell population in adult tissues. Pecam+ endothelial cells increased significantly from E13.5 to E15.5 and remained stable at E17.5 and adult tissues.

Proliferation rate was significantly different between embryonic cell populations with distinct proliferative peaks at E13.5 in epithelial cells and at E15.5 in endothelial cells (22±2% BrdU$^+$), while fibroblasts showed a constant proliferation rate in embryonic tissues. In adult tissues, BrdU$^+$ cells were below 1% in all cell types.

Finally, an unknown cell population was revealed by our gating strategy that was found to be Nkx2-1$^-$/CD45$^-$/Pecam$^-$/PDGFRa$^-$/EpCam$^-$/Ter119$^-$ negative. From histological studies, such a cell population is not evident. So a detailed characterization by transcriptome analysis and use of further surface markers, e.g. stem cell markers, could provide more insight into the origin and putative role of this yet unknown cell population.

In summary, we established a flow cytometry protocol for quantification of developmental dynamics in thyroid cell populations providing a new tool for functional analysis in murine thyroid disease models. The detailed discussion is mentioned in the manuscript (Section 4.1.4). The flow cytometry protocol was the basis for detailed investigation on epigenetic regulation of thyroid development - the second main aim of this thesis. For this, the gating strategy was adapted and extended to allow cell type specific quantification of changes at distinct epigenetic histone marks (H3K9ac, H3K9me3), as detailed in the results section and discussed below.

5.2. Epigenetic regulation of thyroid development: A new hypothesis

The three main arguments from clinics and biology suggesting epigenetic cause of TD are:
1. High discordance rate (92%) for TD between monozygotic twins and the sporadic occurrence of TD due to non-Mendelian inheritance pattern in majority of the cases (98%).
2. Loss of histone acetylation during thyroid carcinogenesis being associated with loss of structural and functional differentiation marker of TFCs.
3. Inhibition of HDAC activity during development of pancreas, intestine and kidney caused abnormal organogenesis and differentiation.

The developing human thyroid undergoes a series of complex changes during embryogenesis to become functional at the end of the first trimester as summarized in Table 1 in the introduction. Developmental defects at any stage might lead to TD. TD is the most prevalent form of CH representing 85% of all cases and is mainly a sporadic disorder associated with a non-Mendelian inheritance pattern. Only 2% of TD cases are familial (Castanet et al., 2000). Further, the key argument for an epigenetic cause of TD is the observation that monozygotic twins - thus genetically identical individuals - exhibit a high discordance rate (92%) for TD (Perry et al., 2002). This suggests post zygotic and thus somatic mutations or epigenetic mechanisms being involved in TD (Vassart & Dumont, 2005; Deladoëy et al., 2007). Finally, monogenetic forms of TD caused by mutations in thyroid enriched transcription factors (PAX8, NKX2-1, FOXE1, TSHR) that regulate thyroid development, are found in only 5% of the TD cases in large cohorts (De Felice and Di Lauro, 2004; Szinnai, 2014). The cause in the remaining cases still remains unknown. In summary, the hypothesis of epigenetic rather than monogenetic cause of TD is supported by clinical and genetic data in different cohorts of patients with TD.

Epigenetic changes also play an important role in thyroid tumourigenesis affecting differentiation and proliferation. Epigenetic silencing due to loss of histone acetylation is associated with loss of differentiation markers of TFCs such as TPO, NIS, Tg and TSHR (Russo et al., 2011). Redifferentiation of the TFCs with HDACi to restore NIS expression and make thyroid tumors radioiodine sensitive has become a new therapeutic goal in treatment of thyroid cancer (Kogai et al., 2006). Cooperative effects of suberoylanilide hydroxamic acid

(SAHA) and VPA on BCPAP, a papillary thyroid carcinoma derived cell line, and FRO, an anaplastic thyroid carcinoma cell line, was observed on *NIS* gene expression (Puppin et al., 2012). HDACi VPA, TSA and depsipeptide have been shown to restore NIS expression at mRNA and protein level in papillary, follicular, and anaplastic cell lines, while iodide uptake in papillary and anaplastic thyroid cancer cell lines have only been shown for VPA and depsipeptide (Kitanzono 2001, Fortunati 2004, Furuya, 2004). New HDACi Belinostat, Panobinostat and classical HDACi VPA have been shown to induce apoptosis and cell cycle arrest in poorly differentiated thyroid carcinoma cell lines (Chan et al., 2013; Catalano et al., 2005). Also, over-expression of proteins with HAT activity (pCAF and p300) in HeLa cells resulted in stimulation of the NIS promoter (Puppin et al., 2005). These findings strongly suggest a putative role of histone acetylation, and more specifically the balance between HDACs and HATs for differentiation and de-differentiation in TFCs.

Epigenetic changes due to histone modifications have recently been shown to play crucial roles in the transcriptional regulation of most eukaryotic genes during organ development and have been linked to control cell differentiation in cardiac (Backs & Olson, 2006) and muscle cells (McKinsey et al., 2001). Studies in early mouse embryonic reprogramming events such as during oocyte maturation have shown dynamic changes of specific histone modifications during early murine development (Sarmento et al., 2004). Histone modifying enzymes HATs and HDACs play an important role in developmental processes and their deregulation has been linked to various congenital diseases. During development, HDACs regulate directly or indirectly the timing of coordinated cellular differentiation in several cell types (e.g. pancreas, intestine, kidney)(Haumaitre et al., 2008, Tou et al., 2005, Chen et al., 2011). HDAC1 knockout mice show proliferative defects (Lagger et al., 2002). HDAC2 knockout mice show cardiac malformations (Trivedi et al., 2007). These studies reveal that HDACs play a key role for development of distinct cell types and are not functionally redundant.

In summary, all these data from human genetics, thyroid cancer and developmental biology suggest a putative regulatory role of epigenetic mechanisms, such as histone acetylation, for thyroid development. However, very few studies have investigated how thyroid development is regulated at the epigenetic level. The first study to hint the involvement of epigenetics in thyroid differentiation was on canine thyroid cell culture. Treatment of these cells with 12-O-tetradecanoylphorbol-13-acetate (TPA) or EGF completely decreased the expression of specialized thyroid genes (Tg and Tpo) (Dumont et al., 1992). On treatment with TSH or

with any agent that enhanced cAMP accumulation, these cells again fully expressed their specialized genes. Thus, on treatment with TPA or EGF TFCs remained determined but lost their differentiation expression and recovered it later again when exposed to TSH or other agents causing cAMP increase. Dumont et al concluded "this suggested the involvement of proteins in specific thyroid cell control and of the chromatin".

Only in 2010, possible involvement of DNA methylation in the pathogenesis of TD was studied by Abu-Khudir et al by comparing dysgenetic thyroid tissue from TD patients with normal thyroid tissues (Abu-Khudir et al., 2010). However, no difference in global DNA methylation profiles between the dysgenetic and normal thyroid tissues was observed.

Very recently, Abu- Khudir et al provided the first evidence for epigenetic regulation of thyroid function by identifying a tissue dependent differentially methylated region in the promoter of *FOXE1*, and showed reduced expression of this transcription factor by epigenetic modulation (Abu-Khudir et al., 2014).

In summary, disrupted epigenetic regulation of thyroid development represents a new hypothesis to explain TD in patients after exclusion of the rare known monogenetic forms.

5.3. HDAC expression, HDAC activity and histone acetylation during normal thyroid development *in vivo*: an observational approach

In a first line of research, we aimed at describing dynamics of general HDAC activity, expression of HDAC1 and 2, and the level of histone acetylation during normal thyroid development *in vivo* compared to adult tissues.

During *in vivo* thyroid development, we observed a decline in total HDAC activity in differentiating TFCs (E15.5), and in adult TFCs (Figure 10) compared to TFC precursors (E13.5). This result was in accordance with high HDAC activity at the precursor state, and low HDAC activity in the fully differentiated state in other organs, e.g. pancreas or kidney (Haumaitre et al., 2008; Chen et al., 2011), providing a first argument for a regulatory role of HDACs during thyroid development.

In a second step, we analyzed by flow cytometry the cell type specific expression levels of HDAC1 and 2, the major HDACs. For HDAC1, we observed a significant decline in its expression in all cell types from E13.5 to adult stage, except for epithelial cells, exhibiting a decline at E13.5 and E15.5, but reaching again levels comparable to E13.5 in the adult tissue (Figure 11). For HDAC2, expression levels were higher at E13.5, and showed a distinct decline in all three cell types (Figure 12). In summary, HDAC1 expression in endothelial cells and fibroblasts and HDAC2 expression in all three cell types are in analogy with data from intestine, pancreas and kidney. Further, the decrease in expression levels of HDAC1 and HDAC2 from E13.5 to adult thyroid (Figure 11 and 12) is correlated with decreased total HDAC enzymatic activity. Similar pattern has been observed during pancreatic differentiation (Haumaitre et al., 2008), adipogenesis (Yoo et al., 2006) and osteogenesis (Lee et al., 2006). Thus, we are able to show that HDAC1 and HDAC2 show differential expression during various stages of thyroid development suggesting their differential roles correlating to various developmental events.

As explained above, histone acetylation levels at distinct stages and in different cell types are the result of a balance between HDAC and HAT activity. Thus, to investigate the effect of developmentally decreasing HDAC activity and expression, we analyzed histone acetylation levels in all cell types throughout thyroid development. However, we decided not to analyze general H3 acetylation, but acetylation at one of the well characterized histone residues, associated with active gene transcription if acetylated (H3K9). Surprisingly, H3K9ac levels were not inversely correlated with general HDAC activity or HDAC1 and 2 expressions, but showed a decrease over time. Several reasons could cause this unexpected result:

First, H3K9 is only one of the several residues in the tail of histone H3 being acetylated as shown in Figure 7. It remains to be shown, whether general H3 acetylation or acetylation at the other residues (e.g. H3K4, H3K14, H3K18, H3K27) would exhibit the expected inverse correlation of H3K9ac to that of general HDAC activity.

Secondly, our assumption of inverse correlation of acetylation with HDAC activity is simplistic. It does not consider possible developmental dynamics of general HAT activity, the counterpart of HDAC activity (Figure 8). Thus, to understand *in vivo* changes of histone acetylation, the complex balance of both enzyme groups modifying histone acetylation needs to be analyzed. Nevertheless, these data provide evidence that acetylation of histone H3K9 shows dynamic pattern in different cell types at various developmental stages during mouse thyroid development.

In summary, this first line of research during *in vivo* development of the thyroid provided arguments for dynamic stage dependent changes of general HDAC activity, of HDAC expression and of histone acetylation. However, with this first set of experiments performed, it was not possible to encompass the global complexity of developmentally regulated dynamics in histone acetylation in the physiological *in vivo* situation. More and more complex experiments such as ChIP-Seq with HDACs and histone marks are underway to get a more general insight into the complexity of the acetylome during thyroid development.

5.4. HDAC inhibition efficiently modified histone acetylation in *ex vivo* cultured thyroids

In a second line of research, we decided to study the role of HDACs and histone acetylation for thyroid development in a more controlled *ex vivo* system after pharmacological HDAC inhibition, being aware that data gathered would be more discriminative than *in vivo*, but the biological relationships simpler than during physiological, not perturbed thyroid differentiation.

In a first set of experiments, we investigated and quantified the changes of epigenetic parameters in control and HDACi exposed thyroid tissues to confirm efficacy of HDAC inhibition. In a second set of experiments we focused on characterization of the effects of perturbed histone acetylation on growth and differentiation of the *ex vivo* cultured thyroid tissues (see 5.5.)

Validation of the *ex vivo* culture model for research on HDACs and dose finding of VPA

To define the role of histone acetylation in embryonic thyroid development, we used an *ex vivo* culture model that recapitulates all key steps of structural and functional differentiation of the embryonic thyroid gland (unpublished data Szinnai). E13.5 thyroids when cultured for 3 days *ex vivo*, exhibit the features of an E15.5 thyroid *in vivo*, with onset of follicle formation and angiogenesis. E13.5 thyroids cultured for 7 days *ex vivo* demonstrate onset of thyroid hormone synthesis as in E17.5 *in vivo*.

In a first step, we were able to show that *ex vivo* cultured thyroid tissues recapitulated the decrease of HDAC activity *in vivo* at discrete stages, thus validating the model for planned

epigenetic research focusing on HDACs (Figures 10 and 14).
Secondly, since most HDACs were expressed during thyroid development, we chose an overall HDAC inhibition strategy rather than specifically but arbitrarily inactivating each HDAC. We used VPA as a general HDACi of class I and class II HDACs widely used in epigenetic research such as in several cell lines (Chen et al., 2011; Balasubramanian et al., 2015), and validated their use in thyroid explants, an approach similar to that used with intestinal explants (Tou et al., 2004) and pancreatic explants (Haumaitre et al., 2008).
Dose titration of VPA from 0.5 mM to 1.5 mM on E13.5 thyroids cultured for 3 and 7 days allowed to determine an effective VPA dose (1mM). It resulted in significant decrease of HDAC activity and exhibited no toxic effects on explants compared to control as assessed by comparable levels of apoptosis by Annexin V-PI staining and by TUNEL assay. Hence, VPA 1mM was the dose of choice throughout the study. Our data validate the use of VPA for potently modulating HDAC activity in thyroid explants.

Effect of HDAC inhibition on histone acetylation

In a next step, we aimed at determining the effect of HDAC inhibition on histone acetylation levels in control versus treated explants. HATs acts as transcription activators and co-activators and are associated with gene activation (Sterner and Berger, 2000; Backs and Olson, 2006) and HDACs can reverse the action of HATs. This interplay between HATs and HDACs results in dynamic transitions in chromatin structure and hence in switches between permissive and repressive chromatin states (Wolffe and Hayes, 1999; Roth et al., 2001). Thus, HDAC inhibition is expected to perturb the balance between HATs and HDACs and consecutively the balance between acetylated, deacteylated and methylated state of specific histone residues. Histone H3K9 mark has double duty, it can turn genes ‘on’ when acetylated and ‘off’ when methylated. Acetylation of H3K9 is highly correlated with active promoters (Wang et al., 2008; Karmodiya et al., 2012), whereas tri-methylation of H3K9 is highly correlated with inactive promoters (Barski et al., 2007).

Immunohistochemical analysis revealed an inverse labeling of H3K9ac and H3K9me3 labeling in control tissues, while treated explants showed no differential staining pattern throughout the explant. However, VPA treated explants exhibited a more intense H3K9ac labeling as expected.

To get a more precise picture, H3K9ac levels were quantified in individual cell types by flow cytometry: HDAC inhibition caused a significant increase in H3K9ac levels in all three cell populations after 3 days and in epithelial cells after 7 days of culture providing evidence for an effective modulation of histone acetylation in treated explants.

Epigenetic switch from repressive to permissive chromatin state at residue H3K9

Despite the crucial importance of bivalent combinations of histone modifications, very few methods exist to detect these combinations, such as with the sequential-chromatin immunoprecipitation (sequential-ChIP) assay (Bernstein et al., 2006; Geisberg and Struhl, 2004) or a new approach with immunoprecipitation-mass spectrometry assay (Voigt, 2012). However, it is impossible to identify cells with a specific bivalent combination of histone modifications in samples with heterogeneous cell populations, such as in tissues. This complexity is even further difficult to address in situations where cells having a specific bivalent modification in samples derived from tissues at various stages of differentiation.

In order to overcome these limitations, we developed a new protocol to study bivalent histone modifications in cells from heterogeneous population derived from thyroid tissue at various developmental stages using flow cytometry. We extended the initial flow cytometry experiment using H3K9ac antibody alone by combining quantification of H3K9ac and H3K9me3 levels in the same flow cytometry experiment. By this approach, we could show an epigenetic switch at the histone H3 tail residue K9 with significant increase of acetylation with concomitant decrease in tri-methylation in the total thyroid as well as for each cell type. This experimental setup was, to our knowledge, not used before and provided the most convincing proof of a specific effect of HDAC inhibition on acetylation levels (Figure 18 and 27).

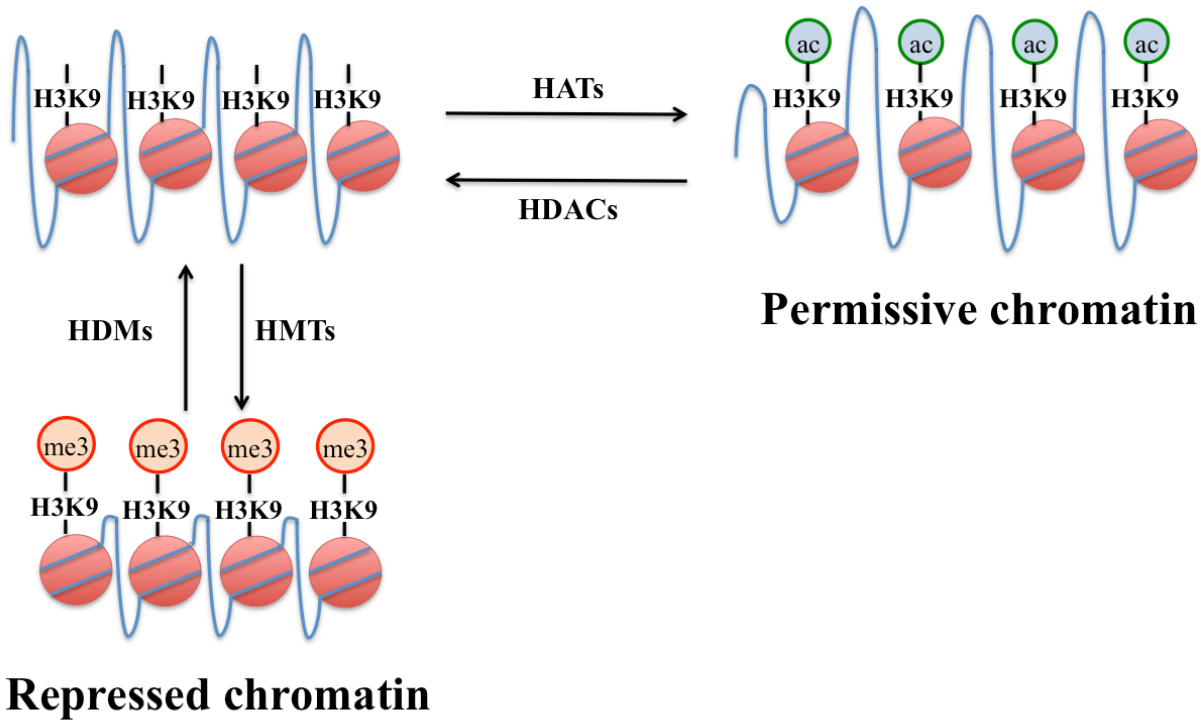

Figure 27. The epigenetic switch at H3K9ac. HATs- Histone acetyl transferases, HDACs- Histone deacetylases, HMTs- Histone methyl transferases and HDMs- Histone demethylases. Acetylated histone tails due to transfer of acetyl groups by HATs on H3K9 residue, represent permissive chromatin. This action is reversed by HDACs. On HDAC inhibition, HMTs add tri-methyl groups on deacetylated histone tails representing repressed chromatin. On HDAC inhibition, the balance between acetylated and trimethylated H3K9 is shifted to the right, as HAT activity is maintained.

In summary, our data confirmed by different approaches that HDAC inhibition in our *ex vivo* explant model significantly reduced HDAC activity and resulted in an efficient modulation of the balance between acetylation and methylation.

5.5 HDAC inhibition caused profoundly disordered thyroid development

After having provided evidence for significant changes in histone acetylation by HDAC inhibition in our model, the next step was to analyze the effect of modified histone acetylation on thyroid development. Structural and functional key steps of thyroid terminal differentiation are follicle formation, angiogenesis, proliferation and thyroid hormone synthesis (Shepard et al., 1964; De Felice and de Lauro, 2004; Szinnai et al., 2007).

Follicle formation

The thyroid follicle is the functional unit of the thyroid. Thyroid hormone synthesis and storage is only possible in the follicular lumen, but not within the TFCs (Dumont et al., 1992). HDAC inhibition in our *ex vivo* model caused a significant decrease of follicle number and total follicle surface per tissue surface. This effect was dose dependent and follicle formation was almost completely blocked in the highest VPA dose tested (Table 3, Figure 19). Thus, these data provided evidence that disturbed balance between HDACs and HATs had major impact on follicle formation, the key morphogenetic step of thyroid development. Reduced follicle number and surface results in reduced functional endocrine surface area, ultimately leading to insufficient endocrine function.

Angiogenesis

A second condition for normal function of an endocrine organ is the presence of a capillary net for secretion of the synthesized hormones into the blood stream. The spherical thyroid follicles are surrounded by a dense capillary net, the complete structure also called angiofollicular unit (Dumont et al., 1992; Colin et al., 2013). VPA treated explants exhibited a significantly reduced capillary net compared to control in immunohistochemistry (Figure 21) after 3 and 7 days of culture. In conclusion, not only follicle formation but also angiogenesis was blocked by HDAC inhibition, resulting in a disordered formation of angiofollicular units in the developing thyroid. This observation is in accordance with previous data. Hick et al have recently shown epithelial-endothelial paracrine crosstalk for angiogenesis and follicle formation. According to their data, TFCs secrete VEGF-A to attract endothelial cells, which invade the thyroid from the periphery of the organ at E14.5 and E15.5. Follicle formation of the unpolarized TFCs occurred only in close contact to invading endothelial cells, and was blocked by an angiogenesis inhibitor (Hick et al., 2013).

Arguments for direct effect of HDAC inhibition on follicle formation

However, based on this observation, it remained unclear whether HDAC inhibition had direct effect on angiogenesis and follicle formation, or whether decreased follicle formation was a consequence of impaired angiogenesis and impaired paracrine interaction between the two cell types (Figure 28).

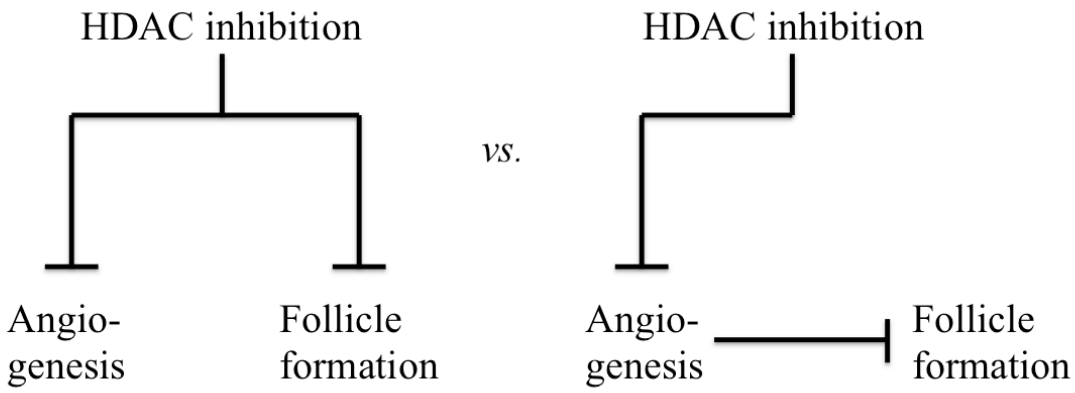

Figure 28. Schematic representation of two possible ways of HDAC inhibition to block follicle formation. Left: Follicle formation is directly inhibited by HDAC inhibition. Right: Decreased follicle formation is a consequence of direct inhibition of angiogenesis by HDAC inhibition.

To answer this question, a selective angiogenesis inhibitor (Sunitinib) was used in our explant model. Under these conditions, angiogenesis was completely blocked, as shown by immunohistochemistry and flow cytometry, despite some but reduced follicle formation (Figure 23). In contrast, in VPA treated explants, some but reduced angiogenesis was observed, but follicle formation was almost completely blocked compared to Sunitinib treated explants. In summary, these results are 1) in accordance with the notion that angiogenesis triggers follicle formation and 2) suggest that HDAC inhibition itself has a direct effect on follicle formation independently of reduced angiogenesis.

Proliferation and growth dynamic of cell populations

A direct effect of HDAC inhibition was visible by eye: VPA treated explants were smaller than control explants (Figure 19). This effect was dose dependent as shown in Figure 20. As stated above, toxic effects of VPA 1.0mM were excluded by TUNEL staining and flow cytometry (Figure 22). As HDAC inhibitors are known to have anti-proliferative effects (Mottamal et al., 2015), we investigated by immunohistochemistry as well as by flow cytometry using BrdU differences in proliferative rate in control versus VPA treated tissues. While immunohistochemistry revealed a higher number of BrdU positive cells in control tissues compared to HDACi treated explants, it provided no clear picture on cell specific proliferation rate. Quantification of absolute numbers of BrdU positive cells in each cell population was possible by flow cytometry and revealed significant reduction in epithelial (day 3 of culture 95%, day 7 of culture 75%) and endothelial cells (day 3 of culture 90%, day 7 of culture 97%), respectively (Figure 24).

As a direct consequence, absolute cell numbers of epithelial cells and endothelial cells were significantly decreased at day 3 and 7 of culture. These data are in accordance with previous reports of growth arrest in HDAC exposed organs during development, e.g. pancreas and kidney (Haumaitre et al., 2008, Chen et al., 2011).

Gene expression

Effect of HDAC inhibition on the expression of thyroid specific genes was performed comparing genes belonging to transcription factors regulating thyroid development (*Pax8*), genes encoding functional proteins necessary for thyroid hormone synthesis (*Nis, Tg, Tpo*), and genes encoding adhesion molecules of epithelial cells (*E-cadherin, KSP-cadherin*) and endothelial cells (*Pecam*).

Time course analysis revealed distinct expression patterns at day 3 and day 7 of culture: In analogy with results from intestine, pancreas and kidney, hyperacetylation caused a stage specific change in gene expression. The most dynamic expression pattern was observed for the gene encoding key proteins of thyroid hormone synthesis, *Nis* and *Tpo*, being reduced at day 3 and increased at day 7 of culture. In contrast, the only gene with unchanged expression pattern, thus non-responsive to HDAC inhibition and hyperacetylation, was *Epcam*. As HDAC inhibition is not only acting on promoters of genes encoding differentiation markers but also on promoters of transcription factors and transcriptional repressors, the gene expression pattern of functional genes is a result of this complex interplay between stage specific expression of regulators, and their sensitivity to HDAC inhibition. Such effects were also observed in other developing organs treated with HDAC inhibition (Tou et al., 2005; Haumaitre et al., 2008; Chen et al., 2011).

In summary, these results reveal important changes in gene expression after HDAC inhibition dependent on stage of analysis, gene function, and sensitivity to HDAC inhibition. However, a more specific approach such as ChIP-Seq is needed to understand which genes are directly regulated by HDACs or acetylation, and which genes are not direct targets of HDACs. These experiments were not possible until 1) flow cytometry protocol for cell sorting of TFCs was established and 2) before low cell number ChIP-Seq became technically feasible. Now such experiments are underway.

Summarizing the effects of HDAC inhibition and disordered histone acetylation on thyroid

development, we observed profoundly disordered thyroid development at all key steps of terminal differentiation: First, follicle formation was blocked, reducing the functional endocrine epithelial surface of the developing organ. Secondly, angiogenesis was strongly reduced, thus reducing the blood flow in the endocrine organ to secrete synthesized hormones. Finally, endocrine cell mass was significantly reduced, ultimately causing endocrine insufficiency, thus hypothyroidism.

In conclusion, HDAC inhibition during terminal differentiation of the thyroid caused hypoplastic and dysgenetic thyroid, reminiscent of thyroid dysgenesis in patients with congenital hypothyroidism. As hypothesized initially, these results suggest, that disordered HDAC function or histone acetylation could be a new molecular mechanism for TD (Figure 29).

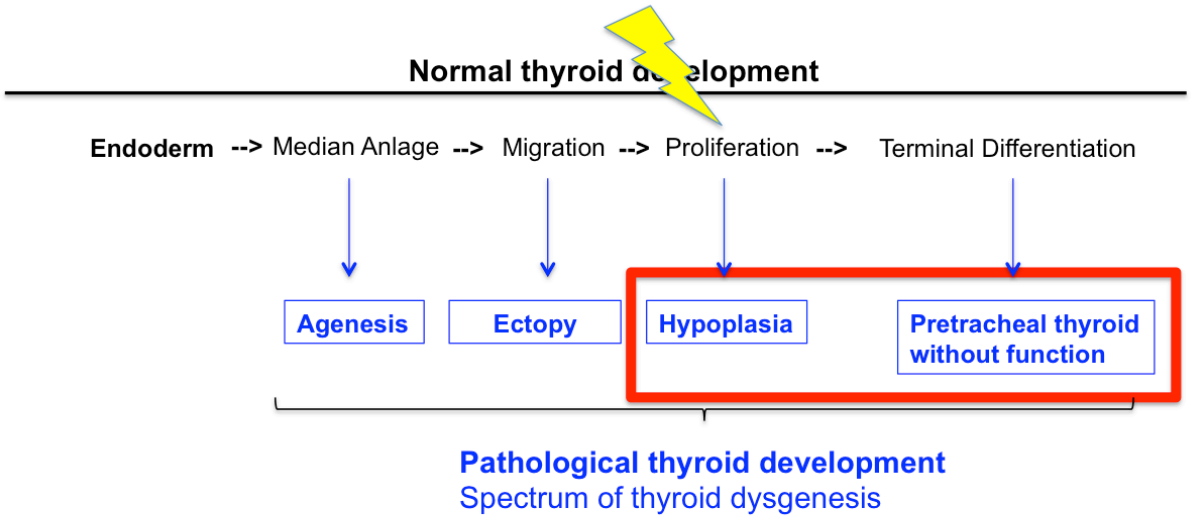

Figure 29. Disturbed epigenetic regulation could be a new molecular mechanism for thyroid dysgenesis in patients with thyroid hypoplasia and pretracheal thyroid without function.

This hypothesis is further supported by very recent data from kidney development. After having established the critical role of general HDAC activity for kidney development, Chen et al showed that HDAC1 and HDAC2 deletion caused renal dysgenesis / hypoplasia. Further, the authors provided insight into the molecular mechanism of hypoplasia, in as revealing a regulatory role of HDAC1 and HDAC2 of the Wnt and p53 pathways (Chen et al 2011, 2015).

6. CONCLUSIONS AND PERSPECTIVES

This work focused on two main aims and projects:

Project 1: First, we aimed to establish a flow cytometry protocol to identify and quantify the various cell populations in the developing and adult murine thyroid.
Project 2: Second, we aimed to analyze the role of HDACs and of histone acetylation for the regulation of thyroid development.

Project 1: A new tool for thyroid research: Flow cytometry of the thyroid gland

My data provides for the first time in the field of thyroid development a new tool for the detection of individual cell populations, and quantification of their proliferation, apoptosis, and epigenetic changes by flow cytometry. In summary, 1) we present a detailed gating strategy to characterize 7 cell populations in the embryonic and adult thyroid gland, 2) we provide a detailed analysis of the cell population changes and proliferation in individual cell types in embryonic and differentiated mouse thyroid *in vivo*, and 3) we reveal a yet unknown and uncharacterized cell population present in embryonic and adult thyroids at a frequency between 5-20%. We believe that our approach will provide a useful new tool for cell function analysis in murine thyroid disease models.

As a direct consequence of our study, the following aspects need to be studied more in detail:
First, as shown in the submitted manuscript, a major change in frequencies of cell populations occurs between E17.5 and 8 weeks old adult thyroid tissues. Thus, in a follow-up study, later embryonic and postnatal stages will be analyzed in the same way to provide a complete picture of *in vivo* cell growth dynamics from E13.5 to adult stage.
Second, the identified unknown cell population needs to be investigated to shed light on its origin, and function within the thyroid gland. Transcriptome analysis of sorted cells will provide a first approach to characterize the nature of this cell population.

Project 2: A new concept: Epigenetic regulation of thyroid development

The gathered data provide for the first time clear arguments for epigenetic regulation of thyroid development and a possible new mechanism for TD.

In summary, 1) we observed developmentally regulated dynamic changes of HDAC activity, HDAC expression and histone acetylation in different cell types during thyroid development *in vivo*, 2) we developed a new protocol by which we quantified the effect of HDAC inhibition on acetylation and tri- methylation at the bivalent histone tail residue H3K9 (epigenetic switch), and 3) we revealed profoundly disordered thyroid development after HDAC inhibition compatible with all aspects of TD in patients with CH: reduced follicle formation, decreased endocrine cell mass, and disturbed angiogenesis.

Based on this first set of experiments, the following aspects need to be analyzed in more depth to further extend our knowledge on the role of HDACs and histone acetylation for thyroid development. Some of the proposed experiments are underway:

First, to confirm the concept, the results need to be replicated by new and more specific pharmacological HDAC inhibitors, e.g. selective HDAC1 blockers, which can be validated in conditional knockout mouse models of specific HDACs to provide *in vivo* proof.

Second, we applied HDAC inhibition during a long period (3 or 7 days). It remains open, whether and at what critical time windows short-term HDAC inhibition can also result in disordered thyroid development in our model.

Third, as our experimental HDAC inhibition was applied only from E13.5 on in our model, our results do not provide insights into the role of HDACs and histone acetylation at the early stages of thyroid development. Thus, the role of HDACs and histone acetylation remains to be characterized in non-lineage committed endodermal stem cells, and TFC precursors between E8.5-E13.5. Such experiments might give an answer to whether more severe forms of TD (agenesis or ectopy) might be caused by disrupted histone acetylation.

Fourth, our study provides a detailed analysis of effects of HDAC inhibition but no insights into target genes and pathways regulated by HDACs and histone acetylation. ChIP-Seq experiments with HDAC2 and H3K9ac *in vivo* at E13.5, E15.5, and E17.5 are underway to provide a complete picture of the complex epigenetic regulatory network.

7. REFERENCES

1. Abramowicz, M. J., Duprez, L., Parma, J., Vassart, G., & Heinrichs, C. (1997). Familial congenital hypothyroidism due to inactivating mutation of the thyrotropin receptor causing profound hypoplasia of the thyroid gland. *Journal of Clinical Investigation*, *99*(12), 3018.
2. Abu-Khudir, R., Paquette, J., Lefort, A., Libert, F., Chanoine, J. P., Vassart, G., & Deladoëy, J. (2010). Transcriptome, methylome and genomic variations analysis of ectopic thyroid glands. *PloS one*, *5*(10), e13420.
3. Ahmed, K., Dehghani, H., Rugg-Gunn, P., Fussner, E., Rossant, J., & Bazett-Jones, D. P. (2010). Global chromatin architecture reflects pluripotency and lineage commitment in the early mouse embryo. *PloS one*, *5*(5), e10531.
4. Al Taji, E., Biebermann, H., Límanová, Z., Hníková, O., Zikmund, J., Dame, C., Grüters, A., Lebl, J., & Krude, H. (2007). Screening for mutations in transcription factors in a Czech cohort of 170 patients with congenital and early-onset hypothyroidism: identification of a novel PAX8 mutation in dominantly inherited early-onset non-autoimmune hypothyroidism. *European Journal of Endocrinology*, *156*(5), 521-529.
5. Alland, L., Muhle, R., Hou, H., Jr, Potes, J., Chin, L., Schreiber-Agus, N., & DePinho, R. A. (1997). Role for N-CoR and histone deacetylase in Sin3-mediated transcriptional repression. *Nature* 387, 49-55.
6. Ambros, V. (2004). The functions of animal microRNAs. *Nature*, *431*(7006), 350-355.
7. Amendola, E., De Luca, P., Macchia, P. E., Terracciano, D., Rosica, A., Chiappetta, G., Kimura, S., Mansouri, A., Affuso, A., Arra, C., Macchia, V., Di Lauro, R., & De Felice, M. (2005). A mouse model demonstrates a multigenic origin of congenital hypothyroidism. *Endocrinology*, *146*(12), 5038-5047.
8. Ang, S. L., & Rossant, J. (1994). HNF-3β is essential for node and notochord formation in mouse development. *Cell*, *78*(4), 561-574.
9. Antonica, F., Kasprzyk, D. F., Opitz, R., Iacovino, M., Liao, X. H., Dumitrescu, A. M., Refetoff, S., Peremans, K., Manto, M., Kyba, M., & Costagliola, S. (2012). Generation of functional thyroid from embryonic stem cells. *Nature*, *491*(7422), 66-71.
10. Avbelj, M., Tahirovic, H., Debeljak, M., Kusekova, M., Toromanovic, A., Krzisnik, C., & Battelino, T. (2007). High prevalence of thyroid peroxidase gene mutations in patients with thyroid dyshormonogenesis. *European Journal of Endocrinology*, *156*(5), 511-519.

11. Backs, J., & Olson, E. N. (2006). Control of cardiac growth by histone acetylation/deacetylation. *Circulation Research*, *98*(1), 15-24.
12. Balasubramanian, D., Deng, A. X., Doudney, K., Hampton, M. B., & Kennedy, M. A. (2015). Valproic acid exposure leads to upregulation and increased promoter histone acetylation of sepiapterin reductase in a serotonergic cell line. *Neuropharmacology*, *99*, 79-88.
13. Barbera, J. M., Clements, M., Thomas, P., Rodriguez, T., Meloy, D., Kioussis, D., & Beddington, R. S. (2000). The homeobox gene Hex is required in definitive endodermal tissues for normal forebrain, liver and thyroid formation. *Development*, *127*(11), 2433-2445.
14. Barski, A., Cuddapah, S., Cui, K., Roh, T. Y., Schones, D. E., Wang, Z., Wei, G., Chepelev, I., & Zhao, K. (2007). High-resolution profiling of histone methylations in the human genome. *Cell*, *129*(4), 823-837.
15. Beck-Peccoz, P., Persani, L., Calebiro, D., Bonomi, M., Mannavola, D., & Campi, I. (2006). Syndromes of hormone resistance in the hypothalamic–pituitary–thyroid axis. *Best Practice & Research Clinical Endocrinology & Metabolism*, *20*(4), 529-546.
16. Bernstein, B. E., Mikkelsen, T. S., Xie, X., Kamal, M., Huebert, D. J., Cuff, J., Fry, B., Meissner, A., Wernig, M., Plath, K., Jaenisch, R., Wagschal, A., Feil, R., Schreiber, SL, & Lander, E. S. (2006). A bivalent chromatin structure marks key developmental genes in embryonic stem cells. *Cell*, *125*(2), 315-326.
17. Bernstein, B. E., Meissner, A., & Lander, E. S. (2007). The mammalian epigenome. *Cell*, *128*(4), 669-681.
18. Bhaskara, S., Chyla, B. J., Amann, J. M., Knutson, S. K., Cortez, D., Sun, Z. W., & Hiebert, S. W. (2008). Deletion of histone deacetylase 3 reveals critical roles in S phase progression and DNA damage control. *Molecular Cell*, *30*(1), 61-72.
19. Bizhanova, A., & Kopp, P. (2009). The sodium-iodide symporter NIS and pendrin in iodide homeostasis of the thyroid. *Endocrinology*, *150*(3), 1084-1090.
20. Bogue, C. W., Ganea, G. R., Sturm, E., Ianucci, R., & Jacobs, H. C. (2000). Hex expression suggests a role in the development and function of organs derived from foregut endoderm. *Developmental Dynamics*, *219*(1), 84-89.
21. Bolden, J. E., Peart, M. J., & Johnstone, R. W. (2006). Anticancer activities of histone deacetylase inhibitors. *Nature Reviews Drug Discovery*, *5*(9), 769-784.

22. Braverman, L. E., & Cooper, D. (2012). Iodine deficiency and endemic Cretinism. In *Werner & Ingbar's the thyroid: a fundamental and clinical text* (pp 217-240). Lippincott Williams & Wilkins, Philadelphia, USA.
23. Brown, R. S., & Demmer, L. A. (2002). The etiology of thyroid dysgenesis—still an enigma after all these years. *The Journal of Clinical Endocrinology & Metabolism*, *87*(9), 4069-4071.
24. Brunmeir, R., Lagger, S., & Seiser, C. (2009). Histone deacetylase 1 and 2-controlled embryonic development and cell differentiation. *International Journal of Developmental Biology*, *53*(2), 275-289.
25. Calvo, R. M., Jauniaux, E., Gulbis, B., Asunción, M., Gervy, C., Contempré, B., & Morreale de Escobar, G. (2002). Fetal tissues are exposed to biologically relevant free thyroxine concentrations during early phases of development. *The Journal of Clinical Endocrinology & Metabolism*, *87*(4), 1768-1777.
26. Cardoso, W. V., & Lü, J. (2006). Regulation of early lung morphogenesis: questions, facts and controversies. *Development*, *133*(9), 1611-1624.
27. Carneiro, K., Donnet, C., Rejtar, T., Karger, B. L., Barisone, G. A., Díaz, E., Kortagere, S., Lemire, J. M., & Levin, M. (2011). Histone deacetylase activity is necessary for left-right patterning during vertebrate development. *BMC Developmental Biology*, *11*(1), 29.
28. Carre, A., Rachdi, L., Tron, E., Richard, B., Castanet, M., Schlumberger, M., Bidart, J.M., Szinnai, G., & Polak, M. (2011). Hes1 is required for appropriate morphogenesis and differentiation during mouse thyroid gland development. *PloS one*, *6*(2), e16752.
29. Castanet, M., Lyonnet, S., Bonaïti-Pellié, C., Polak, M., Czernichow, P., & Léger, J. (2000). Familial forms of thyroid dysgenesis among infants with congenital hypothyroidism. *New England Journal of Medicine*, *343*(6), 441-442.
30. Castanet, M., Park, S. M., Smith, A., Bost, M., Léger, J., Lyonnet, S., Pelet, A., Czernichow, P., Chatterjee, K., & Polak, M. (2002). A novel loss-of-function mutation in TTF-2 is associated with congenital hypothyroidism, thyroid agenesis and cleft palate. *Human Molecular Genetics*, *11*(17), 2051-2059.
31. Castanet, M., Sura-Trueba, S., Chauty, A., Carré, A., de Roux, N., Heath, S., Léger, J., Lyonnet, S., Czernichow, P., & Polak, M. (2005). Linkage and mutational analysis of familial thyroid dysgenesis demonstrate genetic heterogeneity implicating novel genes. *European Journal of Human Genetics*, *13*(2), 232-239.
32. Catalano, M. G., Fortunati, N., Pugliese, M., Costantino, L., Poli, R., Bosco, O., & Boccuzzi, G. (2005). Valproic acid induces apoptosis and cell cycle arrest in poorly

differentiated thyroid cancer cells. *The Journal of Clinical Endocrinology & Metabolism*, *90*(3), 1383-1389.

33. Chadwick, B. P., Obermayr, F., & Frischauf, A. M. (1997). FKHL15, a new human member of the forkhead gene family located on chromosome 9q22. *Genomics*, *41*(3), 390-396.
34. Chan, D., Zheng, Y., Tyner, J. W., Chng, W. J., Chien, W. W., Gery, S., Leong, G., Braunstein, G. D., & Koeffler, H. P. (2013). Belinostat and panobinostat (HDACI): in vitro and in vivo studies in thyroid cancer. *Journal of Cancer Research and Clinical Oncology*, *139*(9), 1507-1514.
35. Chang, S., McKinsey, T. A., Zhang, C. L., Richardson, J. A., Hill, J. A., & Olson, E. N. (2004). Histone deacetylases 5 and 9 govern responsiveness of the heart to a subset of stress signals and play redundant roles in heart development. *Molecular and Cellular Biology*, *24*(19), 8467-8476.
36. Chang, S., Young, B. D., Li, S., Qi, X., Richardson, J. A., & Olson, E. N. (2006). Histone deacetylase 7 maintains vascular integrity by repressing matrix metalloproteinase 10. *Cell*, *126*(2), 321-334.
37. Chen, H., Tini, M., & Evans, R. M. (2001). HATs on and beyond chromatin. *Current Opinion in Cell Biology*, *13*(2), 218-224.
38. Chen, S., Bellew, C., Yao, X., Stefkova, J., Dipp, S., Saifudeen, Z., Bachvarov, D., & El-Dahr, S. S. (2011). Histone deacetylase (HDAC) activity is critical for embryonic kidney gene expression, growth, and differentiation. *Journal of Biological Chemistry*, *286*(37), 32775-32789.
39. Chen, S., Yao, X., Li, Y., Saifudeen, Z., Bachvarov, D., & El-Dahr, S. S. (2015). Histone deacetylase 1 and 2 regulate Wnt and p53 pathways in the ureteric bud epithelium. *Development*, *142*(6), 1180-1192.
40. Christophe, D. (2004). The control of thyroid-specific gene expression: what exactly have we learned as yet?. *Molecular and Cellular Endocrinology*, *223*(1), 1-4.
41. Civitareale, D., Lonigro, R., Sinclair, A. J., & Di Lauro, R. (1989). A thyroid-specific nuclear protein essential for tissue-specific expression of the thyroglobulin promoter. *The EMBO Journal*, *8*(9), 2537-2542.
42. Clifton-Bligh, R. J., Wentworth, J. M., Heinz, P., Crisp, M. S., John, R., Lazarus, J. H., Ludgate, M., & Chatterjee, V. K. (1998). Mutation of the gene encoding human TTF-2 associated with thyroid agenesis, cleft palate and choanal atresia. *Nature Genetics*, *19*(4), 399-401.

43. Colin, I. M., Denef, J. F., Lengelé, B., Many, M. C., & Gérard, A. C. (2013). Recent insights into the cell biology of thyroid angiofollicular units. *Endocrine reviews*, *34*(2), 209-238.
44. Contor, L., Lamy, F., Lecocq, R., Roger, P. P., & Dumont, J. E. (1988). Differential protein phosphorylation in induction of thyroid cell proliferation by thyrotropin, epidermal growth factor, or phorbol ester. *Molecular and Cellular Biology*, *8*(6), 2494-2503.
45. Costa-e-Sousa, R. H., & Hollenberg, A. N. (2012). Minireview: the neural regulation of the hypothalamic-pituitary-thyroid axis. *Endocrinology*, *153*(9), 4128-4135.
46. Cunliffe, V. T. (2008). Eloquent silence: developmental functions of Class I histone deacetylases. *Current Opinion in Genetics & Development*, *18*(5), 404-410.
47. Dai, G., Levy, O., & Carrasco, N. (1996). Cloning and characterization of the thyroid iodide transporter. *Nature*, *379*(6564), 458–460.
48. Damante, G., & Di Lauro, R. (1994). Thyroid-specific gene expression. *Biochimica et Biophysica Acta (BBA)-Gene Structure and Expression*, *1218*(3), 255-266.
49. Darrouzet, E., Lindenthal, S., Marcellin, D., Pellequer, J. L., & Pourcher, T. (2014). The sodium/iodide symporter: state of the art of its molecular characterization. *Biochimica et Biophysica Acta (BBA)-Biomembranes*, *1838*(1), 244-253.
50. Dathan, N., Parlato, R., Rosica, A., De Felice, M., & Di Lauro, R. (2002). Distribution of the titf2/foxe1 gene product is consistent with an important role in the development of foregut endoderm, palate, and hair. *Developmental Dynamics*, *224*(4), 450-456.
51. De Felice, M., Ovitt, C., Biffali, E., Rodriguez-Mallon, A., Arra, C., Anastassiadis, K., Macchia PE, Mattei, M.G., Mariano, A., Schöler, H., Macchia, V., Di Lauro, R., & Di Lauro, R. (1998). A mouse model for hereditary thyroid dysgenesis and cleft palate. *Nature Genetics*, *19*(4), 395-398.
52. De Felice, M., & Di Lauro, R. (2004). Thyroid development and its disorders: genetics and molecular mechanisms. *Endocrine Reviews*, *25*(5), 722-746.
53. Deladoëy, J., Vassart, G., & Van Vliet, G. (2007). Possible non-Mendelian mechanisms of thyroid dysgenesis. *Endocrine Development,* 10, 29-42.
54. Dentice, M., Luongo, C., Elefante, A., Ambrosio, R., Salzano, S., Zannini, M., Nitsch, R., Di Lauro, R., Rossi, G., Fenzi, G., Salvatore, D., & Salvatore, D. (2005). Pendrin is a novel in vivo downstream target gene of the TTF-1/Nkx-2.1 homeodomain transcription factor in differentiated thyroid cells. *Molecular and Cellular Biology*, *25*(22), 10171-10182.

55. Dentice, M., Cordeddu, V., Rosica, A., Ferrara, A. M., Santarpia, L., Salvatore, D., Chiovato, L., Perri, A., Moschini, L., Fazzini, C., Olivieri, A., Costa, P., Stoppioni V, Baserga M, De Felice M, Sorcini M, Fenzi G, Di Lauro R, Tartaglia M, & Macchia, P. E. (2006). Missense mutation in the transcription factor NKX2–5: a novel molecular event in the pathogenesis of thyroid dysgenesis. *The Journal of Clinical Endocrinology & Metabolism*, *91*(4), 1428-1433.
56. Devos, H., Rodd, C., Gagné, N., Laframboise, R., & Van Vliet, G. (1999). A search for the possible molecular mechanisms of thyroid dysgenesis: sex ratios and associated malformations. *The Journal of Clinical Endocrinology & Metabolism*, *84*(7), 2502-2506.
57. Di Palma, T., Nitsch, R., Mascia, A., Nitsch, L., Di Lauro, R., & Zannini, M. (2003). The paired domain-containing factor Pax8 and the homeodomain-containing factor TTF-1 directly interact and synergistically activate transcription. *Journal of Biological Chemistry*, *278*(5), 3395-3402.
58. Dohan, O., De la Vieja, A., Paroder, V., Riedel, C., Artani, M., Reed, M., Ginter, C., & Carrasco, N. The sodium/iodide symporter (NIS): characterization, regulation, and medical significance. *Endocrine Reviews*, *24*(1), 48-77 (2003).
59. Dokmanovic, M., Clarke, C., & Marks, P. A. (2007). Histone deacetylase inhibitors: overview and perspectives. *Molecular Cancer Research*, *5*(10), 981-989.
60. Dow, C. J., Dumont, J. E., & Ketelbant, P. (1986). [Percentage of epithelial cells, fibroblasts and endothelial cells in the dog thyroid]. *Comptes rendus des seances de la Societe de biologie et de ses filiales*, *180*(6), 629-632.
61. Dumont, J. E., Lamy, F., Roger, P., & Maenhaut, C. (1992). Physiological and pathological regulation of thyroid cell proliferation and differentiation by thyrotropin and other factors. *Physiological Reviews*, *72*(3), 667-97.
62. Dunn, J. T., & Dunn, A. D. (2001). Update on intrathyroidal iodine metabolism. *Thyroid*, *11*(5), 407-414.
63. Dupont, C., Armant, D. R., & Brenner, C. A. (2009). Epigenetics: definition, mechanisms and clinical perspective. *Seminars in Reproductive Medicine, 27*(5), 351-357.
64. Erdogan, F., Larsen, L. A., Zhang, L., Tümer, Z., Tommerup, N., Chen, W., Jacobsen, J.R., Schubert, M., Jurkatis, J., Tzschach, A., Ropers, H.H., & Ullmann, R. (2008). High frequency of submicroscopic genomic aberrations detected by tiling path array comparative genome hybridisation in patients with isolated congenital heart disease. *Journal of Medical Genetics*, *45*(11), 704-709.

65. Everett, L. A., Glaser, B., Beck, J. C., Idol, J. R., Buchs, A., Adawi, F., Hazani, E., Nassir, E., Baxevanis, A.D., Sheffield, V.C., & Green, E. D. (1997). Pendred syndrome is caused by mutations in a putative sulphate transporter gene (PDS). *Nature Genetics*, *17*(4), 411-422.
66. Fagman, H., Grande, M., Edsbagge, J., Semb, H., & Nilsson, M. (2003). Expression of classical cadherins in thyroid development: maintenance of an epithelial phenotype throughout organogenesis. *Endocrinology*, *144*(8), 3618-3624.
67. Fagman, H., Grände, M., Gritli-Linde, A., & Nilsson, M. (2004). Genetic deletion of sonic hedgehog causes hemiagenesis and ectopic development of the thyroid in mouse. *The American Journal of Pathology*, *164*(5), 1865-1872.
68. Fagman, H., Andersson, L., & Nilsson, M. (2006). The developing mouse thyroid: embryonic vessel contacts and parenchymal growth pattern during specification, budding, migration, and lobulation. *Developmental Dynamics*, *235*(2), 444-455.
69. Fernández, L. P., López-Márquez, A., & Santisteban, P. (2015). Thyroid transcription factors in development, differentiation and disease. *Nature Reviews Endocrinology*, *11*(1), 29-42.
70. Ferrara, A. M., De Michele, G., Salvatore, E., Di Maio, L., Zampella, E., Capuano, S., Del Prete, G., Rossi, G., Fenzi, G., Filla, A., & Macchia, P. E. (2008). A novel NKX2. 1 mutation in a family with hypothyroidism and benign hereditary chorea. *Thyroid*, *18*(9), 1005-1009.
71. Fortunati, N., Catalano, M. G., Arena, K., Brignardello, E., Piovesan, A., & Boccuzzi, G. (2004). Valproic acid induces the expression of the Na+/I-symporter and iodine uptake in poorly differentiated thyroid cancer cells. *The Journal of clinical endocrinology and metabolism*, *89*(2), 1006-1009.
72. Fry, C. J., & Peterson, C. L. (2001). Chromatin remodeling enzymes: who's on first?. *Current Biology*, *11*(5), R185-R197.
73. Fugazzola, L., Cerutti, N., Mannavola, D., Vannucchi, G., Fallini, C., Persani, L., & Beck-Peccoz, P. (2013). Monoallelic expression of mutant thyroid peroxidase allele causing total iodide organification defect. *The Journal of Clinical Endocrinology & Metabolism*, *88*(7), 3264-3271.
74. Fujiwara, H., Tatsumi, K. I., Miki, K., Harada, T., Miyai, K., Takai, S. I., & Amino, N. (1997). Congenital hypothyroidism caused by a mutation in the Na+/l− symporter. *Nature Genetics*, *16*(2), 124-125.

75. Furuya, F., Shimura, H., Suzuki, H., Taki, K., Ohta, K., Haraguchi, K., Onaya, T., Endo, T., & Kobayashi, T. (2004). Histone deacetylase inhibitors restore radioiodide uptake and retention in poorly differentiated and anaplastic thyroid cancer cells by expression of the sodium/iodide symporter thyroperoxidase and thyroglobulin. *Endocrinology*, *145*(6), 2865-2875.
76. Geisberg, J. V., & Struhl, K. (2004). Quantitative sequential chromatin immunoprecipitation, a method for analyzing co-occupancy of proteins at genomic regions in vivo. *Nucleic Acids Research*, *32*(19), e151-e151.
77. Ghosh, B., Jacobs, H. C., Wiedemann, L. M., Brown, A., Bedford, F. K., Nimmakayalu, M. A., Ward, D.C., & Bogue, C. W. (1999). Genomic structure, cDNA mapping, and chromosomal localization of the mouse homeobox gene, Hex. *Mammalian Genome*, *10*(10), 1023-1025.
78. Giraldez, A. J., Cinalli, R. M., Glasner, M. E., Enright, A. J., Thomson, J. M., Baskerville, S., Hammond, S.M., Bartel, D.P. & Schier, A. F. (2005). MicroRNAs regulate brain morphogenesis in zebrafish. *Science*, *308*(5723), 833-838.
79. Glozak, M. A., Sengupta, N., Zhang, X., & Seto, E. (2005). Acetylation and deacetylation of non-histone proteins. *Gene*, *363*, 15-23.
80. Goll, M. G., & Bestor, T. H. (2005). Eukaryotic cytosine methyltransferases. *Annual Review of Biochemistry*, *74*, 481-514.
81. Grant, D. B., Smith, I., Fuggle, P. W., Tokar, S., & Chapple, J. (1992). Congenital hypothyroidism detected by neonatal screening: relationship between biochemical severity and early clinical features. *Archives of Disease in Childhood*, *67*(1), 87-90.
82. Grasberger, H. (2010). Defects of thyroidal hydrogen peroxide generation in congenital hypothyroidism. *Molecular and Cellular Endocrinology*, *322*(1), 99-106.
83. Grasberger, H., & Refetoff, S. (2011). Genetic causes of congenital hypothyroidism due to dyshormonogenesis. *Current Opinion in Pediatrics*, *23*(4), 421-428.
84. Greenberg, A. H., Czernichow, P., Reba, R. C., Tyson, J., & Blizzard, R. M. (1970). Observations on the maturation of thyroid function in early fetal life. *Journal of Clinical Investigation*, *49*(10), 1790-1803.
85. Grewal, S. I., & Moazed, D. (2003). Heterochromatin and epigenetic control of gene expression. *Science*, *301*(5634), 798-802.
86. Grozinger, C. M., & Schreiber, S. L. (2002). Deacetylase enzymes: biological functions and the use of small-molecule inhibitors. *Chemistry & Biology*, *9*(1), 3-16.

87. Guazzi, S., Price, M., De Felice, M., Damante, G., Mattei, M. G., & Di Lauro, R. (1990). Thyroid nuclear factor 1 (TTF-1) contains a homeodomain and displays a novel DNA binding specificity. *The EMBO Journal*, *9*(11), 3631-3639.
88. Haberland, M., Montgomery, R. L., & Olson, E. N. (2009a). The many roles of histone deacetylases in development and physiology: implications for disease and therapy. *Nature Reviews Genetics*, *10*(1), 32-42.
89. Haberland, M., Mokalled, M. H., Montgomery, R. L., & Olson, E. N. (2009b). Epigenetic control of skull morphogenesis by histone deacetylase 8. *Genes & Development*, *23*(14), 1625-1630.
90. Haumaitre, C., Lenoir, O., & Scharfmann, R. (2008). Histone deacetylase inhibitors modify pancreatic cell fate determination and amplify endocrine progenitors. *Molecular and Cellular Biology*, *28*(20), 6373-6383.
91. Heinzel, T., Lavinsky, R. M., Mullen, T. M., Söderstrom, M., Laherty, C. D., Torchia, J., Yang, W. M., Brard, G., Ngo, S. D., Davie, J. R., Seto E, Eisenman, R. N., Rose, D. W., Glass, C. K., & Rosenfeld M. G. (1997). A complex containing N-CoR, mSin3 and histone deacetylase mediates transcriptional repression. *Nature 387*(6628), 43-48.
92. Hermanns, P., Grasberger, H., Refetoff, S., & Pohlenz, J. (2011). Mutations in the NKX2.5 gene and the PAX8 promoter in a girl with thyroid dysgenesis. *The Journal of Clinical Endocrinology & Metabolism*, *96*(6), E977-E981.
93. Hick, A. C., Delmarcelle, A. S., Bouquet, M., Klotz, S., Copetti, T., Forez, C., Van Der Smissen, P., Sonveaux, P., Collet, J., Feron, O., Courtoy, P., & Pierreux, C. E. (2013). Reciprocal epithelial: endothelial paracrine interactions during thyroid development govern follicular organization and C-cells differentiation. *Developmental Biology*, *381*(1), 227-240.
94. Himmelbauer, H., Harvey, R. P., Copeland, N. G., Jenkins, N. A., & Silver, L. M. (1994). High-resolution genetic analysis of a deletion on mouse chromosome 17 extending over the fused, tufted, and homeobox Nkx2-5 loci. *Mammalian Genome*, *5*(12), 814-816.
95. Hitz, M. P., Lemieux-Perreault, L. P., Marshall, C., Feroz-Zada, Y., Davies, R., Yang, S. W., Lionel, A. C., D'Amours, G., Lemyre, E., Cullum, R., Bigras, J. L., Thibeault, M., Chetaille, P., Montpetit, A., Khairy, P., Overduin, B., Klaassen, S., Hoodless, P., Awadalla, P., Hussin, J., Idaghdour, Y., Nemer, M., Stewart, A. F., Boerkoel, C., Scherer, S. W., Richter, A., Dubé, M. P., & Andelfinger, G. (2012). Rare copy number variants contribute to congenital left-sided heart disease. *PLoS Genetics*, *8*(9), 1-13.

96. Hodges, R. E., Evans, T. C., Bradbury, J. T., & Keetel, W. C. (1955). The accumulation of radioactive iodine by human fetal thyroids. *The Journal of Clinical Endocrinology & Metabolism*, *15*(6), 661-667.
97. Hromas, R., Radich, J., & Collins, S. (1993). PCR cloning of an orphan homeobox gene (PRH) preferentially expressed in myeloid and liver cells. *Biochemical and Biophysical Research Communications*, *195*(2), 976-983.
98. Hubbert, C., Guardiola, A., Shao, R., Kawaguchi, Y., Ito, A., Nixon, A., Yoshida M., Wang, X.F., & Yao, T. P. (2002). HDAC6 is a microtubule-associated deacetylase. *Nature*, *417*(6887), 455-458.
99. Iglesias, A., García-Nimo, L., de Juan, J. A. C., & Moreno, J. C. (2014). Towards the pre-clinical diagnosis of hypothyroidism caused by iodotyrosine deiodinase (DEHAL1) defects. *Best Practice & Research Clinical Endocrinology & Metabolism*, *28*(2), 151-159.
100. Ishibashi, M., Ang, S. L., Shiota, K., Nakanishi, S., Kageyama, R., & Guillemot, F. (1995). Targeted disruption of mammalian hairy and Enhancer of split homolog-1 (HES-1) leads to up-regulation of neural helix-loop-helix factors, premature neurogenesis, and severe neural tube defects. *Genes & Development*, *9*(24), 3136-3148.
101. Issa, J. P. (2000). CpG-island methylation in aging and cancer. *Current Topics in Microbiology and Immunology*, *249*, 101-118.
102. Jaenisch, R., & Bird, A. (2003). Epigenetic regulation of gene expression: how the genome integrates intrinsic and environmental signals. *Nature Genetics*, *33*, 245-254.
103. Jaworska, J., Ziemka-Nalecz, M. & Zalewska, T. (2015). Histone deacetylases 1 and 2 are required for brain development. *The International Journal of Developmental Biology*.
104. Jenuwein, T., & Allis, C. D. (2001). Translating the histone code. *Science*, *293*(5532), 1074-1080.
105. Kaestner, K. H., Lee, K. H., Schlöndorff, J., Hiemisch, H., Monaghan, A. P., & Schütz, G. (1993). Six members of the mouse forkhead gene family are developmentally regulated. *Proceedings of the National Academy of Sciences*, *90*(16), 7628-7631.
106. Kageyama, R., Ohtsuka, T., & Kobayashi, T. (2007). The Hes gene family: repressors and oscillators that orchestrate embryogenesis. *Development*, *134*(7), 1243-1251.
107. Kageyama, S. I., Liu, H., Nagata, M., & Aoki, F. (2006). Stage specific expression of histone deacetylase 4 (HDAC4) during oogenesis and early preimplantation development in mice. *Journal of Reproduction and Development*, *52*(1), 99-106.

108. Kambe, F., & Seo, H. (1997). Thyroid-specific transcription factors. *Endocrine Journal*, *44*(6), 775-784.
109. Karmodiya, K., Krebs, A. R., Oulad-Abdelghani, M., Kimura, H., & Tora, L. (2012). H3K9 and H3K14 acetylation co-occur at many gene regulatory elements, while H3K14ac marks a subset of inactive inducible promoters in mouse embryonic stem cells. *BMC Genomics*, *13*(1), 424.
110. Kenyon, K. L., Ranade, S. S., Curtiss, J., Mlodzik, M., & Pignoni, F. (2003). Coordinating proliferation and tissue specification to promote regional identity in the Drosophila head. *Developmental Cell*, *5*(3), 403-414.
111. Khier, H., Bartl, S., Schuettengruber, B., & Seiser, C. (1999). Molecular cloning and characterization of the mouse histone deacetylase 1 gene: integration of a retrovirus in 129SV mice. *Biochimica et Biophysica Acta (BBA)-Gene Structure and Expression*, *1489*(2), 365-373.
112. Kimura, S., Hara, Y., Pineau, T., Fernandez-Salguero, P., Fox, C. H., Ward, J. M., & Gonzalez, F. J. (1996). The T/ebp null mouse: thyroid-specific enhancer-binding protein is essential for the organogenesis of the thyroid, lung, ventral forebrain, and pituitary. *Genes & Development*, *10*(1), 60-69.
113. Kimura, S., Ward, J. M., & Minoo, P. (1999). Thyroid-specific enhancer-binding protein/thyroid transcription factor 1 is not required for the initial specification of the thyroid and lung primordia. *Biochimie*, *81*(4), 321-327.
114. Kitazono, M., Robey, R., Zhan, Z., Sarlis, N. J., Skarulis, M. C., Aikou, T., Bates, S., & Fojo, T. (2001). Low concentrations of the histone deacetylase inhibitor, depsipeptide (FR901228), increase expression of the Na+/I− symporter and iodine accumulation in poorly differentiated thyroid carcinoma cells. *The Journal of Clinical Endocrinology & Metabolism*, *86*(7), 3430-3435.
115. Kleinau, G., Neumann, S., Grüters, A., Krude, H., & Biebermann, H. (2013). Novel insights on thyroid-stimulating hormone receptor signal transduction. *Endocrine Reviews*, *34*(5), 691-724.
116. Knobel, M., & Medeiros-Neto, G. (2003). An outline of inherited disorders of the thyroid hormone generating system. *Thyroid*, *13*(8), 771-801.
117. Kogai, T., Taki, K., & Brent, G. A. (2006). Enhancement of sodium/iodide symporter expression in thyroid and breast cancer. *Endocrine-Related Cancer*, *13*(3), 797-826.
118. Kondo, T., Asa, S. L., & Ezzat, S. (2008). Epigenetic dysregulation in thyroid neoplasia. *Endocrinology and Metabolism Clinics of North America*, *37*(2), 389-400.

119. Kopp, P., & Bizhanova, A. (2011). Clinical and molecular characteristics of Pendred syndrome. *Annales d'endocrinologie*, *72*(2), 88-94.
120. Kouzarides, T. (2007). Chromatin modifications and their function. *Cell*, *128*(4), 693-705.
121. Kratz, A., Arner, E., Saito, R., Kubosaki, A., Kawai, J., Suzuki, H., Carninci, P., Arakawa, T., Tomita, M., Hayashizaki, Y., & Daub, C. O. (2010). Core promoter structure and genomic context reflect histone 3 lysine 9 acetylation patterns. *BMC Genomics*, *11*(1), 257.
122. Kraus, M. R., & Grapin-Botton, A. (2012). Patterning and shaping the endoderm in vivo and in culture. *Current Opinion in Genetics & Development*, *22*(4), 347-353.
123. Krude, H., Schütz, B., Biebermann, H., von Moers, A., Schnabel, D., Neitzel, H., Tönnies, H., Weise, D., Lafferty, A., Schwarz, S., De Felice, M., von Deimling, A., van Landeghem, F., Di Lauro, R. & Grüters, A. (2002). Choreoathetosis, hypothyroidism, and pulmonary alterations due to human NKX2-1 haploinsufficiency. *The Journal of Clinical Investigation*, *109*(109 (4)), 475-480.
124. Kumar, J., Gordillo, R., Kaskel, F. J., Druschel, C. M., & Woroniecki, R. P. (2009). Increased prevalence of renal and urinary tract anomalies in children with congenital hypothyroidism. *The Journal of Pediatrics*, *154*(2), 263-266.
125. Kuo, C. T., Morrisey, E. E., Anandappa, R., Sigrist, K., Lu, M. M., Parmacek, M. S., Soudais, C., & Leiden, J. M. (1997). GATA4 transcription factor is required for ventral morphogenesis and heart tube formation. *Genes & Development*, *11*(8), 1048-1060.
126. Kurdistani, S.K. (2007). Histone modifications as markers of cancer prognosis: a cellular view. *British Journal of Cancer*. *97*(1), 1-5.
127. Kusakabe, T., Kawaguchi, A., Hoshi, N., Kawaguchi, R., Hoshi, S., & Kimura, S. (2006a). Thyroid-specific enhancer-binding protein/NKX2. 1 is required for the maintenance of ordered architecture and function of the differentiated thyroid. *Molecular Endocrinology*, *20*(8), 1796-1809.
128. Kusakabe, T., Hoshi, N., & Kimura, S. (2006_b). Origin of the ultimobranchial body cyst: T/ebp/Nkx2. 1 expression is required for development and fusion of the ultimobranchial body to the thyroid. *Developmental Dynamics*, *235*(5), 1300-1309.
129. Lado-Abeal, J., Castro-Piedras, I., Palos-Paz, F., Labarta-Aizpún, J. I., & Albero-Gamboa, R. (2011). A family with congenital hypothyroidism caused by a combination of loss-of-function mutations in the thyrotropin receptor and adenylate cyclase-stimulating G alpha-protein subunit genes. *Thyroid*, *21*(2), 103-109.

130. Lagger, G., O'Carroll, D., Rembold, M., Khier, H., Tischler, J., Weitzer, G., Schuettengruber, B., Hauser, C., Brunmeir, R., Jenuwein, T., & Seiser, C. (2002). Essential function of histone deacetylase 1 in proliferation control and CDK inhibitor repression. *The EMBO Journal*, *21*(11), 2672-2681.
131. Laherty, C. D., Yang, W. M., Sun, J. M., Davie, J. R., Seto, E. & Eisenman, R. N. (1997). Histone deacetylases associated with the mSin3 corepressor mediate mad transcriptional repression. *Cell,* 89, 349-356.
132. Lazzaro, D., Price, M., De Felice, M., & Di Lauro, R. (1991). The transcription factor TTF-1 is expressed at the onset of thyroid and lung morphogenesis and in restricted regions of the foetal brain. *Development*, *113*(4), 1093-1104.
133. Lee, C. S., Friedman, J. R., Fulmer, J. T., & Kaestner, K. H. (2005). The initiation of liver development is dependent on Foxa transcription factors. *Nature*, *435*(7044), 944-947.
134. Lee, J., Wang, X., Di Jeso, B., & Arvan, P. (2009). The cholinesterase-like domain, essential in thyroglobulin trafficking for thyroid hormone synthesis, is required for protein dimerization. *Journal of Biological Chemistry*, *284*(19), 12752-12761.
135. Li, Y., Wang, J., Xie, Y., Liu, S., & Tian, Y. (2014). Pattern of change in histone 3 lysine 9 acetylation and histone deacetylases in development of zebrafish embryo. *Journal of Genetics*, *93*(2), 539-544.
136. Libert, F., Passage, E., Lefort, A., Vassart, G., & Mattei, M. G. (1990). Localization of human thyrotropin receptor gene to chromosome region 14q31 by in situ hybridization. *Cytogenetic and Genome Research*, *54*(1-2), 82-83.
137. Luger, K., Mäder, A. W., Richmond, R. K., Sargent, D. F., & Richmond, T. J. (1997). Crystal structure of the nucleosome core particle at 2.8 Å resolution. *Nature*, *389*(6648), 251-260.
138. Luo, J., Su, F., Chen, D., Shiloh, A., & Gu, W. (2000). Deacetylation of p53 modulates its effect on cell growth and apoptosis. *Nature*, *408*(6810), 377-381.
139. Macchia, P. E., Lapi, P., Krude, H., Pirro, M. T., Missero, C., Chiovato, L., Souabni, A., Baserga, M., Tassi, V., Pinchera, A., Fenzi, G., Grüters, A., Busslinger, M., & Di Lauro, R. (1998). PAX8 mutations associated with congenital hypothyroidism caused by thyroid dysgenesis. *Nature Genetics*, *19*(1), 83-86.
140. Magliano, M. P., Di Lauro, R., & Zannini, M. (2000). Pax8 has a key role in thyroid cell differentiation. *Proceedings of the National Academy of Sciences*, *97*(24), 13144-13149.

141. Mansouri, A., Chowdhury, K., & Gruss, P. (1998). Follicular cells of the thyroid gland require Pax8 gene function. *Nature Genetics*, *19*(1), 87-90.
142. Margueron, R., Trojer, P., & Reinberg, D. (2005). The key to development: interpreting the histone code?. *Current Opinion in Genetics & Development*, *15*(2), 163-176.
143. Marians, R. C., Ng, L., Blair, H. C., Unger, P., Graves, P. N., & Davies, T. F. (2002). Defining thyrotropin-dependent and-independent steps of thyroid hormone synthesis by using thyrotropin receptor-null mice. *Proceedings of the National Academy of Sciences*, *99*(24), 15776-15781.
144. Marin-Husstege, M., Muggironi, M., Liu, A., & Casaccia-Bonnefil, P. (2002). Histone deacetylase activity is necessary for oligodendrocyte lineage progression. *The Journal of Neuroscience*, *22*(23), 10333-10345.
145. Marks, P. A., & Xu, W. S. (2009). Histone deacetylase inhibitors: Potential in cancer therapy. *Journal of Cellular Biochemistry*, *107*(4), 600-608.
146. Martínez-Balbás, M. A., Bauer, U. M., Nielsen, S. J., Brehm, A., & Kouzarides, T. (2000). Regulation of E2F1 activity by acetylation. *The EMBO Journal*, *19*(4), 662-671.
147. McKinsey, T. A., Zhang, C. L., & Olson, E. N. (2001). Control of muscle development by dueling HATs and HDACs. *Current Opinion in Genetics & Development*, *11*(5), 497-504.
148. Meshorer, E., Yellajoshula, D., George, E., Scambler, P. J., Brown, D. T., & Misteli, T. (2006). Hyperdynamic plasticity of chromatin proteins in pluripotent embryonic stem cells. *Developmental Cell*, *10*(1), 105-116.
149. Mizuno, K., Gonzalez, F. J., & Kimura, S. (1991). Thyroid-specific enhancer-binding protein (T/EBP): cDNA cloning, functional characterization, and structural identity with thyroid transcription factor TTF-1. *Molecular and Cellular Biology*, *11*(10), 4927-4933.
150. Moerch, U., Nielsen, H. S., Lundsgaard, D., & Oleksiewicz, M. B. (2007). Flow sorting from organ material by intracellular markers. *Cytometry Part A*, *71*(7), 495-500.
151. Montgomery, R. L., Davis, C. A., Potthoff, M. J., Haberland, M., Fielitz, J., Qi, X., Hill, J.A., Richardson, J.A., & Olson, E. N. (2007). Histone deacetylases 1 and 2 redundantly regulate cardiac morphogenesis, growth, and contractility. *Genes & Development*, *21*(14), 1790-1802.
152. Moreno, J. C., Klootwijk, W., van Toor, H., Pinto, G., D'Alessandro, M., Lèger, A., Goudie, D., Polak, M., Grueters, A., & Visser, T. J. (2008). Mutations in the iodotyrosine deiodinase gene and hypothyroidism. *New England Journal of Medicine*, *358*(17), 1811-1818.

153. Morrisey, E. E., Tang, Z., Sigrist, K., Lu, M. M., Jiang, F., Ip, H. S., & Parmacek, M. S. (1998). GATA6 regulates HNF4 and is required for differentiation of visceral endoderm in the mouse embryo. *Genes & Development*, *12*(22), 3579-3590.
154. Morgans, M. E., & Trotter, W. R. (1958). Association of congenital deafness with goitre the nature of the thyroid. *The Lancet*, *271*(7021), 607-609.
155. Mottamal, M., Zheng, S., Huang, T. L., & Wang, G. (2015). Histone deacetylase inhibitors in clinical studies as templates for new anticancer agents. *Molecules*, *20*(3), 3898-3941.
156. Moya, C. M., de Nanclares, G. P., Castaño, L., Potau, N., Bilbao, J. R., Carrascosa, A., Bargadá, M., Coya, R., Martul, P., Vicens-Calvet, E., & Santisteban, P. (2006). Functional study of a novel single deletion in the TITF1/NKX2. 1 homeobox gene that produces congenital hypothyroidism and benign chorea but not pulmonary distress. *The Journal of Clinical Endocrinology & Metabolism*, *91*(5), 1832-1841.
157. Murata, K., Hattori, M., Hirai, N., Shinozuka, Y., Hirata, H., Kageyama, R., Sakai, N., & Minato, N. (2005). Hes1 directly controls cell proliferation through the transcriptional repression of p27Kip1. *Molecular and cellular biology*, *25*(10), 4262-4271.
158. Narumi, S., Muroya, K., Asakura, Y., Adachi, M., & Hasegawa, T. (2010). Transcription factor mutations and congenital hypothyroidism: systematic genetic screening of a population-based cohort of Japanese patients. *The Journal of Clinical Endocrinology & Metabolism*, *95*(4), 1981-1985.
159. Narumi, S., Nagasaki, K., Ishii, T., Muroya, K., Asakura, Y., Adachi, M., & Hasegawa, T. (2011a). Nonclassic TSH resistance: TSHR mutation carriers with discrepantly high thyroidal iodine uptake. *The Journal of Clinical Endocrinology & Metabolism*, *96*(8), 1340-1345.
160. Narumi, S., Yoshida, A., Muroya, K., Asakura, Y., Adachi, M., Fukuzawa, R., Kameyama, K., & Hasegawa, T. (2011b). PAX8 mutation disturbing thyroid follicular growth: a case report. *The Journal of Clinical Endocrinology & Metabolism*, *96*(12), 2039-2044.
161. Nilsson, M., & Fagman, H. (2013). Mechanisms of thyroid development and dysgenesis: an analysis based on developmental stages and concurrent embryonic anatomy. *Current Topics in Developmental Biology*, *106*, 123-170.
162. Okano, M., Bell, D. W., Haber, D. A., & Li, E. (1999). DNA methyltransferases Dnmt3a and Dnmt3b are essential for de novo methylation and mammalian development. *Cell*, *99*(3), 247-257.

163. Olin, P., Ekholm, R., & Almqvist, S. (1970). Biosynthesis of thyroglobulin related to the ultrastructure of the human fetal thyroid gland. *Endocrinology*, *87*(5), 1000-1014.
164. Park, S. M., & Chatterjee, V. K. K. (2005). Genetics of congenital hypothyroidism. *Journal of Medical Genetics*, *42*(5), 379-389.
165. Parlato, R., Rosica, A., Rodriguez-Mallon, A., Affuso, A., Postiglione, M. P., Arra, C., Mansouri, A., Kimura, S., Di Lauro, R., De Felice, M., & De Felice, M. (2004). An integrated regulatory network controlling survival and migration in thyroid organogenesis. *Developmental Biology*, *276*(2), 464-475.
166. Parmentier, M., Libert, F., Maenhaut, C., Lefort, A., Gerard, C., Perret, J., Van Sande, J., Dumont, J.E., & Vassart, G. (1989). Molecular cloning of the thyrotropin receptor. *Science*, *246*(4937), 1620-1622.
167. Perry, R., Heinrichs, C., Bourdoux, P., Khoury, K., Szöts, F., Dussault, J. H., Vassart, G., & Van Vliet, G. (2002). Discordance of monozygotic twins for thyroid dysgenesis: implications for screening and for molecular pathophysiology. *The Journal of Clinical Endocrinology & Metabolism*, *87*(9), 4072-4077.
168. Pesce, L., Bizhanova, A., Caraballo, J. C., Westphal, W., Butti, M. L., Comellas, A., & Kopp, P. (2011). TSH regulates pendrin membrane abundance and enhances iodide efflux in thyroid cells. *Endocrinology*, *153*(1), 512-521.
169. Peserico, A., & Simone, C. (2010). Physical and functional HAT/HDAC interplay regulates protein acetylation balance. *BioMed Research International*, *2011*, 1-10.
170. Plachov, D., Chowdhury, K., Walther, C., Simon, D., Guenet, J. L., & Gruss, P. (1990). Pax8, a murine paired box gene expressed in the developing excretory system and thyroid gland. *Development*, *110*(2), 643-651.
171. Poduri, A., Evrony, G. D., Cai, X., & Walsh, C. A. (2013). Somatic mutation, genomic variation, and neurological disease. *Science*, *341*(6141), 1237758.
172. Pohlenz, J., Dumitrescu, A., Zundel, D., Martiné, U., Schönberger, W., Koo, E., Weiss, R.E., Cohen, R.N., Kimura, S., & Refetoff, S. (2002). Partial deficiency of thyroid transcription factor 1 produces predominantly neurological defects in humans and mice. *The Journal of Clinical Investigation*, *109*(4), 469-473.
173. Polak, M., & Szinnai, G. (2013). Chapter 84 – Thyroid Disorders. *Emery and Rimoin's Principles and Practice of Medical Genetics* (pp 1-24). Churchill Livingstone, London, UK.
174. Portulano, C., Paroder-Belenitsky, M., & Carrasco, N. (2014). The Na+/I− symporter (NIS): mechanism and medical impact. *Endocrine Reviews*, *35*(1), 106-149.

175. Postiglione, M. P., Parlato, R., Rodriguez-Mallon, A., Rosica, A., Mithbaokar, P., Maresca, M., Marians R. C., Davies T. F., Zannini M.S., De Felice, M., & Di Lauro, R. (2002). Role of the thyroid-stimulating hormone receptor signaling in development and differentiation of the thyroid gland. *Proceedings of the National Academy of Sciences*, *99*(24), 15462-15467.
176. Price, M., Lazzaro, D., Pohl, T., Mattei, M. G., Rüther, U., Olivo, J. C., Duboule, D., & Di Lauro, R. (1992). Regional expression of the homeobox gene Nkx-2.2 in the developing mammalian forebrain. *Neuron*, *8*(2), 241-255.
177. Puppin, C., D'Aurizio, F., D'Elia, AV., Cesaratto, L., Tell, G., Russo, D., Filetti, S., Ferretti, E., Tosi, E., Mattei, T., Pianta, A., Pellizzari, L., Damante, G. (2005). Effects of histone acetylation on sodium iodide symporter promoter and expression of thyroid-specific transcription factors. *Endocrinology*, *146*(9), 3967-74.
178. Puppin, C., Passon, N., Hershman, J. M., Filetti, S., Bulotta, S., Celano, M., Russo, D., & Damante, G. (2012). Cooperative effects of SAHA and VPA on *NIS* gene expression and proliferation of thyroid cancer cells. *Journal of Molecular Endocrinology*, *48*(3), 217-227.
179. Rada-Iglesias, A., Bajpai, R., Swigut, T., Brugmann, S. A., Flynn, R. A., & Wysocka, J. (2011). A unique chromatin signature uncovers early developmental enhancers in humans. *Nature*, *470*(7333), 279-283.
180. Rastogi, M. V., & LaFranchi, S. H. (2010). Congenital hypothyroidism. *Orphanet J Rare Dis*, *5*(1), 1-22.
181. Reddington, J. P., Pennings, S., & Meehan, R. R. (2013). Non-canonical functions of the DNA methylome in gene regulation. *Biochemical Journal*, *451*(1), 13-23.
182. Refetoff, S. (2003). Resistance to thyrotropin. *Journal of Endocrinological Investigation*, *26*(8), 770-779.
183. Reichert, N., Choukrallah, M. A., & Matthias, P. (2012). Multiple roles of class I HDACs in proliferation, differentiation, and development. *Cellular and Molecular Life Sciences*, *69*(13), 2173-2187.
184. Reik, W. (2007). Stability and flexibility of epigenetic gene regulation in mammalian development. *Nature*, *447*(7143), 425-432.
185. Rivas, M & Santisteban, P. TSH-activated signaling pathways in thyroid tumorigenesis. *Molecular and Cellular Endocrinology* 213, 31-45 (2003).
186. Rivolta, C. M., Moya, C. M., Gutnisky, V. J., Varela, V., Miralles-García, J. M., González-Sarmiento, R., & Targovnik, H. M. (2005). A new case of congenital goiter

with hypothyroidism caused by a homozygous p. R277X mutation in the exon 7 of the thyroglobulin gene: a mutational hot spot could explain the recurrence of this mutation. *The Journal of Clinical Endocrinology & Metabolism*, *90*(6), 3766-3770.

187. Roger, P. P., Baptist, M., & Dumont, J. E. (1992). A mechanism generating heterogeneity in thyroid epithelial cells: suppression of the thyrotropin/cAMP-dependent mitogenic pathway after cell division induced by cAMP-independent factors. *The Journal of Cell Biology*, *117*(2), 383-393.
188. Roth, S. Y., & Allis, C. D. (1996). Histone acetylation and chromatin assembly: a single escort, multiple dances?. *Cell*, *87*(1), 5-8.
189. Roth, S. Y., Denu, J. M., & Allis, C. D. (2001). Histone acetyltransferases. *Annual Review of Biochemistry*, *70*(1), 81-120.
190. Royaux, I. E., Suzuki, K., Mori, A., & Katoh, R. (2000) Pendrin, the protein encoded by the Pendred syndrome gene (PDS), is an apical porter of iodide in the thyroid and is regulated by thyroglobulin in FRTL-5 cells. *Endocrinology 141*(2), 839-845.
191. Russo, D., Damante, G., Puxeddu, E., Durante, C., & Filetti, S. (2011). Epigenetics of thyroid cancer and novel therapeutic targets. *Journal of Molecular Endocrinology*, *46*(3), 73-81.
192. Sarmento, O. F., Digilio, L. C., Wang, Y., Perlin, J., Herr, J. C., Allis, C. D., & Coonrod, S. A. (2004). Dynamic alterations of specific histone modifications during early murine development. *Journal of Cell Science*, *117*(19), 4449-4459.
193. Schott, J. J., Benson, D. W., Basson, C. T., Pease, W., Silberbach, G. M., Moak, J. P., Maron, B.J., Seidman, C.E., & Seidman, J. G. (1998). Congenital heart disease caused by mutations in the transcription factor NKX2-5. *Science*, *281*(5373), 108-111.
194. Shepard, T. H., Andersen, H., & Andersen, H. J. (1964). Histochemical studies of the human fetal thyroid during the first half of fetal life. *The Anatomical Record*, *149*(3), 363-379.
195. Shepard, T. H. (1967). Onset of Function in the Human Fetal Thyroid: Biochemical and Radioautographic Studies from Organ Culture 1. *The Journal of Clinical Endocrinology & Metabolism*, *27*(7), 945-958.
196. Song, Y., Driessens, N., Costa, M., De Deken, X., Detours, V., Corvilain, B., Maenhaut, C., Miot, F., Van Sande, J., Many, M.C., & Dumont, J. E. (2007). Roles of hydrogen peroxide in thyroid physiology and disease. *The Journal of Clinical Endocrinology & Metabolism*, *92*(10), 3764-3773.

197. Southard, A. E., Edelmann, L. J., & Gelb, B. D. (2012). Role of copy number variants in structural birth defects. *Pediatrics*, *129*(4), 755-763.
198. Spitzweg, C., & Morris, J. C. (2010). Genetics and phenomics of hypothyroidism and goiter due to NIS mutations. *Molecular and Cellular Endocrinology*, *322*(1), 56-63.
199. Sriphrapradang, C., Tenenbaum-Rakover, Y., Weiss, M., Barkoff, M. S., Admoni, O., Kawthar, D., Caltabiano, G., Pardo, L., Dumitrescu, A.M., & Refetoff, S. (2011). The coexistence of a novel inactivating mutant thyrotropin receptor allele with two thyroid peroxidase mutations: a genotype-phenotype correlation. *The Journal of Clinical Endocrinology & Metabolism*, *96*(6), 1001-1006.
200. Stanbury, J., & Chapman, E. (1960). Congenital hypothyroidism with goitre absence of an iodide-concentrating mechanism. *The Lancet*, *275*(7135), 1162-1165.
201. Stapleton, P., Weith, A., Urbánek, P., Kozmik, Z., & Busslinger, M. (1993). Chromosomal localization of seven PAX genes and cloning of a novel family member, PAX-9. *Nature Genetics*, *3*(4), 292-298.
202. Stathatos, N. (2006). Anatomy and Physiology of the Thyroid Gland Clinical Correlates to Thyroid Cancer, Thyroid Cancer A Comprehensive Guide to Clinical Management. *Humana Press Inc, Totowa, New Jersey*, *1*, 3-9.
203. Stein, S. A., Oates, E. L., Hall, C. R., Grumbles, R. M., Fernandez, L. M., Taylor, N. A., Puett, D., & Jin, S. (1994). Identification of a point mutation in the thyrotropin receptor of the hyt/hyt hypothyroid mouse. *Molecular Endocrinology*, *8*(2), 129-138.
204. Sterner, D. E., & Berger, S. L. (2000). Acetylation of histones and transcription-related factors. *Microbiology and Molecular Biology Reviews*, *64*(2), 435-459.
205. Strahl, B. D., & Allis, C. D. (2000). The language of covalent histone modifications. *Nature*, *403*(6765), 41-45.
206. Sunthornthepvarakul, T., Gottschalk, M. E., Hayashi, Y., & Refetoff, S. (1995). Resistance to thyrotropin caused by mutations in the thyrotropin-receptor gene. *New England Journal of Medicine*, *332*(3), 155-160.
207. Suzuki, K., Kobayashi, Y., Katoh, R., Kohn, L. D., & Kawaoi, A. (1998). Identification of thyroid transcription factor-1 in C cells and parathyroid cells. *Endocrinology*, *139*(6), 3014-3017.
208. Svaren, J., & Hörz, W. (1993). Histones, nucleosomes and transcription. *Current Opinion in Genetics & Development*, *3*(2), 219-225.
209. Szinnai, G., Lacroix, L., Carré, A., Guimiot, F., Talbot, M., Martinovic, J., Delezoide, A.L., Vekemans, M., Michiels, S., Caillou, B., Schlumberger, M., Bidart, J.M., & Polak,

M. (2007). Sodium/iodide symporter (NIS) gene expression is the limiting step for the onset of thyroid function in the human fetus. *The Journal of Clinical Endocrinology & Metabolism*, *92*(1), 70-76.

210. Szinnai, G. (2014a). Genetics of normal and abnormal thyroid development in humans. *Best Practice & Research Clinical Endocrinology & Metabolism*, *28*(2), 133-150.
211. Szinnai, G. (2014b). Clinical genetics of congenital hypothyroidism. *Endocrine Development*, 26, 60-78.
212. Targovnik, H. M., Esperante, S. A., & Rivolta, C. M. (2010). Genetics and phenomics of hypothyroidism and goiter due to thyroglobulin mutations. *Molecular and Cellular Endocrinology*, *322*(1), 44-55.
213. Taylor, B. A., Grieco, D., & Kohn, L. D. (1996). Localization of gene encoding the thyroid stimulating hormone receptor (Tshr) on mouse chromosome 12. *Mammalian Genome*, *7*(8), 626-628.
214. Thiagalingam, S. Cheng, K. H., Lee, H. J., Mineva, N., Thiagalingam, A., & Ponte, J. F. (2003). Histone deacetylases: unique players in shaping the epigenetic histone code. *Annals of the New York Academy of Sciences*, *983*(1), 84-100.
215. Thomas, P. Q., Brown, A., & Beddington, R. S. (1998). Hex: a homeobox gene revealing peri-implantation asymmetry in the mouse embryo and an early transient marker of endothelial cell precursors. *Development*, *125*(1), 85-94.
216. Thorpe-Beeston, J. G., Nicolaides, K. H., Felton, C. V., Butler, J., & McGregor, A. M. (1991). Maturation of the secretion of thyroid hormone and thyroid-stimulating hormone in the fetus. *New England Journal of Medicine*, *324*(8), 532-536.
217. Thorwarth, A., Mueller, I., Biebermann, H., Ropers, H. H., Grueters, A., Krude, H., & Ullmann, R. (2010). Screening chromosomal aberrations by array comparative genomic hybridization in 80 patients with congenital hypothyroidism and thyroid dysgenesis. *The Journal of Clinical Endocrinology & Metabolism*, *95*(7), 3446-3452.
218. Tortora, G. J., & Derrickson, B. H. (2008). The Endocrine sytem. *Principles of Anatomy and Physiology* (pp 656-660). Wiley, NJ, USA.
219. Tou, L., Liu, Q., & Shivdasani, R. A. (2004). Regulation of mammalian epithelial differentiation and intestine development by class I histone deacetylases. *Molecular and Cellular Biology*, *24*(8), 3132-3139.
220. Trivedi, C. M., Luo, Y., Yin, Z., Zhang, M., Zhu, W., Wang, T., Floss, T., Goettlicher, M., Noppinger, P.R., Wurst, W., Ferrari, V.A., Abrams, C.S., Gruber P.J., & Epstein, J.

A. (2007). Hdac2 regulates the cardiac hypertrophic response by modulating Gsk3β activity. *Nature Medicine*, *13*(3), 324-331.

221. Trueba, S. S., Augé, J., Mattei, G., Etchevers, H., Martinovic, J., Czernichow, P., Vekemans, M., Polak, M., & Attié-Bitach, T. (2005). PAX8, TITF1, and FOXE1 gene expression patterns during human development: new insights into human thyroid development and thyroid dysgenesis-associated malformations. *The Journal of Clinical Endocrinology & Metabolism*, *90*(1), 455-462.
222. Tsai, S. C., & Seto, E. (2002). Regulation of histone deacetylase 2 by protein kinase CK2. *Journal of Biological Chemistry*, *277*(35), 31826-31833.
223. Turbay, D., Wechsler, S. B., Blanchard, K. M., & Izumo, S. (1996). Molecular cloning, chromosomal mapping, and characterization of the human cardiac-specific homeobox gene hCsx. *Molecular Medicine*, *2*(1), 86-96.
224. Van Vliet, G., & Czernichow, P. (2004). Screening for neonatal endocrinopathies: rationale, methods and results. *Seminars in Neonatology, 9*(1), 75-85.
225. Vassart, G., & Dumont, J. E. (1992). The Thyrotropin Receptor and the Regulation of Thyrocyte Function and Growth. *Endocrine Reviews*, *13*(3), 596-611.
226. Vassart, G., & Dumont, J. E. (2005). Thyroid dysgenesis: multigenic or epigenetic... or both?. *Endocrinology*, *146*(12), 5035-5037.
227. Vega, R. B., Matsuda, K., Oh, J., Barbosa, A. C., Yang, X., Meadows, E., McAnally, J., Pomajzl, C., Shelton, J.M., Richardson, J.A., Karsenty, G., & Olson, E. N. (2004). Histone deacetylase 4 controls chondrocyte hypertrophy during skeletogenesis. *Cell*, *119*(4), 555-566.
228. Vieira, A. R., Avila, J. R., Daack-Hirsch, S., Dragan, E., Félix, T. M., Rahimov, F., Harrington, J., Schultz, R.R., Watanabe, Y., Johnson, M., Fang, J., O'Brien, S.E., Orioli, I.M., Castilla, E.E., Fitzpatrick, D.R., Jiang, R., Marazita, M.L., & Murray, J. C. (2005). Medical sequencing of candidate genes for nonsyndromic cleft lip and palate. *PLoS Genetics*, *1*, 0651–0659.
229. Vilain, C., Rydlewski, C., Duprez, L., Heinrichs, C., Abramowicz, M., Malvaux, P., Renneboog, B., Parma, J., Costagliola, S., & Vassart, G. (2001). Autosomal Dominant Transmission of Congenital Thyroid Hypoplasia Due to Loss-of-Function Mutation of PAX8 1. *The Journal of Clinical Endocrinology & Metabolism*, *86*(1), 234-238.
230. Vissenberg, R., Manders, V. D., Mastenbroek, S., Fliers, E., Afink, G. B., Ris-Stalpers, C., Goddijn, M., & Bisschop, P. H. (2015). Pathophysiological aspects of thyroid

hormone disorders/thyroid peroxidase autoantibodies and reproduction. *Human Reproduction Update*, *21*(3), 378-387.

231. Voigt, P., LeRoy, G., Drury, W. J., Zee, B. M., Son, J., Beck, D. B., Young, N. L., Garcia, B.A., & Reinberg, D. (2012). Asymmetrically modified nucleosomes. *Cell*, *151*(1), 181-193.
232. Wan, H., Dingle, S., Xu, Y., Besnard, V., Kaestner, K. H., Ang, S. L., Wert, S., Stahlman, M. T., & Whitsett, J. A. (2005). Compensatory roles of Foxa1 and Foxa2 during lung morphogenesis. *Journal of Biological Chemistry*, *280*(14), 13809-13816.
233. Wang, Z., Zang, C., Rosenfeld, J. A., Schones, D. E., Barski, A., Cuddapah, S., Cui, K., Roh, T., Peng, W., Zhang. M., & Zhao, K. (2008). Combinatorial patterns of histone acetylations and methylations in the human genome. *Nature genetics*, *40*(7), 897-903.
234. Wienholds, E., Kloosterman, W. P., Miska, E., Alvarez-Saavedra, E., Berezikov, E., de Bruijn, E., Horvitz, H.R., Kauppinen, S., & Plasterk, R. H. (2005). MicroRNA expression in zebrafish embryonic development. *Science*, *309*(5732), 310-311.
235. Willemsen, M. A., Breedveld, G. J., Wouda, S., Otten, B. J., Yntema, J. L., Lammens, M., & de Vries, B. B. (2005). Brain-Thyroid-Lung syndrome: a patient with a severe multi-system disorder due to a de novo mutation in the thyroid transcription factor 1 gene. *European Journal of Pediatrics*, *164*(1), 28-30.
236. Wolff J & Chaikoff I.L. (1948). The inhibitory action of excessive iodide upon the synthesis of diiodotyrosine and of thyroxine in the thyroid gland of the normal rat. Endocrinology, *43*(3), 174-179.
237. Wolffe, A. P., & Hayes, J. J. (1999). Chromatin disruption and modification. *Nucleic Acids Research*, *27*(3), 711-720.
238. Xu, W. S., Parmigiani, R. B., & Marks, P. A. (2007). Histone deacetylase inhibitors: molecular mechanisms of action. *Oncogene*, *26*(37), 5541-5552.
239. Yang, X. J., & Seto, E. (2008). Lysine acetylation: codified crosstalk with other posttranslational modifications. *Molecular Cell*, *31*(4), 449-461.
240. Yen, P. M. (2001). Physiological and molecular basis of thyroid hormone action. *Physiological Reviews*, *81*(3), 1097-1142.
241. Yoo, E. J., Chung, J. J., Choe, S. S., Kim, K. H., & Kim, J. B. (2006). Down-regulation of histone deacetylases stimulates adipocyte differentiation. *Journal of Biological Chemistry*, *281*(10), 6608-6615.

242. Yuzyuk, T., Fakhouri, T. H. I., Kiefer, J., & Mango, S. E. (2009). The polycomb complex protein mes-2/E (z) promotes the transition from developmental plasticity to differentiation in C. elegans embryos. *Developmental Cell*, *16*(5), 699-710.
243. Zamproni, I., Grasberger, H., Cortinovis, F., Vigone, M. C., Chiumello, G., Mora, S., Onigata, K., Fugazzola, L., Refetoff, S., Persani, L., & Weber, G. (2008). Biallelic inactivation of the dual oxidase maturation factor 2 (DUOXA2) gene as a novel cause of congenital hypothyroidism. *The Journal of Clinical Endocrinology & Metabolism*, *93*(2), 605-610.
244. Zannini, M., Avantaggiato, V., Biffali, E., Arnone, M. I., Sato, K., Pischetola, M., Taylor, B.A., Phillips, S.J., Simeone, A., & Di Lauro, R. (1997). TTF-2, a new forkhead protein, shows a temporal expression in the developing thyroid which is consistent with a role in controlling the onset of differentiation. *The EMBO Journal*, *16*(11), 3185-3197.
245. Zaret, K. S. (2008). Genetic programming of liver and pancreas progenitors: lessons for stem-cell differentiation. *Nature Reviews Genetics*, *9*(5), 329-340.
246. Zhang, C. L., McKinsey, T. A., Chang, S., Antos, C. L., Hill, J. A., & Olson, E. N. (2002). Class II histone deacetylases act as signal-responsive repressors of cardiac hypertrophy. *Cell*, *110*(4), 479-488.
247. Zhang, J., Wang, Y., Liu, X., Jiang, S., Zhao, C., Shen, R., Guo, X., Ling, X., & Liu, C. (2015). Expression and Potential Role of microRNA-29b in Mouse Early Embryo Development. *Cellular Physiology and Biochemistry*, *35*(3), 1178-1187.
248. Zhang, Y., Kwon, S., Yamaguchi, T., Cubizolles, F., Rousseaux, S., Kneissel, M., Cao, C., Li, N., Cheng, H.L., Chua, K., Lombard, D., Mizeracki, A., Matthias, G., Alt, F.W., & Matthias, P. (2008). Mice lacking histone deacetylase 6 have hyperacetylated tubulin but are viable and develop normally. *Molecular and Cellular Biology*, *28*(5), 1688-1701.
249. Zorn, A. M., & Wells, J. M. (2009). Vertebrate endoderm development and organ formation. *Annual Review of Cell and Developmental Biology*, *25*, 221.

8. ACKNOWLEDGEMENTS

First of all, I owe my most sincere gratitude to my supervisor, PD Dr. Gabor Szinnai (Pediatric Endocrinology/ Diabetology, University Children's Hospital UKBB, Basel, Switzerland and Pediatric Endocrinology, Department of Biomedicine, University of Basel, Switzerland) for giving me the opportunity to carry out my PhD work under his excellent guidance. Thank you for the continuous encouragement, excellent advice and fruitful discussions on the research projects and manuscripts, I learned a lot from you.

I would also like to acknowledge Prof. Antonius Rolink for accepting to be my faculty supervisor for my dissertation and Prof. Goerg Hollander as my PhD examiner. I would like to thank Prof. Ed Palmer for accepting to be the chair for my PhD exam.

I am greatly indebted to my laboratory supervisor, Frau. Katrin Hafen for her excellent technical assistance in the laboratory. A big thanks to Thomas, Saulius, Gretel, Javier and Noriko for your expert suggestions in the project. A special thank you to Carlos Mayer for introducing me to Swiss culture, life in Basel and showing around in Switzerland. Thank you Simone, Angela, Hong Ying, Elli, Marco, Elisa, Saule, Martha, Annick and Caroline for all the wonderful moments inside and outside of the lab. Thank you Pankaj, Kapil, Sumit, Sameer and Vindhya for all your support in Basel.

Finally and most deeply, I thank my wife Swati for her never failing support. Last but not the least, I would like to thank my parents for their support and strength to help me achieve all the goals in my life.

9. APPENDIX

Yearbook 2015 THYROID CHAPTER

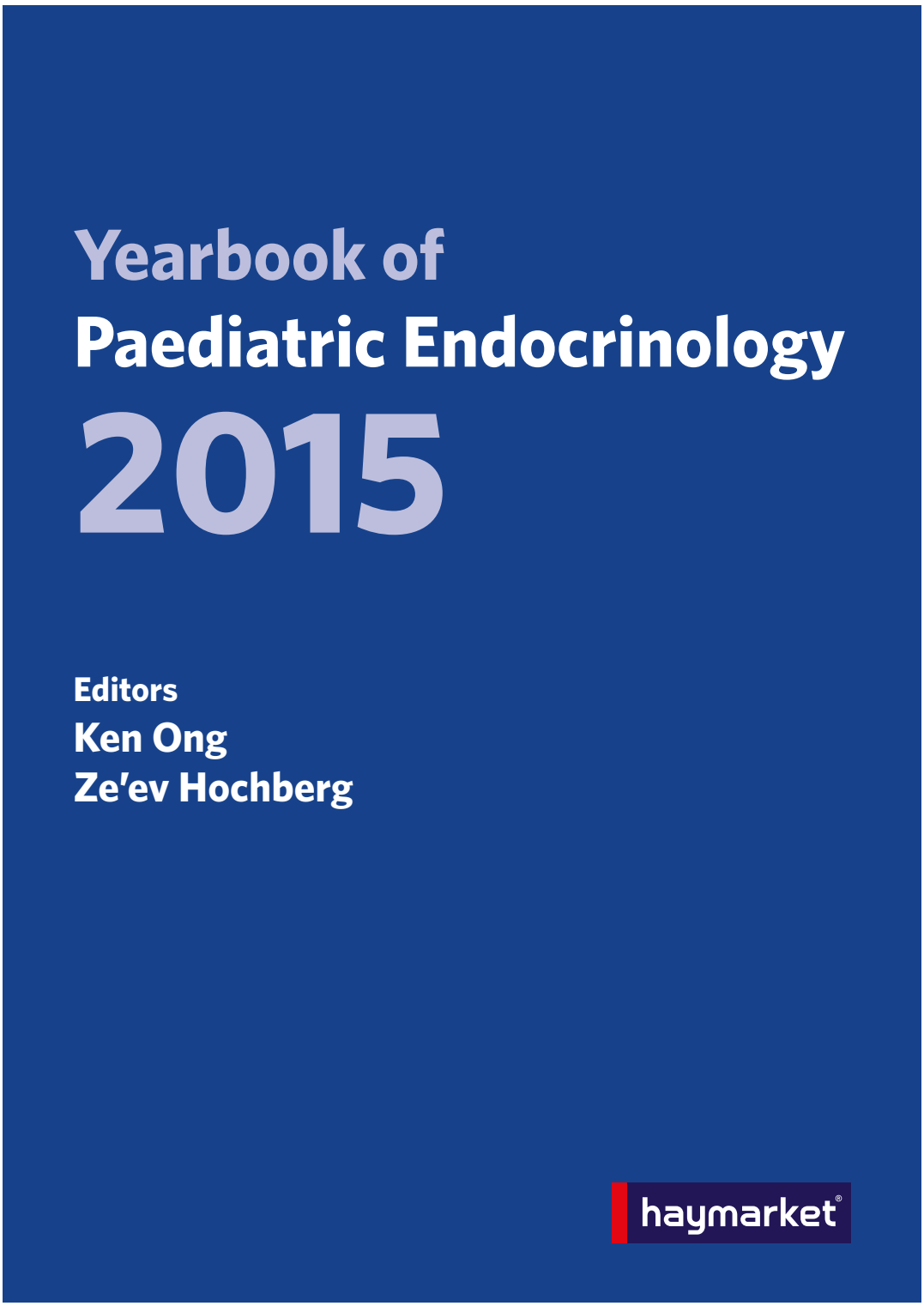

Thyroid

Gabor Szinnai[a], Athanasia Stoupa[b,c], Dulanjalee Kariyawasam[b,d], Sanjay Gawade[a], Aurore Carré[c,d] and Michel Polak[b–d]

[a]Pediatric Endocrinology, University Children's Hospital Basel, and Department of Biomedicine, University of Basel, Basel, Switzerland

[b]Pediatric Endocrinology, Gynecology and Diabetology, Necker Enfants-Malades Hospital, Assistance Publique-Hôpitaux de Paris, IMAGINE Institute, Université Paris Descartes, Sorbonne Paris Cité, Paris, France

[c]Imagine Institute, Paris Descartes-Sorbonne Paris Cité University, France

[d]INSERM U1016, Université Paris Descartes, Faculté de Médecine, Hôpital Cochin, Paris, France

To present the last year's clinically and experimentally most relevant and innovative manuscripts in the field of thyroid disease is the task when preparing the Yearbook. During the year, a large number of papers are saved in the folder 'Yearbook 2015', however, only a few finally make it into this chapter. We picked out a range of papers covering clinical, translational and fundamental work that in our opinion could either change our clinical approach to patients or open new avenues in the molecular understanding of thyroid diseases from congenital hypothyroidism to thyroid cancer. We hope you enjoy reading this year's selection.

Clinical aspects of hypothyroidism

Systematic appraisal of lactose intolerance as cause of increased need for oral thyroxine

Cellini M, Santaguida MG, Gatto I, Virili C, Del Duca SC, Brusca N, Capriello S, Gargano L, Centanni M
Department of Medico-Surgical Sciences and Biotechnologies, «Sapienza» University of Roma, and Endocrinology Unit, Azienda Unita Sanitaria Locale Latina, Latina, Italy
J Clin Endocrinol Metab 2014;99:E1454–E1458

Background: There is a lack of systematic studies assessing the need for T4 dose modification in hypothyroid patients with lactose intolerance, a widespread and often occult disorder.
Methods: The authors assessed the dose required in hypothyroid patients with lactose intolerance and non-compliance with lactose-free diet in a monocentre cohort study.
Results: In all patients with isolated Hashimoto's thyroiditis, target TSH (median TSH 1.02mU/L) was obtained at a median T4 dose of 1.31 microgram/kg/d. In patients also with both Hashimoto's thyroiditis and lactose intolerance, only 5/34 patients reached the desired TSH (median TSH 0.83mU/L) with a similar T4 dose (1.29 microgram/kg/d). In 29/34 patients, the T4 dose was progressively increased and the target TSH (median TSH 1.21mU/L) was only attained at a median T4 dose of 1.81 microgram/kg/d (+38%, P<0.0001). In the 23/29 patients with isolated lactose intolerance, a median T4 dose of 1.72 microgram/kg/d (+31%, P<0.0001) was required to attain normal thyroid function, while in 6/29 patients, other gastrointestinal disorders were diagnosed, and their median T4 requirement was even higher (2.04 microgram/kg/d; +55%; P=0.0032).
Conclusions: Lactose intolerance increased the necessary oral LT4 dose to reach normal TSH levels in hypothyroid patients.

An increased need for T4 has been described in patients with various gastrointestinal disorders, due to the reduced resorptive capacity of the intestine. Besides coeliac disease, lactose intolerance should be considered if unusually high doses of LT4 substitution are necessary to reach euthyroidism, and in patients with known lactose intolerance higher doses should be prescribed.

The severity of congenital hypothyroidism of central origin should not be underestimated

Zwaveling-Soonawala N, van Trotsenburg AS, Verkerk PH
Department of Pediatric Endocrinology, Emma Children's Hospital, Academic Medical Center, University of Amsterdam, Amsterdam, The Netherlands
J Clin Endocrinol Metab 2015;100:E297–E300

Background: Only a few screening programmes measure total or free T4 and TSH simultaneously or stepwise, enabling detection of congenital hypothyroidism of thyroidal (CHT) as well as congenital hypothyroidism of central origin (CHC). The authors aimed to assess disease severity of CHC compared with CHT in a Dutch cohort of CH patients.
Methods: Pretreatment FT4 concentrations were analysed in all children with CH detected by the Dutch neonatal T4+TSH+T4-binding-globulin (TBG) screening between 1995 and 2011. Disease severity was classified using the FT4-based ESPE classification.
Results: 1,288 children were diagnosed with CH between 1995 and 2011. Data of 1,200 (143 CHC and 1,057 CHT) were available for analysis. Based on FT4 concentrations, four children with CHC (2.8%) had severe, 75 (52.4%) had moderate and 64 (44.8%) had mild CH. In the CHT group, 280 children (26.5%) had severe, 341 (32.3%) moderate and 436 (41.2%) mild CH.
Conclusion: Based on initial FT4 values, severe CH was much more prevalent in CHT compared with CHC. However, more than half of CHC patients have moderate CH with initial FT4 below 10pmol/L (0.78ng/dL).

Systematic detection of central congenital hypothyroidism is only possible by combined TSH and T4 based screening programs. A frequently used argument against screening for central congenital hypothyroidism by combined TSH and T4 screening is its presumed mild hypothyroid character. However, the article presented here systematically reviewed the severity of central congenital hypothyroidism in the Netherlands, where neonatal screening is based on T4+TSH+T4-binding globulin measurements. Central congenital hypothyroidism occurred in 12% of all patients. Two messages are important: the severity of central hypothyroidism should not be underestimated; and the policy of neonatal screening should be re-evaluated with these data.

Pregnancy outcomes and relationship to treatment adequacy in women treated early for congenital hypothyroidism: a longitudinal population-based study

Léger J, dos Santos S, Larroque B, Ecosse E
Assistance Publique-Hopitaux de Paris, Hopital Robert Debre, Service d'Endocrinologie Diabetologie Pediatrique, Centre de Reference des Maladies Endocriniennes Rares de la Croissance, Paris, France
J Clin Endocrinol Metab 2015;100:860–869

Background: Hypothyroidism during pregnancy is well known to be associated with adverse outcomes in the mother and her children. So far no data are available on pregnancy outcomes in mothers diagnosed and treated for congenital hypothyroidism (CH) and on the outcome of their children.
Methods: In a cohort of 1,158 women with CH, 207 singleton pregnancies ending >22 weeks were identified retrospectively by questionnaire, and 174 pregnancies were studied prospectively in the three years following the initial questionnaire survey. The reference group comprised 7,245 subjects from the French National Perinatal Survey.
Results: In both the overall and prospective analyses, CH was associated with gestational hypertension, emergency caesarean delivery, induced labour for vaginal delivery and prematurity. In the prospective study, the adjusted odds ratios (aOR) (95% confidence intervals [CI]) were 2.19 (1.26–3.81), 1.88 (1.17–3.02), 1.58 (1.12–2.24) and 1.85 (1.06–3.25), respectively. TSH concentrations at least 10mIU/L during the first three or six months of pregnancy were associated with a higher risk of preterm delivery (aOR, 5.6; 95% CI 1.6–20.0) and fetal macrosomia (aOR, 4.5; 95% CI 1.03–20.1), respectively, whereas no such relationship was observed for TSH concentrations of 5.0–9.9mIU/L.
Conclusion: Adverse pregnancy outcomes in patients with CH treated early in life, can be documented especially when thyroid supplementation is not adequate.

Maternal perchlorate levels in women with borderline thyroid function during pregnancy and the cognitive development of their offspring: data from the Controlled Antenatal Thyroid Study

Taylor PN, Okosieme OE, Murphy R, Hales C, Chiusano E, Maina A, Joomun M, Bestwick JP, Smyth P, Paradice R, Channon S, Braverman LE, Dayan CM, Lazarus JH, Pearce EN
Thyroid Research Group, Institute of Molecular and Experimental Medicine, Cardiff University School of Medicine, Cardiff, UK
J Clin Endocrinol Metab 2014;99:4291–4298

Background: Thyroid dysfunction in the mother is associated with impaired cognitive development of the offspring. Perchlorate decreases thyroidal iodine uptake, potentially reducing thyroid hormone production. The authors investigated the effect of perchlorate exposure in early life on neurodevelopment.
Methods: The authors studied an historical cohort of 21,846 women at gestational age <16 weeks and identified 487 mother–child pairs whose mothers were hypothyroid/hypothyroxinaemic during pregnancy. In these 487 mothers, they analysed whether first trimester maternal perchlorate levels in the highest 10% of the study population were associated with risk of offspring IQ being in the lowest 10% at three years of age.
Results: Urine perchlorate was detectable in all women (median 2.58 microgram/L); iodine levels were low (median 72 microgram/L). Maternal perchlorate levels in the highest 10% of the population increased the risk of offspring IQ being in the lowest 10%; OR=3.14 (95% CI 1.38–7.13), P=0.006, with a greater negative impact observed on verbal OR=3.14 (95% CI 1.42–6.90), P=0.005 than performance IQ. Maternal levothyroxine therapy did not reduce the negative impact of perchlorate on offspring IQ.
Conclusions: High maternal urine perchlorate concentrations were associated with a negative impact on neurocognitive development in the offspring. This effect was independent of maternal levothyroxine therapy.

These two studies underline the importance of an intact thyroid axis in pregnant women for the health of their offspring. The French nationwide study provides the first evidence that maternal congenital hypothyroidism might expose the mother as well as the child to important pregnancy complications such as gestational hypertension, emergency caesarean delivery and prematurity. The study results suggest that better thyroid disease management is required, particularly during the first two trimesters of pregnancy, together with vigilant monitoring of the pregnant woman. These data are in accordance with data from mothers with autoimmune thyroid disease, however, they provide a clearer view on the isolated effect of hypothyroidism versus the combined effect of hypothyroidism and positive thyroid antibodies in studies of pregnancy outcomes in women with autoimmune thyroid disease.

The second study using individual-level patient data to study maternal perchlorate exposure and offspring neurocognitive development suggests that high maternal perchlorate levels in hypothyroid/hypothyroxinaemic pregnant women had an adverse effect on offspring cognitive development at three years of age. However, due to the study protocol, not all questions could be answered definitively. Whether the negative perchlorate effect is due to maternal hypothyroidism or a direct effect on the thyroid function of the fetus, remains open. As stated by the authors, these results require replication in additional studies, including in euthyroid mothers.

Paediatric thyroid nodules and cancer

Ultrasound characteristics of the thyroid in children and adolescents with goiter: a single center experience

Kambalapalli M, Gupta A, Prasad UR, Francis GL
Department of Pediatrics, Children's Hospital of Richmond at Virginia Commonwealth University, Richmond, VA, USA
Thyroid 2015;25:176–182

Background: The authors aimed to evaluate the ultrasound characteristics of the thyroid parenchyma and the prevalence of thyroid nodules in children and adolescents presenting with goitre of autoimmune and non-autoimmune origin.

Methods: Retrospective review of ultrasound exams of the thyroid in 154 children with goitre. Ultrasound characteristics were analysed according to the patient's age, sex, TSH level and thyroid peroxidase antibody titre (TPOAb). Heterogeneity and nodule prevalence were compared between antibody-positive and -negative goitres.
Results: First, heterogeneity was more common in TPOAb-positive (59/71, 83%) compared with TPOAb-negative goitre (24/46, 52%; P<0.001). Second, nodules were equally prevalent in children with (17%) and without (17.4%) TPOAb, and there was no correlation between the serum TSH level or TPOAb titre and the presence of nodules. Third, papillary thyroid cancer (PTC) was diagnosed in 3/71 TPOAb positive patients compared with 1/46 TPOAb negative patients. Finally, pseudonodules were identified in 11/71 TPOAb positive and 0/46 TPOAb negtive patients. However, during follow-up, two pseudonodules were later identified as nodules and one was PTC.
Conclusions: The majority of children and adolescents with goitre had positive TPOAb (71/117). Sonographic heterogeneity was more common among TPOAb-positive patients. Thyroid nodules and PTC were equally common in both groups.

Goitre may appear as a common paediatric condition, especially during adolescence. The data presented support the utility of thyroid ultrasound to detect unsuspected thyroid nodules and papillary thyroid cancer in children with goitre. Only 15% of the nodules and none of the papillary thyroid cancer were palpable. Interestingly, the frequency of thyroid cancer was not decreased in the context of thyroiditis. Therefore a thyroid nodule even in the context of thyroiditis should be investigated as thyroid nodules in patients without autoimmune thyroiditis. Prospective follow-up studies of children with goitre are needed to define recommendations for evaluation with ultrasound and fine-needle aspiration.

Therapeutic effectiveness of screening for multiple endocrine neoplasia type 2A

Machens A, Dralle H
Department of General, Visceral and Vascular Surgery, Martin-Luther-University Halle-Wittenberg, Halle (Saale), Germany
J Clin Endocrinol Metab 2015;100:2539–2545

Background: Genetic screening for mutations in the RET gene allows us to detect patients at risk of hereditary medullary thyroid cancer in the context of multiple endocrine neoplasia type 2A (MEN 2A). The authors aimed to assess the achievements of screening for MEN 2A and identify the challenges and limits.
Methods: Retrospective analysis of 455 carriers at risk of MEN 2A screened and operated between 1963 and 2014. The study comprised 175 carriers of American Thyroid Association (ATA) level C mutations (codon 634); 116 carriers of ATA level B mutations (codons 609, 611, 618, 620 and 630); and 164 carriers of ATA level A mutations (codons 768, 790, 791, 804 and 891) who underwent thyroidectomy. The outcome measures were: 1) percentage of index patients among all carriers, and 2) percentage of MTC, node-positive MTC and biochemical cure among non-index patients.
Results: The percentage of index patients among all carriers fell from 50% (ATA level C) and 100% (ATA level B and A) to 16, 29 and 31%, respectively. Among non-index patients, the percentage of MTC fell for ATA levels C and B but not for ATA level A mutations. The corresponding percentage of node-positive MTC declined since 1963 from 100 to 0% (ATA level C) and since 1995 from 67 to 33% (ATA level B) and from 11 to 10% (ATA level A), whereas biochemical cure increased from 0 to 100% since 1963 (ATA level C), and since 1995 from 0 to 78% (ATA level B) and from 95 to 100% (ATA level A).
Conclusions: Genetic screening clearly improved the outcome in ATA level C patients. More efforts are needed for the less aggressive ATA level B and ATA level A mutations.

Genetic screening for *RET* gene mutations has completely changed the approach in affected families allowing preclinical thyroidectomy in mutation carriers. The authors show clearly a shift to less aggressive stages in patients affected by the ATA C level mutation (c634) with no nodal positive patients at thyroidectomy and 100% biochemical cure nowadays. This is an enormous success bearing in mind the high penetrance of the medullary thyroid carcinoma caused by mutations in codon 634. In contrast, the authors also detect limitations of screening. Based on their results, the focus must now shift to the less aggressive mutations (ATA level B and A). Although improved by use

of genetic testing, the rate of nodal positive patients and biochemical cure after thyroidectomy could be improved by more efforts in identifying and testing family members of index patients with ATA level B and A mutations earlier.

Management guidelines for children with thyroid nodules and differentiated thyroid cancer: The American Thyroid Association Guidelines Task Force on Pediatric Thyroid Cancer

Francis GL, Waguespack SG, Bauer AJ, Angelos P, Benvenga S, Cerutti J, Dinauer CA, Hamilton JK, Hay ID, Luster M, Parisi MT, Rachmiel M, Thompson G, Yamashita S
Virginia Commonwealth University, Pediatric Endocrinology, Richmond, VA, USA
Thyroid 2015;25:716–759

Background: Due to the scarcity of thyroid cancer in children, previous guidelines for the management of thyroid nodules and cancers were focused on adults. However, thyroid neoplasms in the paediatric population exhibit differences in pathophysiology, clinical presentation and long-term outcomes compared with thyroid cancer biology in adults. Furthermore, therapy that may be recommended for an adult may not be appropriate for a child who is at low risk for death but at higher risk for long-term harm from overaggressive treatment. For these reasons, unique guidelines for children and adolescents with thyroid tumours were needed.
Methods: An expert panel commissioned by the American Thyroid Association (ATA) developed clinically relevant questions on the management of children with thyroid nodules and differentiated thyroid cancer. Using an extensive literature search, primarily focused on studies that included subjects ≤18 years of age, the task force identified and reviewed relevant articles through to April 2014. Recommendations were made based upon evidence and expert opinion and were graded using a modified schema from the United States Preventive Services Task Force.
Results: The authors present the first paediatric-specific guidelines for evaluation and management of thyroid nodules and differentiated thyroid cancer, including specific management algorithms for papillary and follicular thyroid cancers.
Conclusions: The ATA task force developed recommendations based on scientific evidence and expert opinion for the management of thyroid nodules and differentiated thyroid cancer in children and adolescents.

These guidelines were long awaited, and provide for the first time specific recommendations for paediatric thyroid cancer diagnosis, treatment and follow-up independently of adult medicine. These represent the current optimal care for children and adolescents with these conditions and are an important tool for critical discussions with adult healthcare providers also involved in treatment of children.

Experiences from Fukushima and Chernobyl

The thyroid status of children and adolescents in Fukushima Prefecture examined during 20–30 months after the Fukushima nuclear power plant disaster: a cross-sectional, observational study

Watanobe H, Furutani T, Nihei M, Sakuma Y, Yanai R, Takahashi M, Sato H, Sagawa F
Radiation Countermeasures Research Institute for Earthquake Disaster Recovery Support, Hirata, Fukushima, Japan; Kasukabe Kousei Hospital, Kasukabe, Saitama, Japan
PLoS One 2014;9:e113804

Background: The authors aimed to: 1) screen for early development of thyroid cancer in children exposed to the Fukushima nuclear accident in 2011; and 2) search for associations between thyroid ultrasonographic findings, thyroid-relevant biochemical markers and iodine-131 ground deposition in the locations of residence during very early days after the accident.

Methods: Cross-sectional study of Fukushima residents <19 years (including fetuses) at the time of the accident including 1) a questionnaire, 2) thyroid ultrasonography, 3) thyroid-related blood tests and 4) urinary iodine measurements. The authors analysed a possible relationship among thyroid ultrasonographic findings (n=1,137), serum hormonal data (n=731), urinary iodine concentrations (n=770) and iodine-131 ground deposition (n=1,137).
Results: No patient with thyroid cancer was identified. Further, no association between thyroid ultrasound anomalies (nodules, cysts) with iodine-131 ground deposits or other parameters were found.
Conclusions: At the early timepoint of 20–30 months after the accident, the authors did not confirm any discernible deleterious effects of the emitted radioactivity on the thyroid of young Fukushima residents.

Initial presentation and late results of treatment of post-Chernobyl papillary thyroid carcinoma in children and adolescents of Belarus

Fridman M, Savva N, Krasko O, Mankovskaya S, Branovan DI, Schmid KW, Demidchik Y
Department of Pathology, Republican Centre for Thyroid Tumors, Minsk, Belarus
J Clin Endocrinol Metab 2014;99:2932–2941

Background: The authors aimed to evaluate the clinical and pathological characteristics and outcome of papillary thyroid carcinoma (PTC) that have arisen in children in Belarus exposed to the radioactive fallout from the Chernobyl accident over a long-term period.
Methods: The long-term treatment results were investigated in 1,078 children and adolescents (<19 years) with PTC who were surgically treated during the years 1990 to 2005.
Results: At presentation, patients suffered from high rates of metastatic PTC, with 73.8% of cases having lymph node involvement and 11.1% having distant spread. The overall survival was 96.9% ± 0.9% with a median follow-up of 16.21 years, and 20-year event-free survival and relapse-free survival were 87.8% ± 1.6% and 92.3% ± 0.9%, respectively. Patients had lower probability of both loco-regional ($P<0.001$) and distant relapses ($P=0.005$) after total thyroidectomy and radioactive iodine therapy. For loco-regional relapses after total thyroidectomy, only radioactive iodine therapy influenced the prognosis ($P<0.001$). For distant relapses after total thyroidectomy, the refusal to treat with radioactive iodine (hazard ratio [HR]=9.26), vascular invasion (HR=8.68) and age at presentation (HR=6.13) were risk factors.
Conclusions: The outcome of PTC both in children and in adolescents exposed to the post-Chernobyl radioiodine fallout was favourable. Total thyroidectomy in combination with radioactive iodine therapy was succesful in minimising loco-regional or distant relapses.

A possible increase in thyroid cancer in the young represents the most critical health problem to be considered after the nuclear accident in Fukushima, Japan (March 2011), which is an important lesson from the Chernobyl disaster (April 1986). Although it was reported that childhood thyroid cancer had started to increase three to five years after the Chernobyl accident, the Japanese authors of the first study speculated that the actual period of latency might have been shorter than reported, considering the delay in initiating thyroid surveillance in the former Soviet Union and also the lower quality of ultrasonographic technology in the 1980s. Fortunately, the thyroid status of young Fukushima residents after the nuclear disaster was normal 20–30 months after the accident. Longer-term follow-up studies are of course necessary to monitor thyroid function and possible thyroid cancer in that population, as the experience of Chernobyl has taught us.

The second study, presenting long-term follow-up data from children and adolescents exposed to the Chernobyl fallout, show rather favourable outcomes of patients with papillary thyroid carcinoma after total thyroidectomy in combination with radioactive iodine treatment, again a key result for a better understanding of the risks of childhood exposure to radiation.

Mutations of the thyroid hormone transporter MCT8 cause prenatal brain damage and persistent hypomyelination

Lopez-Espindola D, Morales-Bastos C, Grijota-Martinez C, Liao XH, Lev D, Sugo E, Verge CF, Refetoff S, Bernal J, Guadano-Ferraz A
Instituto de Investigaciones Biomedicas Alberto Sols, Consejo Superior de Investigaciones Cientificas-Universidad Autonoma de Madrid, Madrid, Spain
J Clin Endocrinol Metab 2014;99:E2799–E2804

Background: The nature of the central nervous system damage is unknown in patients affected with MCT8 mutations. The authors aimed to describe the neuropathology of Allan-Herndon-Dudley syndrome by analysing brain tissue sections from MCT8-deficient subjects.
Methods: They analysed brain sections from a 30th gestational week male fetus and an 11-year-old boy and as controls, brain tissue from a 30th and 28th gestational week male and female fetuses, respectively, a 10-year-old girl and a 12-year-old boy. Staining with haematoxylin-eosin and immunostaining with brain development markers were performed. Thyroid hormone determinations and quantitative PCR for deiodinases were also performed.
Results: The MCT8-deficient fetus showed a delay in cortical and cerebellar development and myelination, impaired axonal maturation and diminished biochemical differentiation of Purkinje cells. The 11-year-old boy showed altered cerebellar structure and deficient myelination. The MCT8-deficient fetal cerebral cortex showed 50% reduction of thyroid hormones and increased type 2 deiodinase and decreased type 3 deiodinase mRNAs.
Conclusions: Brain damage in patients with MCT8 deficiency was diffuse, without evidence of focal lesions and present from fetal stages despite apparent normality at birth. Deficient hypomyelination persisted up to 11 years of age. The neuropathological findings were compatible with the deficient action of thyroid hormones in the developing brain caused by impaired transport to the target neural cells.

Placenta passage of the thyroid hormone analog DITPA to male wild-type and Mct8-deficient mice

Ferrara AM, Liao XH, Gil-Ibanez P, Bernal J, Weiss RE, Dumitrescu AM, Refetoff S
Departments of Medicine and Pediatrics and the Committee on Genetics, The University of Chicago, Chicago, IL, USA
Endocrinology 2014;155:4088–4093

Background: The thyroid hormone (TH) analogue diiodothyropropionic acid (DITPA) corrected thyroid function test (TFT) abnormalities and hypermetabolism of MCT8-deficient children but did not improve the neurological phenotype. The latter result was attributed to the late initiation of treatment. Therefore, the authors gave DITPA to pregnant mice carrying Mct8-deficient embryos to determine whether DITPA, when given prenatally, crosses the placenta and affects the serum TFTs and cerebral cortex of embryos.
Methods: After depletion of the endogenous TH, Mct8-heterozygous pregnant dams carrying both wild-type (Wt) and Mct8-deficient (Mct8KO) male embryos were given DITPA. Effects were compared with those treated with levothyroxine (L-T4).
Results: With DITPA treatment, serum DITPA concentration was not different in the two genotypes, which produced equal effects on serum TSH levels in both groups of pups. In contrast, with L-T4 treatment, TSH did not normalise in Mct8KO pups whereas it did in the Wt littermates and dams despite a higher concentration of serum T4.
Conclusions: DITPA is a candidate for intrauterine treatment of MCT8 deficiency due to: its ability to cross the placenta; its better accessibility of the thyrothrophs in the pituitary gland as shown by negative feedback compared with T4 alone; and its ability to modulate the gene expression of TH-dependent genes in the brain.

In vitro and mouse studies support therapeutic utility of triiodothyroacetic acid in MCT8 deficiency

Kersseboom S, Horn S, Visser WE, Chen J, Friesema EC, Vaurs-Barriere C, Peeters RP, Heuer H, Visser TJ
Erasmus University Medical Center, Rotterdam, The Netherlands
Mol Endocrinol 2014;28:1961–1970

Background: Mutations in MCT8 cause Allan-Herndon-Dudley syndrome and result in severe psychomotor retardation and elevated serum T3 levels. As the neurological symptoms are most likely caused by a lack of thyroid hormone (TH) transport into the CNS, the administration of a TH analogue that does not require MCT8 for cellular uptake may represent a therapeutic strategy. The authors investigated the therapeutic potential of the biologically active T3 metabolite Triac (triiodothyroacetic acid; TA3) by studying TA3 transport, metabolism and action both in vitro and in vivo.
Methods: TA3 uptake and metabolism were studied in neuronal cell lines, fibroblasts of affected patients and in Pax8 and MCT8/Oatp1c1 double knockout mice.
Results: First, fibroblasts from MCT8 patients showed an impaired T3 uptake compared with controls, whereas TA3 uptake was similar in patient and control fibroblasts. Second, in neuronal cell lines, TA3 induced T3-like gene expression. Finally, treatment of athyroid Pax8 knockout mice and Mct8/Oatp1c1 double knockout mice between postnatal day one and 12 with TA3 restored T3-dependent neural differentiation in the cerebral and cerebellar cortex, indicating that TA3 can replace T3 in promoting brain development.
Conclusions: The authors demonstrated uptake of TA3 in neuronal cells and in fibroblasts of MCT8 patients, and similar gene responses to T3 and TA3 in vitro as in vivo.

Monocarboxylate transporter 8 (MCT8; SLC16A2) deficiency causes severe X-linked intellectual and neuropsychological impairment associated with abnormal thyroid function tests producing thyroid hormone deprivation in brain and excess in peripheral tissues (Allan-Herndon-Dudley syndrome, AHDS; OMIM #300523). The time course of brain damage and the pathology of the brain of affected patients was unknown. In the first paper, the authors describe in human fetuses and children neuropathological features of the disease in detail and show that the lesions are compatible with the effects of thyroid hormone deficiency on the brain.

Treatment options for patients with MCT8 deficiency are limited. The administration of propylthiouracil, which blocks thyroid hormone production and inhibits T4 to T3 conversion, combined with L-T4 has shown some metabolic benefits, but no effect on the neurological phenotype. To treat patients with MCT8 deficiency, substances with thyroid hormone effect but alternative cellular uptake mechanisms than by MCT8 are necessary. So far, two thyromimetics, diiodothyropropionic acid (DITPA) and triiodothyroacetic acid (Triac) are under investigation, DIPTA already being used in four patients from nine months of age. The following two papers provide detailed insights into the actions and metabolism of DIPTA and Triac in vitro and in vivo, and pave the way for more effective treatment of affected patients.

In an attempt to treat affected patients as early as in utero, the authors of the second study provided evidence that DIPTA crosses the placenta and reaches the neuronal target cells (neurons, thyrothrophs) in the mice model inducing a T3-like effect. The approach to treat affected patients as early as in utero is even more relevant in the context of the data presented in the first paper showing that brain damage in the human fetus is already induced in utero. In the third study in mice, the authors show new insights into the uptake and action of Triac, and provide further evidence in the mouse model, that Triac fulfils criteria to be used therapeutically in MCT8 patients: MTC8 independent cellular uptake, T3-like effects in neuronal cells and T3-like response in the hypothyroid brain. More clinical research is necessary to confirm these encouraging translational data.

Effects of early thyroxine treatment on development and growth at age 10.7 years: follow-up of a randomized placebo-controlled trial in children with Down's syndrome

Marchal JP, Maurice-Stam H, Ikelaar NA, Klouwer FC, Verhorstert KW, Witteveen ME, Houtzager BA, Grootenhuis MA, van Trotsenburg AS
Department of Pediatric Endocrinology, and Psychosocial Department, Academic Medical Center/Emma Children's Hospital, Amsterdam, The Netherlands
J Clin Endocrinol Metab 2014;99:E2722–E2729

Background: The authors aimed to determine the long-term effects of early T4 treatment on development and growth in children with Down's syndrome (DS) with either an elevated or normal neonatal TSH concentration.
Methods: 123/196 patients participating in a first randomised placebo-controlled study comparing T4 and placebo treatment during the first two years of life were reassessed for mental development and growth parameters at a mean age of 10.7 years. Outcomes were compared between T4- and placebo-treated children, and between treatment groups with either a normal (<5mIU/L), or elevated (≥5mIU/L) TSH concentration at original trial entry.
Results: No differences were found in mental or motor development, communication skills or fine-motor co-ordination between T4-treated (n=64) and placebo-treated children (n=59). T4-treated children had a larger head circumference (HC) (50.4 versus 49.8cm, P=0.04) and tended to be taller (133.2 versus 131.1cm, P=0.06). These differences were somewhat greater in children with TSH ≥5mIU/L (HC: T4, 50.5 versus placebo, 49.7cm; P=0.01; height: T4, 133.8 versus placebo, 130.8cm; P=0.02), but were not found in children with TSH <5mIU/L (HC: T4, 50.1 versus placebo, 50.0cm; P=0.75; height: T4, 132.1 versus placebo, 131.6cm; P=0.22).
Conclusions: Early T4 treatment of children with Down's syndrome did not result in improved mental or motor development at 10 years of age. However, the positive effect on growth was still measurable, especially in children with an elevated plasma TSH concentration in the neonatal period.

In the original study, analysing the effect of early T4 treatment during the first two years of life in children with Down's syndrome, at the end of the intervention at two years of age, the authors found a slightly better motor development and growth. In this unique long-term follow-up study, this effect was not sustained when these children were re-evaluated almost nine years after the initial trial. Whether this is due to a lack of major effect of thyroxine on neurocognitive development in children with Down's syndrome or whether thyroxine treatment should be maintained throughout childhood to obtain favourable results should be tested in further clinical trials.

DYRK1A BAC transgenic mouse: a new model of thyroid dysgenesis in Down syndrome

Kariyawasam D, Rachdi L, Carré A, Martin M, Houlier M, Janel N, Delabar JM, Scharfmann R, Polak M
Inserm U1016, Paris, France
Endocrinology 2015;156:1171–1180

Background: The molecular basis of mild thyroid dysgenesis in children with Down's syndrome is unknown. Transgenic Dyrk1A mice, obtained by bacterial artificial chromosome engineering (mBACTgDyrk1A), have three copies of the *Dyrk1A* gene and are a model of Down's syndrome. The authors aimed to determine whether this transgenic Dyrk1A (Dyrk1A(+/++)) mouse is an adequate murine model for the study of thyroid dysgenesis in Down's syndrome.
Methods: Embryonic thyroid development was analysed in wild-type (WT) and Dyrk1A(+/++) mice by immunofluorescence with markers of early thyroid development, hormonogenesis and final differentiation. The adult phenotype was compared at eight to 12 weeks in Dyrk1A(+/++) and WT mice for T4 and TSH levels, thyroidal weight and histological analysis.
Results: During development at E17.5, thyroglobulin stained surface in Dyrk1A(+/++) thyroids was less than a third as large and their differentiated follicular surface half the size (P=0.004) compared with WT. In adult mice, Dyrk1A(+/++) mice had lower plasma T4 levels (2.4ng/mL versus WT,

3.7ng/mL; P=0.019) while plasma TSH (114mUI/L versus WT, 73mUI/L; P=0.09) were not different. Dyrk1A(+/++) thyroid glands were heavier (P=0.04) and exhibited large disorganised regions.
Conclusions: Dyrk1A overexpression caused functional and morphological impairment of thyroid development. The Dyrk1A(+/++) mouse can be considered a suitable study model for thyroid dysgenesis in Down's syndrome.

The most common abnormalities of thyroid function and morphology in children with Down's syndrome are: mildly elevated TSH, with normal or slightly decreased T4; and thyroid hypoplasia. In contrast, severe congenital hypothyroidism is less frequent at birth, and autoimmune thyroiditis occurs beyond infancy. This paper: 1) provides insight into the disordered development of the thyroid possibly involved in Down's syndrome associated mild thyroid hypothyroidism; 2) confirms earlier results of the group analysing fetal thyroids of children with Down's syndrome, and finally establishes the model of transgenic mice with three copies of the *Dyrk1A* gene as an accurate model of Down's syndrome associated thyroid dysgenesis. Further work should aim at determining the precise molecular mechanism linking *Dyrk1A* and thyroid development.

New insights into molecular mechanisms of congenital hypothyroidism

The paired box transcription factor Pax8 is essential for function and survival of adult thyroid cells

Marotta P, Amendola E, Scarfo M, De Luca P, Zoppoli P, Amoresano A, De Felice M, Di Lauro R
IRGS, Biogem, Ariano Irpino, Avellino, Italy
mario.defelice@unina.it
Mol Cell Endocrinol 2014;396:26–36

Background: The transcription factor Pax8 is known to be essential at very early stages of mouse thyroid gland development, before the onset of thyroid hormone production. The authors aimed to determine the role of Pax8 in late thyroid development.
Methods: Detailed analysis of a mouse line with late embryonic conditional inactivation of Pax8.
Results: The removal of the Pax8 protein at late stages in thyroid gland development resulted in severe hypothyroidism, consequent to a reduced gland size and a deranged differentiation.
Conclusions: These results demonstrate that Pax8 is not only relevant for thyroid gland morphogenesis, but also an essential player in controlling survival and differentiation of adult thyroid follicular cells.

The observation that a transcription factor may control embryonic development as well as maintenance and survival has earlier been shown for Nkx2-1 in the thyroid gland. So far, no data were available on the role of Pax8 in the adult thyroid. The authors nicely show in a conditional knockout model that Pax8 is crucial for normal differentiation and inhibits apoptosis of thyroid follicular cells.

Extreme phenotypic variability of thyroid dysgenesis in six new cases of congenital hypothyroidism due to PAX8 gene loss-of-function mutations

Ramos HE, Carré A, Chevrier L, Szinnai G, Tron E, Cerqueira TL, Léger J, Cabrol S, Puel O, Queinnec C, De Roux N, Guillot L, Castanet M, Polak M
INSERM U1016, Universite Paris Descartes, Sorbonne Paris Cite, Paris, France
Eur J Endocrinol 2014;171:499–507

Background: The authors searched for PAX8 mutations in a cohort of patients with congenital hypothyroidism (CH) and various types of thyroid gland defects.
Methods: The French neonatal screening programme was used for recruiting patients.
Results: 118 patients with CH, including 45 with familial and 73 with sporadic diseases, were studied. The thyroid gland was normal in 23 patients, 28 had hypoplasia, 25 had hemithyroid agenesis, 21 had athyreosis and 21 had ectopy. The authors identified four different PAX8 mutations (p.R31C, p.R31H, p.R108X

and p.I47T) in 10 patients (six patients with CH and four family members), two with sporadic and eight with familial diseases. Imaging studies performed in the index cases showed ectopic thyroid gland (n=2), hypoplasia (n=2), eutopic lobar asymmetry (n=1) and eutopic gland compatible with dyshormonogenesis (n=1). The previously reported p.R31C and the novel p.I47T PAX8 mutations are devoid of activity.
Conclusion: The novel p.I47T PAX8 mutation presented loss of function leading to CH. Thyroid ectopy was observed in two cases of PAX8 (p.R31H) mutation, a finding that has not been reported previously.

In the last two decades, heterozygous loss-of-function *PAX8* mutations have been reported in patients with a range of hypothyroidism and thyroid morphology despite the presence of identical mutations. Thyroid ectopy is the most prevalent phenotype of thyroid dysgenesis, however, genetic defects have not been found in known thyroid transcription factors. First, the presented study extends current knowledge on the variability of thyroid function and type of dysgenesis even within families. Second, the study reports for the first time of molecular defects in known genes causing thyroid ectopy. As a consequence, *PAX8* mutations have to be considered as molecular cause of thyroid ectopy.

Functional zebrafish studies based on human genotyping point to netrin-1 as a link between aberrant cardiovascular development and thyroid dysgenesis

Opitz R, Hitz MP, Vandernoot I, Trubiroha A, Abu-Khudir R, Samuels M, Desilets V, Costagliola S, Andelfinger G, Deladoey J
Institute of Interdisciplinary Research in Molecular Human Biology, Universite Libre de Bruxelles, Brussels, Belgium
Endocrinology 2015;156:377-388

Background: Congenital heart disease is the most frequent associated malformation in patients with thyroid dysgenesis. The authors aimed to identify common genetic or epigenetic factors causing the combination of congenital hypothyroidism and congenital heart disease.
Methods: Genome-wide single-nucleotide polymorphism array and Sanger sequencing to analyse blood DNA samples from three selected patients with co-occurring congenital hypothyroidism caused by thyroid dysgenesis and congenital heart disease to search for de novo copy number variants and coding mutations in candidate genes.
Results: Rare variants were identified in all three patients. The Netrin-1 gene was selected as the biologically most plausible contributory factor for functional studies. In zebrafish, ntn1a and ntn1b were not expressed in thyroid tissue, but ntn1a was expressed in pharyngeal arch mesenchyme, and ntn1a-deficient embryos displayed defective aortic arch artery formation and abnormal thyroid morphogenesis. The functional activity of the thyroid in ntn1a-deficient larvae was, however, preserved. Phenotypic analysis of affected zebrafish indicates that abnormal thyroid morphogenesis resulted from a lack of proper guidance exerted by the dysplastic vasculature of ntn1a-deficient embryos.
Conclusions: Clinical and genetic data in humans and developmental studies in zebrafish identified Netrin-1 as a potential candidate gene for thyroid dysgenesis in the context of congenital heart disease.

Up to 8% of individuals with congenital hypothyroidism caused by thyroid dysgenesis have co-occurring congenital heart disease. The authors conducted careful phenotyping of patients without *NKX2-5* mutations combined with molecular and functional studies in zebrafish and identified Netrin-1 as a potential shared genetic factor for cardiac and thyroid congenital defects. In analogy with other transcription factors associated with thyroid dysgenesis in animal models, in netrin-1 deficiency the primary defect is not within the thyroid precursor cells but within the surrounding mesenchyme. Netrin-1 is proposed as a new candidate gene for thyroid dysgenesis and congenital heart disease.

When an intramolecular disulfide bridge governs the interaction of DUOX2 with its partner DUOXA2

Carré A, Louzada RA, Fortunato RS, Ameziane-El-Hassani R, Morand S, Ogryzko V, de Carvalho DP, Grasberger H, Leto TL, Dupuy C
Universite Paris-Sud, Orsay, France
Antioxid Redox Signal 2015 (Epub ahead of print) Apr 20

Background: Mutations in dual oxidase 2 (DUOX2) and dual oxidase activator 2 (DUOXA2) cause thyroid dyshormonogenesis. DUOX2 forms with DUOXA2 a stable complex at the cell surface that

is crucial for the H_2O_2-generating activity. However, the mechanism of their interaction is unknown. The contribution of some cysteine residues located in the N-terminal ectodomain of DUOX2 in a surface protein–protein interaction is suggested.
Methods: The authors investigated in vitro the involvement of different cysteine residues in the formation of covalent bonds possibly critical for the function of the complex.
Results: The authors report the identification and the characterisation of an intramolecular disulphide bond between cys-124 of the N-terminal ectodomain and cys-1162 of an extracellular loop of DUOX2. This disulphide bridge has important functional implications in both export and activity of DUOX2; and provides structural support for the formation of interdisulphide bridges between the N-terminal domain of DUOX2 and the two extracellular loops of its partner, DUOXA2.
Conclusions: The oxidative folding of DUOX2 that takes place in the endoplasmic reticulum appears to be a key event in the trafficking of the DUOX2/DUOXA2 complex as it promotes an appropriate conformation of the N-terminal region, which is propitious to subsequent covalent interactions with the maturation factor, DUOXA2.

The dual oxidase 2 (DUOX2) protein belongs to the NADPH oxidase (NOX) family. As a H_2O_2 generator, it plays a key role in both thyroid hormone biosynthesis and innate immunity. Both stability and function of the maturation factor, DUOXA2, are dependent on the oxidative folding of DUOX2, indicating that DUOX2 displays a chaperone-like function with respect to its partner. This basic structure/function study provides clues to better understand the impact of different mutations of these enzymes identified in patients with congenital hypothyroidism.

Mechanism of the year: new arguments in an old discussion

Differences in hypothalamic type 2 deiodinase ubiquitination explain localized sensitivity to thyroxine

Werneck de Castro JP, Fonseca TL, Ueta CB, McAninch EA, Abdalla S, Wittmann G, Lechan RM, Gereben B, Bianco AC
Division of Endocrinology, Diabetes and Metabolism, University of Miami School of Medicine, Miami, FL, USA
J Clin Invest 2015;125:769–781

Background: Patients with hypothyroidism are routinely treated with L-T4, which aims to normalise the thyroid stimulating hormone (TSH) level. However, normalisation of serum TSH with L-T4 monotherapy results in relatively low serum 3,5,3′-triiodothyronine (T3) and high serum thyroxine/T3 (T4/T3) ratio. In the hypothalamus–pituitary dyad as well as the rest of the brain, the majority of T3 present is generated locally by T4 deiodination via the type 2 deiodinase (D2); this pathway is self-limited by ubiquitination of D2 by the ubiquitin ligase WSB-1.
Methods: Investigations in WT and astrocyte-specific Wsb-1 knockout mice.
Results: Tissue-specific differences in D2 ubiquitination accounted for the high T4/T3 serum ratio in adult thyroidectomised rats chronically implanted with subcutaneous L-T4 pellets. Whole-body D2-dependent T4 conversion to T3 was decreased by L-T4 treatment. In contrast, D2 activity in the hypothalamus was only minimally affected by L-T4. In vivo studies in Wsb1 knockout mice as well as in vitro analysis of D2 ubiquitination driven by different tissue extracts indicated that D2 ubiquitination in the hypothalamus was relatively less. As a result, in contrast to other D2-expressing tissues, the hypothalamus had increased sensitivity to T4.
Conclusions: Tissue-specific differences in D2 ubiquitination are an inherent property of the TRH/TSH feedback mechanism and indicate that only constant delivery of L-T4 and L-T3 fully normalises T3-dependent metabolic markers and gene expression profiles in thyroidectomised rats.

The type 2 iodothyronine deiodinase (D2) is essential for feedback regulation of TSH by T4. Monotherapy with L-T4 in hypothyroid patients normalises TSH and T4 levels, while in 15% of patients T3 remains below the lower limit of reference. Further, 5–10% of L-T4 treated patients experience persistent symptoms of hypothyroidism despite normalisation of TSH and T4.

The authors investigated in an extensive and elegant animal study the role of D2 activity at different levels and under different substitution regimens in thyroidectomised rats. First, they confirm their own earlier results concerning the benefits of combined L-T4 and L-T3 treatment for normalisation of all thyroid function parameters, providing further arguments for clinical re-evaluation of combined L-T3 and L-T4 treatment regimens in patients experiencing hypothyroid symptoms despite adequate TSH and T4 levels. Second, they add important insights into the differences of L-T4 and L-T3 feedback mechanisms by revealing that deiodination in peripheral tissues as well as in most brain regions is very sensitive to T4-induced D2 ubiquitination in contrast to the hypothalamus, where T4-induced D2 inactivation is not present. As a consequence, TSH is normalised based on adequate T3 conversion from T4 in the hypothalamus, while in the peripheral tissues the conversion of T4 to T3 is blocked by T4 sensitive ubiquitination causing tissue-specific hypothyroidism in the context of normalised TSH and T4 levels. Whether these data are valid in the subgroup of patients experiencing hypothyroid symptoms despite adequate TSH and T4 values remains to be shown in new clinical studies.

Human thyroid stem cells

Human embryonic stem cells form functional thyroid follicles

Ma R, Latif R, Davies TF
Thyroid Research Unit, Department of Medicine, Icahn School of Medicine at Mount Sinai and the James J. Peters VA Medical Center, New York, NY, USA
Thyroid 2015;25:455–461

Background: Overexpression of the regulatory transcription factors PAX8 and NKX2-1 directs murine embryonic stem cells to differentiate into thyroid follicular cells subsequently organised into three-dimensional follicular structures. The authors studied human embryonic stem (hES) cells with the aim of recapitulating this scenario and producing functional human thyroid cell lines.
Methods: Reporter gene tagged pEZ-lentiviral vectors were used to express human PAX8-eGFP and NKX2-1-mCherry in the H9 hES cell line followed by differentiation into thyroid cells directed by Activin A and thyrotropin (TSH).
Results: Both transcription factors were expressed efficiently in hES cells expressing either PAX8 or NKX2-1, or in combination in the hES cells. Further differentiation of the double transfected cells showed the expression of thyroid-specific genes, including thyroglobulin (TG), thyroid peroxidase, the sodium/iodide symporter and the TSH receptor as assessed by qPCR and immunostaining. Activin and TSH-induced differentiation resulted in thyroid follicle formation and abundant TG protein expression within the follicular lumens. On stimulation with TSH, these hES-derived follicles were also capable of dose-dependent cAMP generation and radioiodine uptake, indicating functional thyroid epithelial cells.
Conclusion: In analogy with the murine model, this study provides proof of principle that hES cells can be committed to thyroid cell speciation under appropriate conditions.

After induction of murine embryonic stem cells into functional follicular cells, the authors successfully reproduced the directed differentiation of human embryonic stem cells to follicular cells expressing specific differentiation markers and capable of iodine uptake. These are important technical achievements in the manipulation of human stem cells. However, as also stated by the authors, more research is necessary to replace lentiviral overexpression of NKX2-1 and PAX8 by optimised growth and differentiating protocols avoiding the genetic manipulation of the stem cells.